BIOETHANOL OXIDATION TO VALUE ADDED PRODUCTS

A Thesis submitted to Gujarat Technological University

For the award of

Doctor of Philosophy

In

CHEMICAL ENGINEERING

By

PARESH HARIBHAI RANA

Enrollment no: 129990905003

Under Supervision of

Prof. Dr. Parimal A. Parikh

Gujarat Technological University
Ahmedabad
July - 2017

BIOETHANOL OXIDATION TO VALUE ADDED PRODUCTS

A Thesis submitted to Gujarat Technological University

For the award of

Doctor of Philosophy

In

CHEMICAL ENGINEERING

By

PARESH HARIBHAI RANA

Enrollment no: 129990905003

Under Supervision of

Prof. Dr. Parimal A. Parikh

Gujarat Technological University
Ahmedabad
July - 2017

DECLARATION

I declare that the thesis entitle "**Bioethanol Oxidation to Value added Products**" submitted by me for the degree of Doctor of Philosophy is the record of research work carried out by me during the period from January 2013 to July 2017 under the supervision of **Prof. Dr. Parimal A. Parikh** and this has not formed the basis for the award of any degree, diploma, associateship, Fellowship, titles in this or any other University or other institution of higher learning.

I further declare that the material obtained from other sources has been duly acknowledged in the thesis. I shall be solely responsible for any plagiarism or other irregularities, if notices in the thesis.

Signature of Research scholar: Date:

Name of Research Scholar: **Paresh Haribhai Rana**

Place: Ahmedabad

CERTIFICATE

I certify that the work incorporated in the thesis "**Bioethanol Oxidation to Value Added Product**" submitted by Shri **Paresh Haribhai Rana** was carried out by the candidate under my supervision. To the best of my knowledge:

(i)   The Candidate has not submitted the same research work to any other institution for any degree/diploma, associateship, Fellowship or other similar titles.

(ii)   The thesis submitted is a record of original research work done by the Research Scholar during the period of study under my supervision and

(iii)   The thesis represents independent research work on the part of the Research Scholar.

Signature of Supervision: Date:

Name of Supervisor: **Prof. Dr. Parimal A. Parikh**

Place: Surat

Originality Report Certificate

It is certified that PhD Thesis titled "**Bioethanol Oxidation to Value Added Product**" by Mr. Paresh Haribhai Rana has been examined by us. We undertake the following:

a. Thesis has significant new work/knowledge as compared already published or are under consideration to be published elsewhere. No sentence, equation, diagram, table, paragraph or section has been copied verbatim from previous work unless it is placed under quotation marks and duly referenced.

b. The work presented is original and own work of the author (i.e. there is no plagiarism). No ideas, processes, results or words of others have been presented as Author own work.

c. There is no fabrication of data or results which have been compiled /analyzed.

d. There is no falsification by manipulating research materials, equipment or processes, or changing or omitting data or results such that the research is not accurately represented in the research record.

The thesis has been checked using Turnitin (copy of originality report attached) and found within limits as per GTU Plagiarism Policy and instructions issued from time to time (i.e. permitted similarity index <=25%).

Signature of the Research Scholar: Date:

Name of the Research Scholar: **Paresh Haribhai Rana**

Place: Ahmedabad

Signature of Supervision: Date:

Name of Supervisor: **Prof. Dr. Parimal A. Parikh**

Place: Surat

PhD THESIS Non-Exclusive License to
GUJARAT TECHNOLOGICAL UNIVERSITY

In consideration of being a PhD Research Scholar at GTU and in the interests of the facilitation of research at GTU and elsewhere, I, Paresh Haribhai Rana having Enrollment No. 129990905003 hereby grant a non-exclusive, royalty free and perpetual license to GTU on the following terms:

a) GTU is permitted to archive, reproduce and distribute my thesis, in whole or in part, and/or my abstract, in whole or in part (referred to collectively as the "Work") anywhere in the world, for non-commercial purposes, in all forms of media;

b) GTU is permitted to authorize, sub-lease, sub-contract or procure any of the acts mentioned in paragraph (a);

c) GTU is authorized to submit the Work at any National / International Library, under the authority of their "Thesis Non-Exclusive License";

d) The Universal Copyright Notice (©) shall appear on all copies made under the authority of this license;

e) I undertake to submit my thesis, through my University, to any Library and Archives. Any abstract submitted with the thesis will be considered to form part of the thesis.

f) I represent that my thesis is my original work, does not infringe any rights of others, including privacy rights, and that I have the right to make the grant conferred by this non-exclusive license.

g) If third party copyrighted material was included in my thesis for which, under the terms of the Copyright Act, written permission from the copyright owners is required, I have obtained such permission from the copyright owners to do the acts mentioned in paragraph (a) above for the full term of copyright protection.

h) I retain copyright ownership and moral rights in my thesis, and may deal with the copyright in my thesis, in any way consistent with rights granted by me to my University in this non-exclusive license.

i) I further promise to inform any person to whom I may hereafter assign or license my copyright in my thesis of the rights granted by me to my University in this non-exclusive license.

j) I am aware of and agree to accept the conditions and regulations of PhD including all policy matters related to authorship and plagiarism.

Signature of the Research Scholar:

Name of Research Scholar: **Paresh Haribhai Rana**

Date: Place: Ahmedabad

Signature of Supervisor:

Name of Supervisor: **Prof. Dr. Parimal A. Parikh**

Date: Place: Surat

Seal:

Thesis Approval Form

The viva-voce of the PhD Thesis submitted by Shri Paresh Haribhai Rana (Enrollment No. 129990905003) entitled "**Bioethanol Oxidation to Value Added Product**" was conducted on   at Gujarat Technological University.

(Please tick any one of the following option)

☐ We recommend that he/she be awarded the Ph.D. Degree.

☐   We recommend that the viva-voce be re-conducted after incorporating the following suggestions:

(Briefly specify the modification suggested by the panel)

☐ The performance of the candidate was unsatisfactory. We recommend that   he/she should not be awarded the Ph.D. Degree.

(The panel must give justification for rejection the research work)

…………………….…………   …………………….…………

Name and Signature of Supervisor with Seal   1) External Examiner 1 Name and Signature

…………………….…………   …………………….…………

2) External Examiner 2 Name and Signature   3) External Examiner 3 Name and Signature

ABSTRACT

Coal energized the 19th century while oil worked for the 20th century. The question that remains pending is the future energy source. With the expanding population, growing demands from industrialization and rising concern for environment preventative measure, total dependence on fossil fuel resources is not sustainable. Hence there is an urgent need for a green and sustainable fuel provoked research into biomass as an alternative to fossil fuels. There is a need to identify a suitable biomass derived species, which can provide high value outputs in order to replace conventional fossil fuel resources. Bioethanol is one of such biomass derived platform molecule which has a potential to be a sustainable feedstock of variety of commodity chemicals. For instance, Acetaldehyde which majorly produced from the oxidation of ethylene (Wacker process) can be produced via one - step gas phase conversion of bioethanol. With the growing availability of bioethanol, oxidation of bioethanol to value added chemicals has been considered as feasible process.

With this back - ground, the main goal of the study is to investigate the effect of noble metals, metal oxides and metal/oxide loading on the conversion as a function of temperature for the oxidation of bioethanol in air. In the first part of this work liquid phase oxidation of bioethanol was carried out with Au and Ag supported on various type of zeolites. Reaction parameters like pressure, O_2/ethanol molar ratio, effect of alkali and reaction time has also been studied. It was observed that presence of water hindered that catalytic activity of the catalysts which resulted into poor conversion of bioethanol.

The second part of this work described the preparation, characterization and catalytic study of Au, Ag and Au - Ag over SiO_2, CeO_2 and ZrO_2 in the gas phase oxidation of bioethanol as a function of reaction temperature. Among the 1 wt% Au supported on SiO_2, CeO_2 and ZrO_2 catalysts, Au/ZrO_2 was found to be very active for bioethanol oxidation. The improved catalytic performance of Au/ZrO_2 was due to the oxygen deficiencies generated by Au on ZrO_2 surface. Ag/ZrO_2 and $Au-Ag/ZrO_2$ showed low conversion than Au/ZrO_2 and Au/CeO_2, because Ag is more prone to oxidation than Au. Due to inert nature of SiO_2, Au/SiO_2 exhibited lowest ethanol conversion.

Later on Ag/CeO$_2$ was employed for this work and characterization results indicated that a part of Ag was inserted into the lattice of CeO$_2$ and expanded the support lattice led to increase the lattice oxygen mobility. Also the presence of Ag weakens the Ce-O bond and furthermore promotes the exchange between lattice oxygen and adsorbed oxygen. Stability tests of Ag/CeO$_2$ showed no sign of deactivation even after 36 h of time on stream. Besides that, the catalyst also showed higher selectivity towards acetaldehyde even at higher temperature. Ag/CeO$_2$ catalyst was found to outperform the reported catalyst systems.

A Ce$_x$Zr$_{1-x}$O$_2$ mixed oxide catalyst, prepared by co precipitation method, was also tested in the oxidation of bioethanol. Remarkable effects of Ce$_x$Zr$_{1-x}$O$_2$ and Au supported Ce$_x$Zr$_{1-x}$O$_2$ was observed in the bioethanol oxidation. The results obtained from catalyst characterization indicated that solid solution of Ce$_x$Zr$_{1-x}$O$_2$ mixed oxide was formed. Role of oxygen in bioethanol oxidation was inevitable and Ce$_x$Zr$_{1-x}$O$_2$ mixed oxides are known for their higher thermal stability and high oxygen mobility. In this work, oxygen storage capacity (OSC) of the catalysts was found to enhance the conversion of bioethanol. This could be due to incorporation of zirconium to ceria framework which improved OSC of catalysts. OSC of Ce$_x$Zr$_{1-x}$O$_2$ mixed oxides further increased upon impregnation of Au as Au reduced supports.

Acknowledgements

It gives me great pleasure to thank my parents, my brother, my sisters and children (Chetasi, Maulin and Vileena) and relatives for their love, unfailing support, tremendous patience, trust and encouragement that they have shown to me.

Nothing appropriate can describe the love and support of my dearest wife **Hiral** , whose constant encouragement and admiration sets new horizons for me to reach, in every facet of my life. I would like to acknowledge her endless patience during my study and thank almighty for inspirational strength.

Paresh H. Rana

Dedicated to,

My parents:

Mrs. Tulsiben Haribhai Rana

Mr. Haribhai Kaluji Rana

Table of Contents

List of Abbreviations

GHG: Green house gases

SR: Steam Reforming

SEM: Scanning Electron Microscopy

TEM: Transmission Electron Microscopy

XRD: X-ray Diffraction

FTIR: Fourier Transform Infrared Spectroscopy

TGA: Thermo Gravimetric analysis

EDX: Energy Dispersive Analysis

PPy: Polypyrrole

OSC: Oxygen Storage Capacity

EtOH: Ethanol

TPR: Temperature programmed Reduction

DFT: Density Functional Theory

SAED: Selected Area Electron Diffraction

FID: Flame Ionization Detector

TCD: Thermal Conductivity Detector

GHSV: Gas Hourly Space Velocity

WHSV: Weight Hourly Space Velocity

MWCNT: Multi Walled Carbon Nano Tube

List of Figures

List of Tables

List of Appendix

Chapter – 1

Introduction

CHAPTER – 1

Introduction

This chapter starts with introduction concerning dependency on fossil fuels, needs of new route and production of bioethanol from biomass and then describes the motivation for the study, objective of study, advantage of bioethanol oxidation and outline of thesis.

1.1 Introduction

The cost of various fuels and chemicals is largely governed by the cost of the raw material and the efficiency of the processes involved. Presently, majority of chemicals are produced from the fossil resources. Continuous depletion of available fossil fuels, uncertainty in price and soaring emission of GHG implies challenges to the future chemical industry. Furthermore to meet the increasing demand of bulk and fine chemicals, chemical industries have to find out an alternate way instead of depending on thinning amount of fossils oil. Worldwide, biomass is the fourth largest energy resources after coal, oil and gas that estimated to be about 14% of global primary energy [1]. Biomass is primary alternative compared to expensive fossil oil resources and also a source of sustainable energy, as it reduces GHG. Development of the conversion technologies promises the application of biomass at lower cost and higher conversion efficiency. It is possible to convert biomass derived chemicals to essentially high value commodity chemicals. There could be more advantages in using biomass as a feedstock compared with fossil resources, for example, in the chemical industry the introduction of oxygen functionalities into hydrocarbons can be rather difficult, whereas many products derived from biomass already contain some oxygen [2]. It is possible to produce some chemicals more easily and in few steps from biomass than from fossil resources. The use of biomass as a sustainable resource for production of fuels and commodity chemicals could offer an improved security in supply, since biomass can be grown in most parts of the world.

The oxidation of organic substrates leads to the production of various value added chemicals that are of great commercial and synthetic importance. Particularly, the oxidation of alcohols to carbonyl compounds is a fundamental transformation in organic chemistry as these compounds are widely used as intermediates for fine chemicals [3–5]. For oxidation of alcohols conventionally inorganic oxidants, such as permanganate and

dichromate are used. However, they are known to toxic in nature and produce a large amount of waste. The separation and disposal of this waste material increases cost in chemical processes. Hence, from both economic and environmental benign, there is a need for greener and more efficient methods that will replace traditional toxic oxidants. In this regards, many researchers have reported the use of molecular oxygen as an oxidant for alcohol oxidation using different catalysts [6,7]. With the growing concern towards green environment and uneven price of fossil fuels rose to biomass derived chemicals for production of value added chemicals. Bioethanol is one of such biomass derived chemical, which has high potential to be a sustainable feedstock for the production of commercial chemicals.

1.2 Motivation of the study

Presently, carbonaceous commodity chemicals such as acetaldehyde, acetic acid, ethyl acetate, butanol, acetone etc. are mainly produced from petrochemical sources, but due to a receding amount of fossil fuels, it is necessary to explore new routes. One possibility is to use renewable feedstock such as bioethanol. The production of bioethanol is growing, and it could be economically feasible to convert bioethanol into value added chemicals. Today, ethanol is mainly used in blending with fuel in limited extent and also attracted significant interest as a source for hydrogen production [8]. However, it appears much more feasible to use ethanol as a feedstock for chemical production from both an economical and green perspective. In addition, the demand for commodity chemicals is increasing, which further indicates that it is time to find alternatives to the fossil fuel. Furthermore the price of renewable feedstock is decreasing, whereas the price of fossil fuels is increasing making the ethanol route even more interesting.

The main concern of government regarding the mass production of industrial chemicals from fossil fuels is the environmental impact associated with their application which results in production of GHG. Therefore there is pressure to find more "green" processes for the production of bulk chemicals. For example, route to acetic acid production would be the fermentation of bioethanol, but thus far it seems that this is only cost effective for the production of vinegar not for acetic acid demand by the chemical industry due to small volume. A better route would be the direct oxidation of bioethanol to acetic acid under mild conditions using molecular oxygen (from air). This process would produce enough

acetic acid to meet the demand by the chemical industry, hence the process is facile and the starting materials are easy to get.

1.2.1 Availability of bioethanol

More than 80% of the world's energy consumption and production of chemicals originates from fossil resources. The use of fossil resources coupled with concerns about global warming, as mentioned earlier, results in a big drive to develop new technologies for the generation of energy and chemicals. In this respect, it has recently been considered that biomass could become a major source for the production of energy and chemicals [9].

Bioethanol can be obtained from the fermentation of biomass. It contains about 8-10 vol % of ethanol [10]. It can be concentrated up to 96 vol % by a distillation process [11]. The worldwide production of ethanol was 14.1 billion gallons in 2007 [12], which is reached 30 billion gallons in 2016 [13].

Bioethanol currently accounts for more than 94% of global biofuel production, and mostly of it comes from sugar cane. About 60% of the global bioethanol production comes from sugar cane as the resource and 40% from other agricultural crops. Brazil and the United States are world leaders, which exploit sugar cane and corn, respectively, and they together account for about 62 % of the world bioethanol production [14]. As far as concern to Indian scenario, ethanol production reached to 2 billion liter in 2017. We are importing around 600 million liter mainly from USA, Brazil and exporting around 140 million liter to South African countries. Biomass availability in India is estimated at upwards of 915 million metric tons which covers both agricultural (657 MMT/year) and 'forestry & wasteland' residues (260 MMT/year) [India, Biofuel Annual report, GIAN Report No. IN6088, 24/6/2016].

Bioethanol can be used as an alternative resource for producing chemicals like ethylene, acetaldehyde, butadiene, acetic acid, ethyl acetate etc. The products produced from bioethanol must obviously be more valuable than bioethanol itself for the process to be economically valuable. Instead of using bioethanol for transporting fuel purposes where it seems to have relatively low value nowadays, it could be instead be used as a feedstock for other important chemical products which have a much higher value.

World Ethanol Production
14.1 million gallons
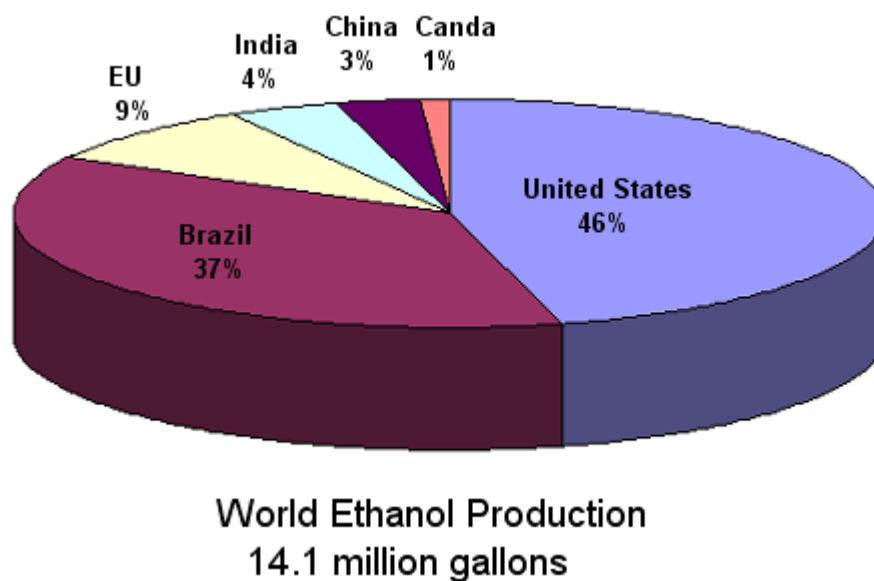
Figure1.1 Worldwide ethanol production [12]

1.2.2. Demand of commercial chemicals

The global demand of commercial chemicals, such as ethylene (production volume 20.3 x 10^6 ton in 2010), acetic acid (10^6 ton in 2011), acetaldehyde (approximately 10^6 ton in 2003), ethyl acetate (1.3 x 10^6 ton in 2004), hydrogen (60 x 10^6 ton in 2007), 1-3 butadiene (9 x 10^6 tonyear^{-1} in 2005) and butanol (3 x 10^6 ton in 2010) and estimated to grow considerably because of their commercial importance or direct involvement in production process as intermediates or (by) products [15].

Ethylene is the most produced organic compound on earth. It is mostly used in the production of polymers (e.g., polyethylene, polyvinylchloride), ethylene oxide, and ethylene glycol, etc. Ethylene is typically obtained from petroleum through thermal cracking, a process involving a complex chain of radical reactions. Processes involved in acetic acid production include methanol carbonylation and catalytic liquid phase oxidation of acetaldehyde and butane. Currently, most acetaldehyde is produced by the so called Wacker process through the direct oxidation of ethylene to acetaldehyde with a $PdCl_2/CuCl_2$ catalyst in water in the presence of air or other oxidants. Industrially, ethyl acetate is mainly produced by the esterification of acetic acid with ethanol. Hydrogen is

considered a very promising future energy source, as it has the highest energy density among all known fuels, with water being the only byproduct of its combustion. Currently, hydrogen is mainly produced by SR of nonrenewable hydrocarbons, such as methane [16]. Butanol is mainly produced by using the so-called oxo process, which consists of propylene hydroformylation followed by butylaldehyde hydrogenation to yield n-butanol. Butadiene is one of the most important bulk chemicals produced in the petrochemical industry. Two ways are mainly pursued for its industrial synthesis: isolation from naphtha steam cracker fractions of paraffinic hydrocarbons for the manufacture of ethylene and its higher homologues, or the catalytic and oxidative dehydrogenation of n-butane and n-butene [17]. All these processes derive their feed from the fossil based feedstock, oil or natural gas, the depleting sources.
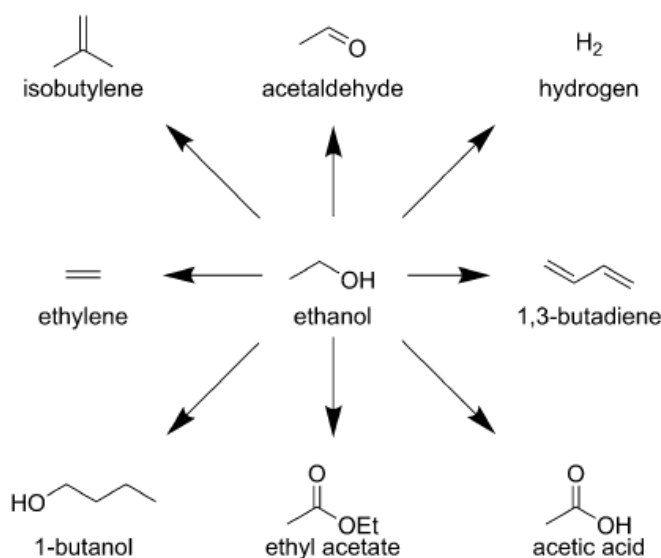
Figure1.2 A number of the important bulk chemicals that can be obtained from bioethanol

The production of bulk chemicals from biomass resources such as bioethanol is important for a number of reasons; firstly, it would limit the dependency on oil resources, thus bringing an immediate economic and strategic benefit. In addition, chemicals produced from biomass can, in principle, be CO_2 neutral and thus contribute to a solution to the important environmental issues.

1.3 Aims and objectives of the present study

The present work principally aims at bioethanol oxidation to value added products by means of liquid phase and gas phase reaction. Wet impregnation method is used for deposition of noble metals on the supports in the search of novel catalyst. The prepared catalyst is fully characterized by SEM, TEM, EDX, XRD, FTIR and TGA.

The specific objectives are:

i.   To study the effect of process parameters like temperature, O_2 pressure, ethanol concentration and time-on-stream.

ii. To evaluate the performance of noble metal over different supports for high conversion and selectivity for the reaction.

1.4 Outline of thesis

The thesis is organized as below,

Chapter 1 gives Introduction, motivation for study and aims and objectives of the present study.

Chapter 2 deals with the recent literature review on ethanol oxidation to different products with liquid phase and gas phase by employing various catalysts and brief on catalyst characterization techniques.

Chapter 3 describes the liquid phase catalytic oxidation of bioethanol using Au supported on various zeolite catalysts.

Chapter 4 comprises valorization of bioethanol to value added products by employing Au, Ag and Au - Ag over various oxides using gas phase oxidation.

Chapter 5 presents selective oxidation of bioethanol to acetaldehyde over Ag/CeO_2 catalyst; it also exploiting the lattice defects of support.

Chapter 6 shows influence of relative proportions of Ce and Zr in their mixed oxides on their catalytic performance for selective bioethanol oxidation.

Chapter 7 summarizes the work and evaluates the contribution of the present study.

References

[1] B.A. Statham, World Energy Council, Deciding the future: energy policy scenarios to 2050, World Energy Council, London, 2007.

[2] S.M. Tembe, G. Patrick, M.S. Scurrell, Acetic acid production by selective oxidation of ethanol using Au catalysts supported on various metal oxide, Gold Bull. 42 (2009) 321–327.

[3] J. Muzart, Palladium-catalysed oxidation of primary and secondary alcohols, Tetrahedron. 59 (2003) 5789–5816. doi:10.1016/S0040-4020(03)00866-4.

[4] J.S. Rafelt, J.H. Clark, Recent advances in the partial oxidation of organic molecules using heterogeneous catalysis, Catal. Today. 57 (2000) 33–44. doi:http://dx.doi.org/10.1016/S0920-5861(99)00308-9.

[5] T. Mallat, A. Baiker, Oxidation of Alcohols with Molecular Oxygen on Solid Catalysts, Chem. Rev. 104 (2004) 3037–3058. doi:10.1021/cr0200116.

[6] H.-B. Ji, J. Song, B. He, Y. Qian, Kinetic evidence for the mechanism of liquid-solid phase oxidation of alcohols, React. Kinet. Catal. Lett. 82 (2004) 97–103. doi:10.1023/B:REAC.0000028810.01091.80.

[7] K. Mori, T. Hara, T. Mizugaki, K. Ebitani, K. Kaneda, Hydroxyapatite-Supported Palladium Nanoclusters: A Highly Active Heterogeneous Catalyst for Selective Oxidation of Alcohols by Use of Molecular Oxygen, J. Am. Chem. Soc. 126 (2004) 10657–10666. doi:10.1021/ja0488683.

[8] G.A. Deluga, J.R. Salge, L.D. Schmidt, X.E. Verykios, Renewable Hydrogen from Ethanol by Autothermal Reforming, Science. 303 (2004) 993–997. doi:10.1126/science.1093045.

[9] N. Dimitratos, J.A. Lopez-Sanchez, G.J. Hutchings, Green Catalysis with Alternative Feedstocks, Top. Catal. 52 (2009) 258–268. doi:10.1007/s11244-008-9162-4.

[10] P. Lens, P. Westermann, M. Haberbauer, A. Moreno, Biofuels for Fuel Cells: Renewable energy from biomass fermentation, IWA Publishing, 2005.

[11] C.H. Christensen, B. Jørgensen, J. Rass-Hansen, K. Egeblad, R. Madsen, S.K. Klitgaard, S.M. Hansen, M.R. Hansen, H.C. Andersen, A. Riisager, Formation of Acetic Acid by Aqueous-Phase Oxidation of Ethanol with Air in the Presence of a Heterogeneous Gold Catalyst, Angew. Chem. Int. Ed. 45 (2006) 4648–4651. doi:10.1002/anie.200601180.

[12] S.L. Baier, M. Clements, C.W. Griffiths, J.E. Ihrig, Biofuels impact on crop and food prices: using an interactive spreadsheet, (2009). https://papers.ssrn.com/soL3/papers.cfm?abstract_id=1372839 (accessed February 8, 2017).

[13] J. Sun, Y. Wang, Recent Advances in Catalytic Conversion of Ethanol to Chemicals, ACS Catal. 4 (2014) 1078–1090. doi:10.1021/cs4011343.

[14] N. Sarkar, S.K. Ghosh, S. Bannerjee, K. Aikat, Bioethanol production from agricultural wastes: An overview, Renew. Energy. 37 (2012) 19–27. doi:10.1016/j.renene.2011.06.045.

[15] C. Angelici, B.M. Weckhuysen, P.C.A. Bruijnincx, Chemocatalytic Conversion of Ethanol into Butadiene and Other Bulk Chemicals, ChemSusChem. 6 (2013) 1595–1614. doi:10.1002/cssc.201300214.

[16] L. Barattini, G. Ramis, C. Resini, G. Busca, M. Sisani, U. Costantino, Reaction path of ethanol and acetic acid steam reforming over Ni–Zn–Al catalysts. Flow reactor studies, Chem. Eng. J. 153 (2009) 43–49. doi:10.1016/j.cej.2009.06.002.

[17] J. Grub, E. Loser, Ullmann's Encyclopedia of Industrial Chemistry, Wiley-VCH, Weinheim, 2012.

Chapter – 2

Literature review and Characterization techniques

CHAPTER – 2

Literature review and Characterization techniques

Catalysis is of tremendous importance for the chemical industry. Approximately two-thirds of the chemical products and ~ 90 % of the chemical processes involve catalysis (e.g., homogeneous, heterogeneous, or enzymatic type) [1]. Generally speaking, a catalyst is a substance that can speed up chemical reactions without itself being consumed in the reaction process; note that in some cases, a catalyst is used to slow down chemical reactions. The power of a catalyst lies in its capability in accelerating chemical reactions by reducing the energy barrier (i.e., activation energy) for the transition state and in controlling reaction pathways for selective synthesis of desired product.

Heterogeneous catalysis plays a major role worldwide, not only from the economic point of view, but it also provides the necessary infrastructure for well being of the society as a whole. It is hard to imagine what modern society would be like without chemicals, polymers, and pharmaceuticals, most of which are prepared industrially by catalytic chemistry. Without effective heterogeneous catalysis the manufacture of many materials such as, pharmaceuticals, foodstuffs etc. would not be possible. It is therefore not surprising; that heterogeneous catalysis is a subject that spans chemistry, chemical engineering and materials science in working together to break new ground. There is intense and broad interest in the design of new catalysts and as well as seeking to understand how these materials function as catalysts.

2.1 Catalytic oxidation of alcohols

Selective oxidation of alcohols is one of the most important transformations in organic synthesis. Although a number of methods have been developed for search of new facile, cost-effective and environmentally friendly procedures that avoid the use of large excess, toxic and expensive metal oxidants are required [2]. An attractive and promising alternative route is the direct oxidation of alcohols catalyzed by reusable heterogeneous solid catalysis, using molecular oxygen (O_2) [3]. The catalytic oxidation of alcohols with air has attracted significant attention as a "green" chemistry reaction in catalysis [4]. Molecular oxygen is a nonpoisonous and inexpensive oxidant for the oxidative

transformation of alcohols. Unlike inorganic oxidants that produce chemical wastes, heterogeneous catalysis can effectively use molecular oxygen to produce only water as side-products, and can be operated under mild temperature and pressure conditions. From a cost-efficiency point of view, supported catalysts have an advantage over homogeneous catalysts by being easily recoverable and they can be used in continuous flow regimes.

From a fundamental point of view, selective oxidation of alcohols is a topic of intense scientific interest; drawing attention from a very diverse group of researchers. So far, literature reports [5] that the selective oxidation of alcohols has focused primarily on oxidizing alcohols into:

- Aldehydes,
- Carboxylic acids or esters, and
- Oxidation of aldehydes to esters,
- Epoxidations of olefins,
- Activation of C–H bonds in alkanes,
- Oxidation of amines,
- Propene epoxidation and alkanes to alcohol

The catalysts used include mainly palladium, platinum, gold, ruthenium, multi component oxides and vanadium over different supports and have shown some promising results in alcohol oxidation. However these metal catalysts generally suffer from rapid deactivation due to leaching as a consequence of over oxidation of the metal active sites. One of the major problems associated with the use of these catalysts in oxidation reactions is product selectivity, since a broad range of products often exist at the end of reaction.

2.2 Ethanol oxidation

Ethanol can be easily produced from agricultural products by fermentation and thus can be considered a renewable resource. The annual amount of bioethanol produced currently 30 billion gallons in 2016 [6] and is increasing. In compared to global demand of commercial chemicals, such as ethylene, acetic acid, acetaldehyde, ethyl acetate, hydrogen, 1-3 butadiene and butanol as mentioned in chapter 1 [7] , a sufficient amount of bioethanol is produced to have a significant impact, even if only part of it is used as a chemical feedstock rather than a fuel additive [8]. Crude bioethanol contains only 8 - 10 vol %

ethanol [9], and thus purification of ethanol by distillation to produce a useful fuel is a very costly process. Consequently, an investigation aimed at determining whether bioethanol can be directly converted to value added chemicals, which could be less expensive to isolate industrially, is of great interest.

Ethanol oxidation to value added products has gain significant interest in last decades. As shown in Figure 1.2 (chapter 1), variety of chemical can be produced from bioethanol oxidation via liquid and gas phase reaction. Following section 2.3 and 2.5 describes literature review on liquid phase and gas phase oxidation of ethanol, respectively.

2.3 Liquid phase catalytic oxidation of ethanol

It has recently been shown that fine chemicals can be synthesized directly from aqueous phase oxidation of ethanol using noble metal as catalysts. The supported nanoparticles have attracted considerable attention recently as promising new materials for alcohol oxidation owing to their higher selectivity and activity. The considerable amount of work has been reported liquid phase ethanol oxidation using Au, Pd and Pt supported on $MgAl_2O_4$ support [4], Au/TiO_2 [10], Au supported on ZnO, TiO_2 and Al_2O_3 [11], Au/SiO_2 [12], Au/TiO_2 [13], $Ru(OH)x$ over TiO_2, Al_2O_3, $MgAl_2O_4$ and CeO_2 [14], Au/NiO [15], $PdO/m\text{-}ZrO_2$ [16] , Pt/Fe_3O_4 and Pt/C [17] catalysts.

Christensen et al. [4] were first to investigated ethanol oxidation (5 wt%) with molecular oxygen on noble metal catalysts in water. The catalytic performance of Pd, Pt, and Au was compared by depositing them on the same support, $MgAl_2O_4$. The results showed that all catalysts had the same catalytic activity, but the only difference was that the Au catalyst showed a high selectivity to acetic acid. They also reported that the highest yield of acetic acid can be achieved when ethanol is oxidized in aqueous phase at 150 ˚C and 30 bar. On Pd the first step to form acetaldehyde and the second step to form acetic acid proceed rapidly, whereas on Pt the first step is the fastest. In contrast, on Au deeper oxidation takes place. The second step to form acetic acid is the fastest and the direct complete oxidation to form CO_2 is also relatively rapid.

Christensen et al. [10] who have first developed $Au/MgAl_2O_4$ catalyst had investigated effect of supports. Au was loaded in different supports ($MgAl_2O_4$ and TiO_2) and results reported in the study showed that Au/TiO_2 also showed similar high catalytic performance

and proposed a kinetic model of ethanol to acetic acid. They also demonstrated that by varying the amount of water in reaction mixture, ethyl acetate can be produced. At lower ethanol concentration acetic acid is main reaction products; at concentrations >60 wt%, it is ethyl acetate.

Tembe et al. [11] extended studied of Au supported on three oxide supports, TiO_2, Al_2O_3 and ZnO. The result revealed that Au/ZnO showed catalytic activity equivalent to that of Au/TiO_2. While Al_2O_3 supported Au showed a somewhat poor performance in ethanol oxidation and evident leaching of Au into solution. Present of excess oxygen, increases the ethanol conversion and selectivity towards acetic acid. They also found that higher initial ethanol concentrations favor the production of ethyl acetate rather than acetic acid similar to Christensen et al. [10].

On the other hand, the size effect of Au nanoparticles has been discussed on SiO_2 support [12]. Au NPs with an average diameter of 5 nm showed higher activity than Au NPs with 3 and 10 nm. The kind of the metal oxide supports and the diameter of Au NPs mainly affect the catalytic activity of oxidation of aqueous ethanol.

Muhler et al. [13] performed 1 wt% and 1.5 wt% Au/TiO_2 for selective oxidation of aqueous ethanol solutions with air. They have studied the process conditions, such as temperature, pressure, catalyst concentration, ethanol concentration, reaction time and stirring rate in detail for both catalysts. They found that influence of pressure on reaction condition was negligible as long as there was an excess of oxygen. Increased amount catalyst has positive effects on ethanol conversion. The selectivity to acetic acid was high at high mass of catalyst and less mass led to higher amount of acetaldehyde. A higher ratio of $n(O_2)/n(ethanol)$ leads to higher conversion, while the selectivity to acetic acid is limited, presumably due to a higher tendency to total oxidation. A shortfall of oxygen led to a decrease in conversion and selectivity to acetic acid, and, at the same time, to an increase in selectivity to aldehyde and ester. High concentrations of ethanol and acetic acid favor the formation of ester.

Haruta and co workers [15] demonstrated use of Au/NiO as catalyst in ethanol oxidation in water by molecular oxygen. Here high conversion was achieved with NiO support in compared to other oxide supports. Further they checked effects of doping of other metal cations into NiO and found that Cu doping to the NiO support enhanced the semi

conductivity resulted in an improvement in the selectivity to acetic acid without the depression of the conversion of ethanol. In case of Fe doping catalytic activity was appreciably decreased with an increase in Fe molar percentage. Similar trend was observed for Co doping also.

PdO/Al$_2$O$_3$ and PdO/m-ZrO$_2$ catalysts were employed by Letichevsky et al. [16] in the selective oxidation of ethanol to acetic acid. PdO/m-ZrO$_2$ catalyst was found to be more active than PdO/Al$_2$O$_3$ due to the adsorption and spillover of the oxygenate species from m-ZrO$_2$ to PdO and vice-versa.

Long et al. [17] made use of Pt/Fe$_3$O$_4$@X (X = PPy, C or SiO$_2$) and catalytic properties of these catalysts were compared with the aerobic oxidations of ethanol to acetic acid. The conversion rates of ethanol oxidation catalyzed by Pt/Fe$_3$O$_4$@PPy, Pt/Fe$_3$O$_4$@C and Pt/Fe$_3$O$_4$@SiO$_2$ was 95%, 91% and 70% respectively.

2.4 Factors effecting alcohol oxidation

The metal particle size is considered to be of the principal importance for aerobic oxidation of alcohol [18]. For example, certain reactions reach an optimum activity and/or selectivity at larger particle diameters of the catalysts while other reactions show superior performance at smaller particle diameters. The shape and symmetry of the particle itself can influence the site population and geometry [19]. It has been shown that support may also play a key role in determining the catalytic activity and selectivity of the reaction [20,21]. Some studies have also shown that the addition of a base can highly affect the oxidation of alcohol [22].

2.4.1 Effect of metal oxides support

The properties of supported catalyst have been shown to depend very sensitively on a number of factors such as particle size; pretreatment, calcinations temperature and preparation method. The nature of support material and its physical state seem to play one of the critical central roles in Au catalysis [23,24]. Transition metal oxides are generally used as support in heterogeneous catalysis. The overall performance of a supported catalyst is highly dependent on the structure and properties of oxides support and the catalyst-oxide interface interactions [25,26]. A wide range of metal oxides and other materials have been studied as supports for various reactions in alcohol oxidation.

However there is still a lot of work needs to be done in order to understand how catalyst works in alcohol oxidation reactions.

Gorbanev et al. [14] have studied the loading effects of Ru(OH)x over TiO_2, Al_2O_3, $MgAl_2O_4$ and CeO_2 supports. Higher proportion lead to larger clusters on supports loosing the activity. Particularly with CeO_2 particles size were increased with increase loading of Ru, whereas for other oxides only minor changes occurred. High Ru loading resulted in decrease in catalyst activity as the larger particles cover the no. of active sites. The lower loading of Ru (0.6 Wt %) provided full conversion, while the conversion with higher (4.7 wt %) loading reached only about 50% for CeO_2. However, in case of $MgAl_2O_4$ lower loading of Ru did not significantly improve the results for oxidation. This could be due to the higher surface area of $MgAl_2O_4$ than CeO_2. Hence the variation in metal loading on $MgAl_2O_4$ did not affect the particle size.

Au supported on various support has been explored by various researchers for ethanol oxidation to acetic acid. Figure 2.1 gives the comparison for the ethanol oxidation to acetic acid using gold over various supports [4,10,11,13].

It is clear from Figure 2.1 that Au supported on TiO_2 and $MgAl_2O_4$ have the higher conversion of ethanol and higher selectivity to acetic acid at the reaction condition. Au/Al_2O_3 has shown the least selectivity towards acetic acid. This may be because of higher particle size (> 10 nm) and leaching of Au from Al_2O_3 support [11]. However after 25 h the conversions achieved were essentially identical for all four catalyst types [4,13].
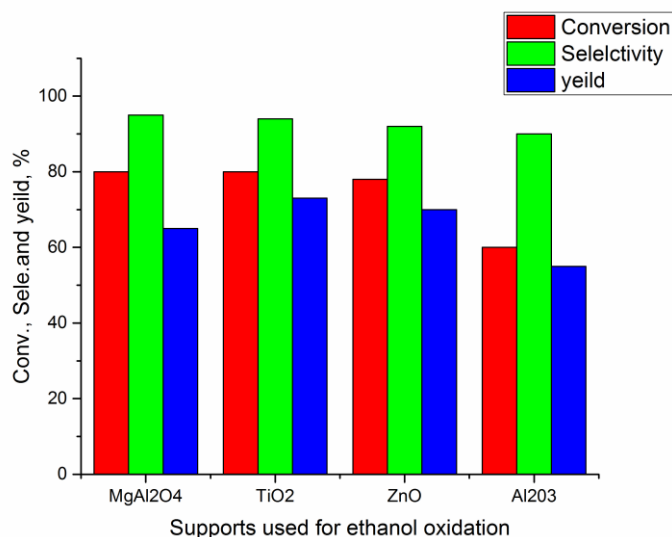
Figure 2.1 Reaction condition: 150 ˚C, 45 bar and 10 h reaction time

2.4.2. Effect of ethanol concentration

Conversion of ethanol and selectivity to acetic acid depends on the initial concentration of ethanol. The conversion and selectivity both decrease with increased initial concentration of ethanol [10,11,13]. At initial ethanol concentration (>40%), production of ethyl acetate become more evident. The yield of acetic acid decrease with increasing initial ethanol concentration (5 – 40 wt %), whereas the yield for acetaldehyde and ethyl acetate increase [11].

2.4.3 Effect of particle size

It has been shown both experimentally and theoretically that the activity of Au nanoparticles in the oxidation of CO increases with decreasing particle size and is strongly affected by the type of supports were used [27–29]. However, bulk Au has been employed in certain oxidation reactions as well indicating that, the presence of larger Au particles can be favorable for certain oxidation reactions [30].

Some studies have shown the effect of the size of Au particles in alcohol oxidation using CeO_2 and TiO_2 as supports for the aerobic oxidation of benzyl alcohol. The Au particle size prepared was in the range of 1.3 to 11.3 nm. The catalysts were then tested for aerobic oxidation of benzyl alcohol. The results showed that there was a huge effect of Au particle size in alcohol oxidation. The optimal activity was observed for the catalysts with an

average particle size of 6.9 nm, whereas smaller and bigger particles showed a poor activity. This behavior was observed irrespective of the support (CeO_2 or TiO_2) and of the reaction conditions applied [31]. Similar results were also reported by Zheng and Stucky for aerobic oxidation of ethanol using Au supported on silica [32]. Three SiO_2 – supported catalysts with 3.5, 6.3, and 8.2 nm Au particles were prepared by depositing the nanoparticles on silica gel from their corresponding chloroform solutions. The catalytic screening of the three catalysts was performed on ethanol oxidation at 200 °C using molecular oxygen as the oxidant. The results showed that Au particle size has a crucial role in alcohol oxidation as shown in Figure 2.2.
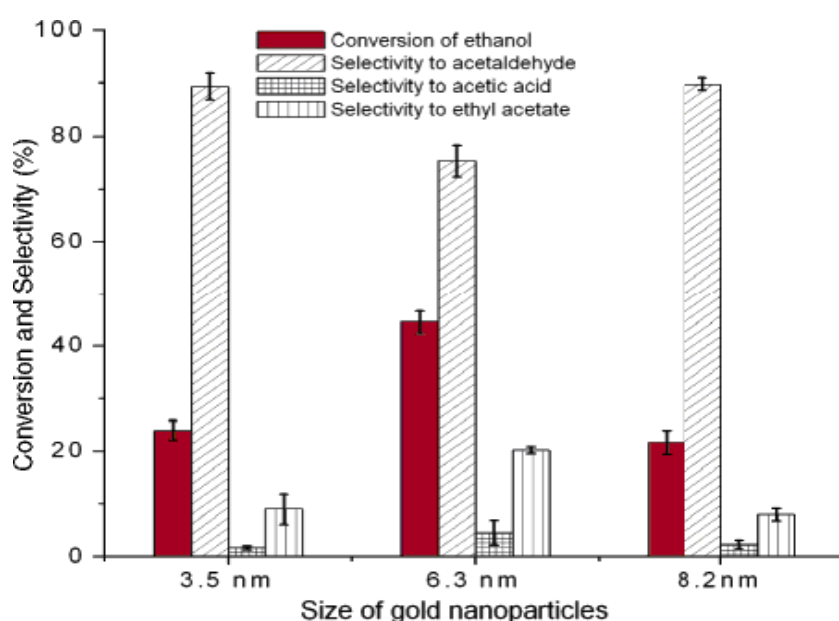
Figure 2.2 Different Au particles size supported on SiO_2, ethanol conversions and selectivity [32]

The catalytic study of three catalysts with different Au particle size showed that the smallest Au nanoparticles did not exhibit as high a catalytic activity as 6.3 nm Au nanoparticles displayed high catalytic activity (45% EtOH conversion). Both 3.5 and 8.2 nm nanoparticles showed lower ethanol conversions of 24% and 22% respectively [32]. Sun et al. [12] also reported the effect of Au particles size on ethanol oxidation using silica as support. The results showed that, Au particles with an average diameter of 5 nm had a high activity, about 3 times higher than that of smaller (3 nm), and 15 times higher than that of larger (10-30 nm) Au particles.

2.4.4 Effect of a base in alcohol oxidation

Prati and Rossi were the first to show that alcohols, specifically diols and sugars can be oxidized to the corresponding acids with Au catalysts but only when base is present [33,34]. A similar observation was also reported by Carretin et al. where 100% selectivity of sodium glycerate was observed in glycerol oxidation reaction when the reaction was carried out with an addition of NaOH [35]. In the absence of NaOH, no glycerol conversion was observed. The presence of a base is essential for some reaction to take place in alcohol oxidation, for example as shown in Figure 2.3 addition of 10% KOH promoted the oxidation of benzyl alcohol to methyl benzoate [22]. It has been shown that heterogeneous CeO_2 supported Au catalysts are able to oxidize several higher alcohols to their corresponding carboxylic acids using air as an oxidant [36].

The presence of small amount of base (KOH) promoted the reaction to give a higher yield of methyl benzoate. Less than 5% yield of methyl benzoate was observed when the base (KOH) was not added, but when the base was added the yield exceeded 80% as shown in Figure 2.3. On the contrary it was noted that catalysts such as Au/Ga_3O_9 can also perform aerobic oxidation of alcohols at room temperature without a base [37].
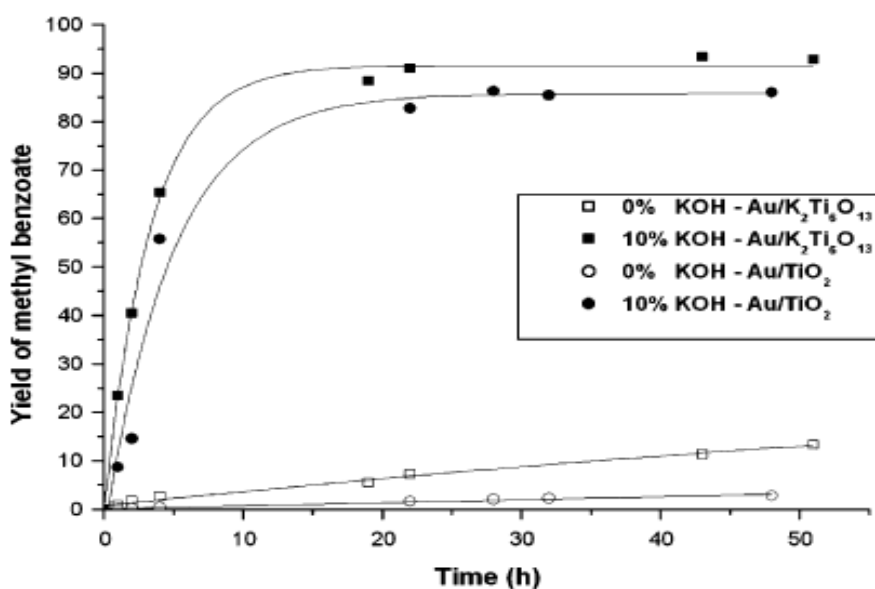
Figure 2.3 The effect of a base added in alcohol oxidation reaction[22]

The effect of having a base in alcohol oxidation is critical for some reactions to take place. Some reactions require a bit of a base to take place, while some do not need a base at all.

For example, for the oxidation of ethanol to acetic acid, no base is required [36,38]. In contrast to this, Zope et al. [39] reported that added NaOH enhanced the rate of oxidation of glycerol and ethanol.

2.5 Gas phase oxidation of ethanol

The gas phase oxidative dehydrogenation of ethanol has been considered as the most important process for the production of hydrogen, acetic acid, acetaldehyde, butanol, ethyl acetate, 1-3 butadienes etc. This process includes dehydrogenation of ethanol over various catalysts like, molybdenum based catalyst, copper-chromium supported catalyst, Palladium and Platinum based catalyst, vanadium catalysts, multi component oxides catalyst, gold based catalyst, silver based catalyst and bimetallic catalyst etc. Figure 2.4 shows reaction network for ethanol transformation in to value added products.
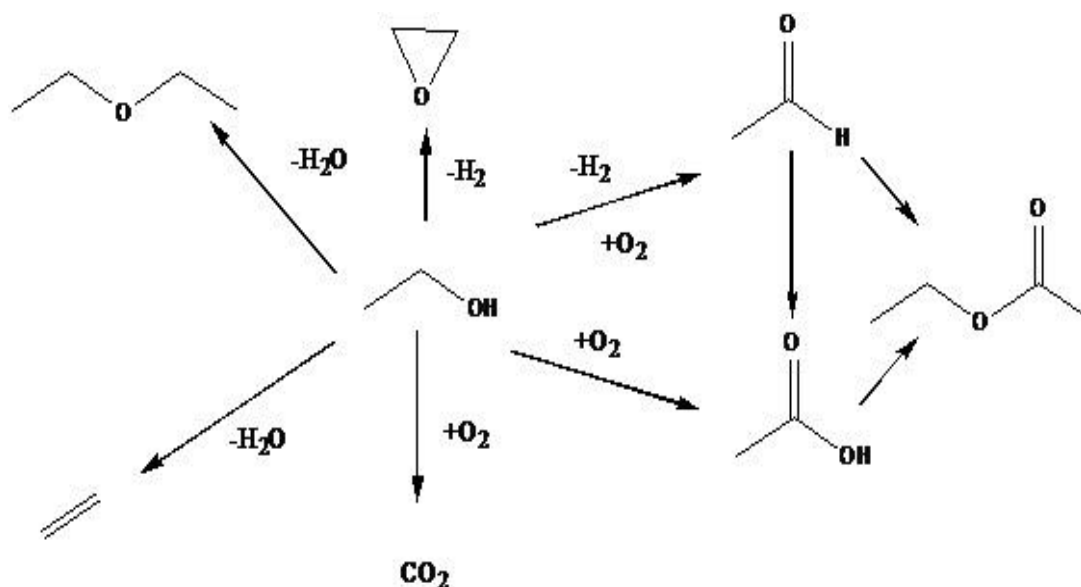
Figure 2.4 Reaction network involved in ethanol transformations

2.5.1 Platinum group metals

Palladium and platinum catalysts are active at lower temperatures (usually below 200 °C) than metal oxide catalysts. Ethanol oxidation over Pd/Al_2O_3 [40] and Pt/Al_2O_3 [41] results in the formation of partially oxidized compounds, such as acetaldehyde and acetic acid, as well as CO_2 at higher temperatures. Over PdO/SiO_2 ethyl acetate was produced with a selectivity of 60% together with acetaldehyde of 20% selectivity [42]. Higher selectivity to

ethyl acetate was obtained at higher oxidation rates, mainly at temperatures above 150 °C. When Pd and Pt were supported on CeO_2 [43] breaking of $C - C$ bond proceeds to form CO, CO_2 and CH_4. High selectivity to ethyl acetate (94.7 %) and ethanol conversion (98.6 %) were obtained over 2Pd/HY catalyst, while acetaldehyde selectivity of 89.0 % was achieved on PdO/HY at a low temperature as 150 °C [44].

2.5.2 Molybdenum based catalyst

Molybdenum based oxides constitute another important group of catalysts for gas phase oxidation of ethanol to acetaldehyde. SnO_2 (Tin dioxide) is the most popular supported Mo oxides for acetaldehyde production. Dispersed four-coordinated molybdates were thought to be the active phase which could also yield acetic acid [45]. At temperatures below 225 °C acetaldehyde was predominant, while at higher temperatures acetic acid exceeds acetaldehyde. Addition of water to feed decreased ethanol conversion and appreciably increased acetic acid production [46].

2.5.3 Vanadium oxide

In gas phase oxidation of ethanol vanadium oxide has been most often studied as major catalyst. Among metal oxide supports for V_2O_5, TiO_2 [47–49], Hydrotalcite, Al_2O_3, TiO_2 and SBA-15 [50], SiO_2, Al_2O_3 and ZrO_2 [51] have been used. TiO_2 was better than most of oxides systems such as hydrotalcite, Al_2O_3, SiO_2, SBA-15 and ZrO_2 in terms of higher selectivity to both acetaldehyde and acetic acid and ethanol conversion. This can be ascribed to (i) oxidation of ethanol mainly depend on the monolayer of the polymeric form of vanadium and they do not depend on the presence of the massive form of V_2O_5 [48] and (ii) oxidation of ethanol proceeds via the redox mechanism where the oxidized catalyst surface oxidizes the reactant and is reoxidized by gas phase oxygen. During the reaction on the V_2O_5/TiO_2 catalyst, titanium cations remain in the Ti^{4+} state, whereas V^{5+} cations undergo a reversible reduction under reaction conditions to V^{4+} and V^{3+} [49,51]. The best catalytic performance was demonstrated by V_2O_5/TiO_2 nanoparticle catalyst that allowed producing acetaldehyde by the gas phase oxidation of aqueous ethanol (50 wt %) at approximately 180 -185 °C with selectivity higher than 90% at a conversion of ethanol above 95% [47]. Furthermore, selectivity over 80% toward acetic acid could be achieved in this reaction at a low gas velocity at temperatures as low as 165 °C.

2.5.4 Copper based catalyst

Copper based catalysts are known to be active and selective for the dehydrogenation to acetaldehyde and ethyl acetate rather than acetic acid and CO_2. Cu/SiO_2 and Cu/ZnO at 160 °C yielded acetaldehyde and ethyl acetate as major products, while at higher temperature of 220 °C producing ethyl acetate with increased selectivities above 50% [52]. However the selectivity towards acetaldehyde was not satisfactory [52–54]. Cu nanoparticle supported on mesoporous carbon (MC) was an active catalyst for dehydrogenation of ethanol to acetaldehyde with excellent selectivity compared with Cu/SBA-15 due to their surface characteristic [55]. Furthermore, the use of carbon materials opens up new gates since the surface properties of a carbon support can be tailored to alter the selectivity and activity of the catalyst. Copper catalyst supported on nitrogen doped graphene materials has shown higher catalytic activity than Cu/SiO_2 owing to superior metal supports interaction and are also selective to acetaldehyde [56].

2.5.5 Multi component oxides

An interesting classical multi-component catalyst $Mo_{0.61}V_{0.31}Nb_{0.08}O_x$ was supported on TiO_2 which yielded > 90% of acetic acid at 100% ethanol conversion at elevated temperature and pressure (16 bar, 237 °C) with a feed of aqueous ethanol and oxygen [57]. Author also reported that presence of water increases acetic acid selectivity by inhibiting acetaldehyde synthesis more strongly than its oxidation to acetic acid, thus minimizing acetaldehyde concentrations and its conversion to COx. Kinetics for ethanol oxidation to acetic acid has also been proposed. In contrast to [57], a quaternary MoVNbTe catalyst [58] was found to be more efficient to yield acetic acid or mixture of acetic acid and ethyl acetate at atmospheric pressure. Further, the authors reported that presence of water is not essential to improve the selectivity of reaction as in case of $Mo_{0.61}V_{0.31}Nb_{0.08}O_x/TiO_2$.

2.5.6 Gold based catalyst

Since the pioneering discoveries were made by Hutchings, who predicted that Au would be the most active catalyst for ethylene hydro chlorination [59] and Haruta, who discovered that Au supported catalysts were very active for low temperature CO oxidation [60], there has been tremendous interest in Au - catalyzed oxidation reactions [3,61]. Ethanol oxidation has also been extensively studied by various researchers using Au based catalysts, among this work it was reported that if the reaction is taking place in aqueous

solution the formation of carboxylic acid was favored as the main product over the aldehyde, but in solvent-free experiments, aldehyde formation was favored as the major product [20]. Idriss et al. investigated the effect of temperature in the gas-phase oxidation of ethanol over Au/CeO_2 catalyst in the temperature range of 100-800 °C and study revealed that the product changed significantly with varying temperature [43]. At low temperature range acetaldehyde was the main product. Takei et al. studied support effects of Au catalyst on ethanol oxidation in gas phase. They found product selectivities highly depend on the type of supports. Au NPs deposited on acidic or basic metal oxides produced acetaldehyde with selectivities above 95% at temperatures above 200°C, while Au NPs on p-type semi conductive metal oxides were active for the complete oxidation to CO_2 and H_2O at temperatures below 200 °C. Au NPs on n-type semi conductive metal oxides produced both acetaldehyde and acetic acid [62].

Guan and Hensen [63] studied Au supported on several silica oxide supports (SBA-15, SBA-16, MCM-41, SiO_2 and SiO_2: Al) prepared by deposition precipitation and wetness impregnation method and evaluated their activity in absence and presence of oxygen for ethanol oxidation. In presence of oxygen dehydrogenation rate of ethanol was substantially higher compared to oxygen free case. The best catalyst performance was Au supported by MCM - 41, which gave a high conversion (60%) and selectivity of 90% to acetaldehyde at 250 °C. The Au/SiO_2 catalyst was found to be least among the catalysts activity (35% conversion) with the lower selectivity to acetaldehyde. The TOF study showed the completely different relation between TOF and Au NPs, where Au NPs with smaller than 7 nm size displayed a constant activity in absence of oxygen and particle size larger than 10 nm have a higher activity per surface atom in presence of oxygen. The results of this study clearly demonstrated that catalytic performance relies on the nature of support and particle size of Au.

The oxidation of ethanol has been investigated by Chen et al. [64] using zeolites (Si/Al = 360) supported on Au catalyst. They found that Au/ZSM5 catalyst pretreated by non thermal O_2 plasma method showed the best oxidative activity compared to low-temperature calcination in air and high-temperature reduction in hydrogen atmosphere. The characterization analysis from microscopy and XRD of Au/ZSM5 catalyst revealed that plasma pretreatment afforded a small Au particle size and a uniform dispersion of Au nanoparticles on ZSM5 surfaces. Characterization results further demonstrated that the

residual ammonia adsorbed on ZSM5 surfaces during the precipitation can be oxidized to nitrate ions by non thermal O_2 plasma treatment, while it converted to NO^+ by low-temperature oxygen calcination and was completely removed by high-temperature hydrogen reduction.

Mielby and co-workers demonstrated use of encapsulate Au NPs in zeolites silicate-1 (Au/Recryst-S1) for catalytic gas phase oxidation of bioethanol (10 wt %) and compared its performance with other three Au/silicate-1, Au/meso-silicate-1 and Au/APS- silicate-1 catalysts. They found that Au/Recryst-S1 was better in compared to other catalysts and obtained 50 % ethanol conversion with 98% selectivity to acetaldehyde and have high site-time yield of acetaldehyde. The outcome of work indicated the three-dimensional distribution and the structure of the Au support interfacial sites played a vital role in the reaction. However selectivity for acetaldehyde was decrease at temperature higher than 200 °C [65]. Later, Zhang et al. [66] have demonstrated solvent free synthesis of silicate -1 (S1) encapsulating Au-Pd bimetallic nanoparticles (Au-Pd@S1). They found that Au-Pd@S1catalyst achieved higher ethanol conversion (92.8%) and outperform the reported Au/Recryst-S1 catalyst [65]. They have also investigated the influence of water in bioethanol oxidation using Au-Pd@S1 and Au-Pd/S-1 (prepared by conventional hydrothermal route) and reported Au-Pd@S1 catalyst exhibited higher catalytic activity (82 % ethanol conversion) in compared to conventionally prepared Au-Pd/S-1 catalyst (2% ethanol conversion) in presence of 90% water. The activity of Au-Pd@S1 was due to the hydrophobicity of the S-1 zeolite, which enabled to efficiently separate the ethanol and water, hindering access of water to the Au-Pd particles in the zeolites micropores.

An investigation impact of TiO_2, SiO_2 and Al_2O_3 on Au NPs catalysts were carried out by Sobolev et al. [67], who reported an unusual behavior of Au/TiO_2 displayed "double peak" catalytic activity in gas phase oxidation of ethanol. In line of this study, further they investigated different Au loadings on a TiO_2 support and results obtained with Au loadings varying from 2 wt% to 7 wt% catalysts displayed two distinct temperatures dependent. The authors proposed that the formation of a specific active oxygen species at the catalytic sites on Au/TiO_2 being responsible for low temperature activity at 125 °C. The generation of the active oxygen species was assumed to be possible under mild conditions in the presence of hydrogen [68]. Surface O^- anion radicals, surface O_2^- superoxide anions, or peroxides were suggested as active species at low temperatures [68,69]. The sharp

decreased in activity was assumed to be due to the decomposition, desorption, or suppressed production of the highly active oxygen species at higher temperatures [67,68]. Strong deactivation due to the deposition of organic species on the catalyst surface via coking was proposed as well, as the initial catalytic activity was restored after an additional oxidative pre-treatment [67]. Even though oxygen is assumed to be needed as an intrinsic promoter of the dehydrogenation reaction the conversion of ethanol follows the non-oxidative pathway at high temperatures. In contrast to this, Muhler et al. [70] proposed that acetaldehyde formation following a Mars–van Krevelen mechanism at high temperature and this was due to the presence of highly dispersed Au nanoparticles on TiO_2 led to a higher reducibility of TiO_2 resulting in more oxygen vacancies and the created oxygen vacancies on TiO_2 act as active sites for the reaction.

The effect of bimetallic Au-Ir NPs catalysts was reported for the oxidation of ethanol with O_2 as oxidant under solvent free conditions at temperature range of 180 °C. Guan and Hensen [71], investigated the effect of synthesized bimetallic Au:Ir supported by SiO_2 prepared by impregnation method and they found that this catalyst has apparent higher activity for the reaction than both monometallic Au/SiO_2 and Ir/SiO_2 over the period of the reaction time; with $Au(26)Ir(74)/SiO_2$ being the most active. With increasing Au content, the conversion decreases slightly but with a concomitant increase in the acetaldehyde selectivity. The selectivities for the Au–Ir bimetallic catalysts were typically above 90% and higher than the selectivity of the Ir catalyst. The results indicated that an intimate contact between Au surface sites for (dissociative) ethanol adsorption and Ir sites covered by O adatoms which catalyze C–H bond cleavage to yield acetaldehyde.

Later on, Redina et al. [72] employed $Au-Cu/SiO_2$ catalyst with different metal loading prepared by redox method for gas phase oxidation of ethanol. The characterization analysis of $Au-Cu/SiO_2$ catalyst by TPR, EXAFS and STEM reveled that introduction of Au NPs directly on the surface of copper oxide or Cu^{2+} species was feasible by redox method. It was observed that with low-loaded bimetallic Au-Cu catalysts highest catalytic activity with almost full conversion and 100% selectivity to acetaldehyde in ethanol oxidation was achieved. The catalyst system with Au:Cu atomic ratio of 1:3 was found to have noticeable synergetic effect of the Au-Cu interaction in comparison with the monometallic samples having the same Au or Cu loadings. The formation of by product CO_2 was observed when the reaction was performed at temperature higher that 300 °C at

the cost decreased selectivity to acetaldehyde. Table 2.1 shows ethanol conversion and selectivity towards acetaldehyde using Au NPs immobilized on different supports in gas phase reaction.

Table 2.1 Ethanol conversion and selectivity towards acetaldehyde using Au NPs immobilized on different supports.

Catalyst	X,%	S,%	Reaction condition (T = °C, P = atm, O_2/ethanol)	Ref.
Au/MCM-41	60	90	250, 1, 2	[63]
Au/ZSM5	30	75	250, 1, 2	[64]
Au/silicate -1	50	65	250 ,1, 1	[65]
Au-Pd/silicate -1	100	0	250, 1 ,60	[66]
Au/TiO$_2$	95	40	250, 1, 9	[67,69,73]
Au/TiO$_2$	50	50	250 ,1, 1	[70]
Au/MgCuCr$_2$O$_4$	95	97	250, 1, 3	[74,75]
Au/Al$_2$O$_3$	80	10	250, 1	[62]
Au-Ir/ SiO$_2$	100	90	250 ,1, 1	[71]
Au-Cu/SiO$_2$	100	95	250, 1, 1.2	[72]

2.5.7 Silver based catalyst

Among the group IB metals, Ag based catalyst is least studied for ethanol oxidation, although catalytically active Ag is used in ethylene oxide synthesis, industrially. Chen et al. [76] investigated Ag-hollandite catalyst prepared by hydrothermal synthesis method and reported high catalytic performance for ethanol oxidation, with ethanol conversion of 100% and acetaldehyde selectivity of 71 % at 250 °C. Authors attributed high activity; selectivity and stability were due to the presence of Ag^+ species which facilitated the activation of molecular oxygen and its transfer to oxidize ethanol through the Ag-O-Mn bridge and was also due to the unique morphology of the Ag-hollandite nanofibers. The X-ray photoelectron spectroscopy surface analysis revealed that the Ag species presented as Ag^+.

Li and co-workers [77] used nanoporous Ag catalyst in oxidation of ethanol was fabricated by the selective leaching of magnesium from a $Ag_{77}Mg_{23}$ alloy foil by using an aqueous solution of tartaric acid (1 wt %) for 1 h at room temperature and found that dealloyed np-Ag-1 (25 nm) demonstrated higher conversion (85%) than np-Ag-2 (50 nm, 75% conversion), thus indicated that a smaller size of the pore of np-Ag was conducive to the oxidation reaction.

Ag-containing ceramic catalysts modified or unmodified with Zr and Al were studied in selective catalytic oxidation of ethylene glycol and ethanol into the corresponding carbonyl compounds in oxygen rich environment by Vodyankina et al. [78]. They reported that Ag-containing ceramic catalysts showed high catalytic efficiency in selective ethanol oxidation to acetaldehyde (ca. 95% yield at 250 °C). The support phase composition does not have any significance influence either on the conversion of ethanol or on the yield of acetaldehyde and these can due to the participation of Fe-containing additives in the process of selective ethanol oxidation over Ag particles. Also, in the case of diol oxidation, adsorption of ethylene glycol on Fe-containing sites was observed which led to the decrease in selectivity with respect to glyoxal and the same was not observed during the ethanol oxidation into acetaldehyde.

Crystalline and silica-supported OMS-2 catalysts with and without the addition of Ag were prepared using co-precipitation, impregnation, and consecutive impregnation techniques and tested in the gas-phase selective oxidation of ethanol to acetaldehyde by Dutov et al. [79]. The characterization results showed that the preparation method influenced the localization of Ag for both the crystalline and supported catalysts and consequently the samples had different active sites. The interaction of Ag with MnO_2 improved both reducing and reoxidation abilities of the samples, resulting in higher activity of the Ag containing catalysts. However, the selectivity to acetaldehyde sharply decreased with increased reaction temperature due to the total oxidation process. On the other hand, formation of Ag-MnOx sites in the supported catalysts by introducing of Ag ions into the channels of the OMS-2 was favorable for oxidation rate, while formation of Ag/MnOx interfaces did not improve conversion of ethanol compared to the Ag/SiO_2 catalyst. The use of silica support for the Ag/OMS-2 composites allowed improving the selectivity toward acetaldehyde in an extended temperature range and increased the yield of acetaldehyde in comparison with the crystalline samples.

Xu et al. [80] used Ag/hydroxyapatite foam (HAp) synthesized by incipient wetness method and evaluated their activity for selective oxidation of ethanol. They have also carried out kinetic study of the reaction. Results of characterization using in-situ and ex-situ XPS, HRTEM and TPSR revealed that metallic Ag nanoparticles stabilized well on the HAp surface during the reaction and adsorbed oxygen played an important role in the reaction. Ag/HAp showed 18 % ethanol conversion with 100 % selectivity to acetaldehyde at 275 °C. Further, raising the temperature resulted to decreased selectivity steadily by the production of CO_2. Moreover, the catalyst showed higher stability (time-on-stream 100 h) with ethanol conversion (15 %) and selectivity (95 %) towards acetaldehyde at 275 °C. The density functional theory (DFT) calculation suggested that ethanol molecules are first weakly adsorbed on Ag (111) and then dissociate to form ethoxy (CH_3CH_2O) and hydroxyl species through an oxygen assisted dehydrogenation mechanism. This indicated that ethanol dissociate in the presence of chemisorbed oxygen atom. The formation of acetaldehyde was completed in presence of chemisorbed oxygen by abstracting a hydrogen atom from ethoxy.

Freitas et al. [81] investigated the loading effect of Ag in the 10 wt % Cu/ZrO_2 performance in ethanol conversion. They found that that increased loading of Ag from 0.3 wt % to 2 wt % led to decrease Cu^0/Cu^+ ratio and also leads to reduced Zr surface. Higher loading of Ag led to decrease activity, whereas acetaldehyde selective increased and for ethyl acetate decreased compared to 10 wt % Cu/ZrO_2. These change in selectivity attributed to the presence of Ag led to enhance Cu^+/Cu^0 ratio makes the catalyst less favorable for ethyl acetate.

The synopsis of the important parameters of the previous literature for ethanol alcohol oxidation suggests that Au supported catalysts is superior to other reported catalysts in catalytic performance and stability. Moreover, the method of synthesis these catalysts are crucial as the important aspect of these catalysts is the size of metal nanoparticle, which affect on the catalysts performance. However, selecting the right support is important as it distributes the particles and the nature of support can effect on catalyst selectivity.

2.6 Oxidative dehydrogenation reaction mechanism

Oxidation is a key reaction in organic synthesis and play a significant role in the development of value added chemicals from biomass. The application of heterogeneous

catalyst and molecular oxygen to oxidation reactions offers a green alternative to traditional, toxic chemical oxidants [38]. The selective oxidation of alcohols to carboxylic compounds over heterogeneous recyclable catalysts is an important process in green organic chemistry. Most efforts in recent years have focused on the aerobic oxidation that uses molecular oxygen as oxidant generating water as the only byproduct, and good results have been obtained with metal based catalysts containing Ru, Ag, Cu, Au, Pt or Pd as discussed in section 2.4 and 2.5.

Oxidative dehydrogenation (ODH) is a process that occurs without any participation of hydrogen and leads to the removal of two hydrogen atoms from the original molecule as water in the presence of oxygen. The original molecule is converted into an unsaturated one.

Different studies agree that the mechanism for aerobic ethanol (CH$_3$CH$_2$OH) oxidation starts with activation of either C–H or O–H bond of ethanol which led to formation of ethoxide (CH$_3$CH$_2$O) followed by removal of β-H from ethoxide to produce acetaldehyde (CH$_3$CHO). Further oxidation of acetaldehyde produces acetic acid (CH$_3$COOH).

Studies of ethanol oxidation over Pt and Pd electro catalysts suggest that C–H activation occurs via the oxidative insertion of the metal into the C–H bond to form hydroxyethylidene (CH3CH*OH) and hydride (H*) surface intermediates [82] as shown in eq. (2.1). However, studies in the heterogeneous catalysts report that alcohol oxidation proceeds via the initial activation of the O–H bond to form ethoxide and H* surface intermediates [38,63,83–85] as shown in eq. (2.2).

$$CH_3CH_2OH^* \rightarrow CH_3CHOH^* + H^* \rightarrow CH_3CH = O^* + 2H^* \qquad (2.1)$$

$$CH_3CH_2OH^* \rightarrow CH_3CH_2O^* + H^* \rightarrow CH_3CH = O^* + 2H^* \qquad (2.2)$$
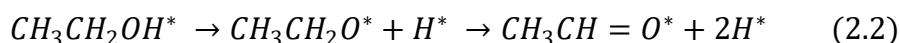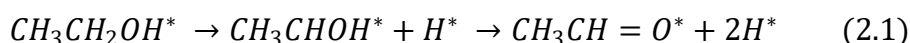
Acetaldehyde oxidation to acetic acid can proceed via most common acetyl (CH3CO) route eq. (2.3) and intermediate (CH$_3$CH(OH)O) eq.(2.4), which can be formed on the surface as well as in the solution [82,86,87].

$$CH_3CHO^* + OH^* + * \rightarrow CH_3O^* + H^* + OH^* \rightarrow CH_3COOH + H^* \quad (2.3)$$

$$CH_3CHO^* + OH^* \rightarrow CH_3CH(OH)O^* + * \rightarrow CH_3COOH + H^* \qquad (2.4)$$
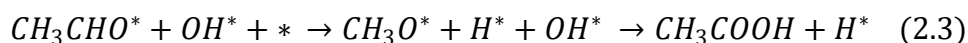
Qingsen et al. [84] have examined reaction pathways for selective oxidation of ethanol on the Au (111) surface via a comprehensive periodic DFT calculations. Authors have suggested three different reaction routes for oxidation of ethanol to ethoxy: (i) dissociation of ethanol to ethoxy, (ii) O-assisted activation of ethanol to ethoxy, and (iii) OH-assisted activation of ethanol to ethoxy. They have found that the diffusion for most of the surface species is rapid and facilitates the reactions leading to selective oxidation where presence of surface oxygen adatom is essential in the O–H bond activation of ethanol. They also showed that activation barrier of the β–H elimination of ethoxy is higher than activation of ethanol and formation of ethyl acetate and formation of the acetic acid is not facile through the reaction between the adsorbed O atom and acetaldehyde due to the high activation barrier.

Guan and Hensen [63] have also demonstrated that dehydrogenation of alcohols proceed via the initial cleavage of the hydroxyl bond, resulting in adsorbed alkoxide and hydrogen intermediates, followed by the removal of a β –H atom from adsorbed ethoxide to produce aldehyde. They concluded from infrared spectroscopy investigation that the first step is easier than the second and β –H removal is the rate limiting step which is in consistent with previous reported by Qingsen et al.[84]. They also observed that in the presence of oxygen, activity of ethanol dehydrogenation is considerably higher than in its absence and subsequent surface science studies have shown that co-adsorbed oxygen on late transition metals acts as a Brønsted base to facilitate O–H bond cleavage.

Xu et al. [80] have also postulated three way mechanisms for ethanol adsorption using Ag(111) surface as for ethanol oxidation, (a) an oxygen-assisted dissociative adsorption, (b) a hydroxyl-assisted dissociative adsorption, and (c) direct dehydrogenation without any assistance. They found that CH_3CH_2OH molecules are adsorbed on Ag(111) and then dissociate to form CH_3CH_2O and OH species with lower barrier through an oxygen-assisted dehydrogenation mechanism which indicates that ethanol can readily dissociate in the presence of chemisorbed oxygen atom. Also the formation of CH_3CHO abstracting H atom from CH_3CH_2O occurred with chemisorbed oxygen having reaction barrier 38.6 kJ/mol which was low in compared to 62.7 kJ.mol offered by OH assisted dissociative adsorption and 46.3 kJ/mol without any assistance. Therefore, they claimed that oxygen-assisted dehydrogenation mechanism favored for this reaction.

Presence of surface oxygen enhanced rate of ethanol oxidation further confirmed by Maihom et al. [85]. They performed DFT calculations over Au exchanged ZSM-5 with and without surface oxygen. They found that for Au/ZSM5 and Au-O/ZSM5 dissociation of the O−H bond is the rate-determining step which is contrast to earlier reports [63,84], where β –H removal was the rate limiting step . Activation barrier of the O−H bond on the Au site for Au-O was found to be very less (9.0 kcal/mol) as compared to Au/ZSM5 (43.0 kcal/mol). They reasoned that this was due to assistance of active oxygen on Au for the O−H bond dissociation. Surface oxygen facilitates ethanol O−H bond dissociation and ethoxide species formation and causes them to become both kinetically and thermodynamically favorable.

In contrast to these, Zope et al. [39] showed that OH species are directly involved in the oxidation of ethanol and glycerol to their corresponding carboxylic acids over Au and Pt catalysts in basic aqueous media. The process was suggested to proceed first through Au catalyzed partial oxidation to generate the corresponding aldehydes which further oxidized to corresponding acid. They investigated that oxygen from water was participated in the reaction. For this, they carried out experiments with isotopically labeled water ($H_2^{18}O$) and molecular oxygen ($^{18}O_2$). Mass spectroscopy results revealed that ^{18}O of water was incorporated in product They also suggested that O_2 acted to scavenge electrons from the Au particles after oxidation of alcohol had occurred via a hydroxyl species, regenerating the hydroxyl and closing the catalytic cycle.

Later, Hibbitts and Neurock [82] examined Pd catalyst for selective oxidation of ethanol and found that OH species act as Bronsted bases which abstract protons from the hydroxyl groups of adsorbed or solution phase alcohols. They have reported mechanism is consistent with the mechanism reported previously for Au-catalyzed alcohol oxidation [39]. Table 2.2 shows the activation barriers for ethanol oxidation calculated over Au (111), Pt(111) and Pd(111) in water

Table 2.2 Activation barriers for ethanol oxidation calculated over Au (111), Pt (111) and Pd (111) in water

Step	Reaction	Au(111) E_{ACT}	Pt(111) E_{ACT}	Pd(111) E_{ACT}
1	$CH_3CH_2OH* + * \rightarrow CH_3CH_2O* + H*$	204	116	106
2	$CH_3CH_2OH* + OH* \rightarrow CH_3CH_2O* + H_2O*$	22	18	0
3	$CH_3CH_2O* + * \rightarrow CH_3CHO* + H*$	46	15	50
4	$CH_3CH_2O* + OH* \rightarrow CH_3CHO* + H_2O*$	12	24	75
5	$CH_3CHO* + OH* \rightarrow CH_3CHOOH* + *$	5	5	24
6	$CH_3CHOOH* + * \rightarrow CH_3COOH* + H*$	21	13	11
7	$CH_3CHOOH* + OH* \rightarrow CH_3COOH* + H_2O*$	29	17	38

The * represents a catalytic site on the surface. All values in kJ mol^{-1}, Au (111) and Pt(111) [39] and Pd(111) [82]

On other hand, Li et al. [57] , Jiang et al. [88] and Holz et al. [70] have proposed Mars van Krevelen mechanism for ethanol oxidation. According to the Mars van Krevelen mechanism, the surface itself is an active part in the reaction. In this mechanism, the oxidation of reactants occurs by two sequential steps, (i) reactant molecule initially reduces an oxidized oxide surface site and (ii) then the reduced surface site is subsequently reoxidized with oxygen that comes from the catalyst itself, the lattice oxygen in this case, and not from gas phase molecular O_2 (Langmuir-Hinshelwood mechanism). When the reaction product desorbs, a vacancy is left behind in the surface. The vacancy is now filled again by a reactant atom from the bulk, rather than directly by the gas phase. As a matter of fact, whether the vacancies are filled by the bulk or the gas phase is still a subject of intense debate in the catalysis community, even though this difference does not influence the relevant processes within the reaction mechanism itself. Below Table 2.3 shows elementary steps for ethanol oxidation derived from Mars van Krevelen mechanism. Where O* represents lattice oxygen, *OH denotes hydroxyl group, * represents a reduced metal center, consisting of an oxygen vacancy in the reducible mixed oxides, CH_3CH_2O* is an ethoxide species attached to a Mi cation (C_2H_5-O-Mi), and CH_3CHO* and CH_3CHO_2* are adsorbed acetaldehyde and acetic acid species, respectively [57,88].

Table 2.3 Elementary steps for ethanol reaction derived from Mars van Krevelen mechanism

Step	Reaction	
1	$CH_3CH_2OH* + O* + *$	$\rightarrow CH_3CH_2O* + *OH$
2	$CH_3CH_2O* + O*$	$\rightarrow CH_3CHO* + *OH$
3	CH_3CHO*	$\rightarrow CH_3CHO + *$
4	$CH_3CHO* + O*$	$\rightarrow CH_3CHO_2* + *$
5	$CH_3CHO_2* + *$	$\rightarrow CH_3COOH + *$
6	$*OH + *OH$	$\rightarrow H_2O + O* + *$
7	$O_2 + * + *$	$\rightarrow O* + O*$

Therefore, no general consensus has been reached on the type of hydrogen involved in the initial deprotonation of ethanol. Whether this rate-determining step is the surface reaction between chemisorbed ethanol and oxygen or β –H elimination of ethoxide is not yet clear.

2.7 Catalyst characterization technique

Many characterization techniques have been used in catalysis research, with the intent to cover the reactant mechanism and analyze the catalyst composition and look at catalyst behavior [89]. In this section, a brief introduction to the theory and principle of various characterization techniques employed in the present study are discussed.

2.7.1 X-ray powder diffraction (XRD)

2.7.1.1 Background

Powder X-ray diffraction is commonly used tool to identify and measure the uniqueness of structure, phase purity, degree of crystallinity and unit cell parameters of crystallite materials. The XRD patterns are recorded by the measurements of the angles at which the X-ray beams are diffracted by the sample. The relation between the distance between two *hkl* planes *(d)* and angle of diffraction (2θ) is given by Bragg's equation as follows (eq. 2.5):

$$n\lambda = 2d \sin\theta \ldots\ldots\ldots\ldots (2.5)$$

Where λ = wavelength of X-rays, n= an integer known as the order of reflection (*h, k,* and *l* represent Miller indices of respective planes) [90,91]. The diffraction patterns provides various information like planes of material, phase purity, degree of crystallinity, and unit cell parameters of material [92]. The identification of phase is based on a comparison of a set of reflections of the sample with that of pure reference phases distributed by International Center for Diffraction Data (ICDD). Unit cell parameter (a) of a cubic lattice can be determined by the following equation (eq 2.6):

$$a = d_{hkl}(h^2 + k^2 + l^2)^{1/2} \ldots\ldots\ldots\ldots\ldots\ldots. (2.6)$$

where d = distance between two consecutive parallel planes having Miller indices h, k, and l [90].

2.7.1.2- Experimental

In this study, powder X-ray Diffraction (XRD) analysis was performed on a Bruker - D8 Discover equipped with Ni-filtered Cu Kα radiation source (λ = 1.542 Å) 40 kV and 30 mA. The diffractograms were recorded in the 2θ range of 20 - 90° with a 2θ step size of 0.02° and a scanning speed of 6° min^{-1}.

2.7.2 Electron microscopy (SEM, EDX and TEM)

2.7.1.2 Background

Scanning electron microscopy (SEM) is well known techniques for characterization of catalyst. In this technique electrons are employed as an alternative source of light to generate the image. It is technique just not provides only topology of the catalyst but combined with energy –dispersive X-ray spectroscopy (EDX), chemical composition of catalyst can also be determined. Generally electrons beam are produced by a metallic filament cathode. The filament heated in vacuum by a passing a voltage on it. Due to high melting point and lowest vapor pressure of tungsten, it is mostly used as filament. Filament generated electrons interact with atoms of the sample which producing a signals. These singles bear various information of the sample regarding to its topography and chemical composition. The electron beam is typically scanned in raster pattern. The interaction between primary beam of electrons and samples, originates two types of electrons, (i) generated from sample surface known as emitted electrons and (ii) secondary

electrons describes as reflected electrons due to emission of electromagnetic radiation (characteristic X-rays) and other photons of various energies. The emitted electrons from the sample have high electron energy and are called backscatter electrons (BSE), which mainly used for showing the contrast in chemical components. Secondary electrons are reflected electrons have low energy than the backscatter electrons as a result of the inelastic interaction of the primary beam with the sample where significant energy loss was occurred. However a secondary electrons detector collects these electrons. Both electrons secondary and backscatter are converted to a signal then sent to a viewing screen. As a result, high resolution topographical images can be obtained in this detection mode. SEM is non-destructive to samples although some electron beam damage is possible. SEM scans over a sample surface with a probe of electrons (5-50 kV) and detects the yield of either secondary or back scattered electrons as a function of the position of the primary beam. Magnification of 10-500,000 times is possible with a resolution of about 1 nm [93].

Energy dispersive X-ray spectroscopy (EDX) also known as EDS, EDXS or XEDS or called energy dispersive X-ray analysis (EDXA) or energy dispersive X-ray microanalysis (EDXMA). It is alternative and useful analytical technique to characterize the chemical composition or element analysis of catalysts. The high energy beam of electron is focused on the sample to stimulate the characteristic emission of X-ray from the sample. The focused beam can excite inner electron. The hole is generated where electron was ejected. The vacate electron hole refills electron from higher energy level. As a result, difference in energy between higher and lower shell released in the form of X-ray which can be qualitative and quantitative measured by energy dispersive spectrometer [94].

Transmission electron microscopy (TEM) is a very powerful tool in the catalyst and material science fields. It determines size, shape and composition of the catalyst. It works on the principle of light microscope using electrons instead of light. Small wavelength of electrons enables high resolution. In the TEM the electrons beam is transmitted through thin film and interacting with specimen. The electrons that transmit through the sample are magnified by electromagnetic lenses and then hit a fluorescent screen are generate the TEM image. Based on atom density metals generally have a higher electrons density than supports, therefore they appear darker in the TEM image. Selected area electron

diffraction (SAED) technique can be done inside the TEM. It is similar to XRD and useful to determine crystal structure [95].

2.7.2.2 Experimental

In this study, surface morphology of the catalyst and chemical composition were investigated with scanning electron microscopy (SEM) and energy dispersive x-ray analysis (EDX) using JEOL make model 7600F FESEM. Transmissions electron microscopy (TEM) images of the catalyst were recorded on a Philips CM 200 microscope operating at 200 kV. The samples were dispersed in ethanol and kept in an ultrasonic bath for 20 min, then deposited on a carbon covered copper grid for each measurement.

2.7.3 Fourier transform infrared spectroscopy (FTIR)

2.7.3.1 Background

Fourier transform infrared (FTIR) spectroscopy deals with the vibration of chemical bonds in a molecule at various frequencies depending on the elements and types of bonds. After absorbing of infrared radiation the frequency of vibration of a bond increases leading to transition between ground state and several excited states. These absorption frequencies represent excitations of vibrations of the chemical bonds and thus are specific to the type of bond (stretching or bending vibration) and the group of atoms involved in the vibration. The obtained infrared absorption bands in the range of 400 - 4000 cm^{-1} are the characteristic for the functional group present in the catalyst. The term Fourier transform (FT) deals a mathematical process to convert data from interference pattern to an infrared absorption spectrum [96].

2.7.3.2 Experimental

In this study, Fourier Transform Infrared Spectroscopy (FTIR) spectra of catalyst samples were collected in reflection mode using ZnSe optics in Bruker Alpha Eco-ATR spectrometer. The instrument was operated in the range of cm^{-1}.

2.7.4 Thermo gravimetric analysis (TGA)

2.7.4.1 Background

Thermo gravimetric analysis (TGA) is a method to evaluate the weight loss of catalyst with increasing temperature. It is a highly sensitive technique, which provides information about the weight percentage of moisture, volatiles and solvent in samples. It is carried out by placing the sample in a weighing balance and heating the sample at a controlled rate. The weight loss is studied in various ambient atmospheres such nitrogen or air [97]. From weight lost of catalyst, the oxygen storage capacity (OSC) of the material can also be determined which may be playing a significant role to enhance the catalytical activity.

2.7.4.2 Experimental

In this study, Oxygen storage capacity (OSC) was measured by thermo gravimetric analysis (TGA) on a Mettler Toledo TG-SDTA apparatus. OSC measurement was carried out for specimen with heating and cooling cycles. Firstly, the sample was heated from ambient temperature to 800 °C under N_2 flow, then cooling to 150 °C in dry air and again heating to 800 °C in N_2 environment. All heating and cooling rates were 5 °C min^{-1}. Weight loss of sample during the second heating cycle was used to determine the oxygen release properties.

Literature shows that various oxides such as TiO_2, Al_2O_3, $MgAl_2O_4$, NiO, and Fe_3O_4 have been explored for the oxidation of ethanol; however less work was reported on CeO_2, while ZrO_2 and mixed oxide of $Ce_xZr_{1-x}O_2$ have not been reported for bioethanol oxidation reaction. Literature also revealed that selectivity towards acetaldehyde is decreased with increased temperature. Majority work has been carried our using higher ethanol concentration (50 - 100 %) in water rather than bioethanol. Catalysts stability has also not well performed.

Therefore it is a necessary that employ catalysts should attain high selectivity towards acetaldehyde and also display higher catalytic stability at the reaction conditions. At present cost of acetaldehyde is higher than acetic acid hence it would be advantage to produce acetaldehyde.

References

[1] Jin Rongchao, The impacts of nanotechnology on catalysis by precious metal nanoparticles, Nanotechnol. Rev. 1 (2012) 31. doi:10.1515/ntrev-2011-0003.

[2] M. Hudlicky, Oxidations in Organic Chemistry, ACS Monogr. Ser 186. American Chemical Society, Washington, DC, (1990), 114

[3] A.S.K. Hashmi, G.J. Hutchings, Gold Catalysis, Angew. Chem. Int. Ed. 45 (2006) 7896–7936. doi:10.1002/anie.200602454.

[4] C.H. Christensen, B. Jørgensen, J. Rass-Hansen, K. Egeblad, R. Madsen, S.K. Klitgaard, S.M. Hansen, M.R. Hansen, H.C. Andersen, A. Riisager, Formation of Acetic Acid by Aqueous-Phase Oxidation of Ethanol with Air in the Presence of a Heterogeneous Gold Catalyst, Angew. Chem. Int. Ed. 45 (2006) 4648–4651. doi:10.1002/anie.200601180.

[5] S.K. Klitgaard, K. Egeblad, U.V. Mentzel, A.G. Popov, T. Jensen, E. Taarning, I.S. Nielsen, C.H. Christensen, Oxidations of amines with molecular oxygen using bifunctional gold–titania catalysts, Green Chem. 10 (2008) 419. doi:10.1039/b714232c.

[6] J. Sun, Y. Wang, Recent Advances in Catalytic Conversion of Ethanol to Chemicals, ACS Catal. 4 (2014) 1078–1090. doi:10.1021/cs4011343.

[7] C. Angelici, B.M. Weckhuysen, P.C.A. Bruijnincx, Chemocatalytic Conversion of Ethanol into Butadiene and Other Bulk Chemicals, ChemSusChem. 6 (2013) 1595–1614. doi:10.1002/cssc.201300214.

[8] J. Rass-Hansen, H. Falsig, B. Jørgensen, C.H. Christensen, Bioethanol: fuel or feedstock?, J. Chem. Technol. Biotechnol. 82 (2007) 329–333. doi:10.1002/jctb.1665.

[9] M. Eds. . W.; Vandamme, E.; Lens, P.; Westermann, P.; Haberbauer, M.; Morena Soetaert, Biofuels for fuel cells, Book. - (2005) 37.

[10] B. Jørgensen, S.E. Christiansen, M.L.D. Thomsen, C.H. Christensen, Aerobic oxidation of aqueous ethanol using heterogeneous gold catalysts: Efficient routes to acetic acid and ethyl acetate, J. Catal. 251 (2007) 332–337. doi:http://dx.doi.org/10.1016/j.jcat.2007.08.004.

[11] S. Tembe, G. Patrick, M. Scurrell, Acetic acid production by selective oxidation of ethanol using Au catalysts supported on various metal oxide, Gold Bull. 42 (2009) 321–327. doi:10.1007/BF03214954.

[12] K.-Q. Sun, S.-W. Luo, N. Xu, B.-Q. Xu, Gold Nano-size Effect in Au/SiO$_2$ for Selective Ethanol Oxidation in Aqueous Solution, Catal. Lett. 124 (2008) 238–242. doi:10.1007/s10562-008-9507-4.

[13] D. Heeskens, P. Aghaei, S. Kaluza, J. Strunk, M. Muhler, Selective oxidation of ethanol in the liquid phase over Au/TiO$_2$, Phys. Status Solidi B. 250 (2013) 1107–1118. doi:10.1002/pssb.201248440.

[14] Y.Y. Gorbanev, S. Kegnæs, C.W. Hanning, T.W. Hansen, A. Riisager, Acetic Acid Formation by Selective Aerobic Oxidation of Aqueous Ethanol over Heterogeneous Ruthenium Catalysts, ACS Catal. 2 (2012) 604–612. doi:10.1021/cs200554h.

[15] T. Takei, J. Suenaga, T. Ishida, M. Haruta, Ethanol Oxidation in Water Catalyzed by Gold Nanoparticles Supported on NiO Doped with Cu, Top. Catal. 58 (2015) 295–301. doi:10.1007/s11244-015-0370-4.

[16] S. Letichevsky, P.C. Zonetti, P.P.P. Reis, J. Celnik, C.R.K. Rabello, A.B. Gaspar, L.G. Appel, The role of m-ZrO$_2$ in the selective oxidation of ethanol to acetic acid employing PdO/m-ZrO$_2$, J. Mol. Catal. Chem. 410 (2015) 177 – 183. doi:http://dx.doi.org/10.1016/j.molcata.2015.09.012.

[17] Y. Long, K. Liang, J. Niu, B. Yuan, J. Ma, Pt NPs immobilized on core-shell magnetite microparticles: novel and highly efficient catalysts for the selective aerobic oxidation of ethanol and glycerol in water, Dalton Trans. 44 (2015) 8660–8668. doi:10.1039/C5DT00779H.

[18] H. Tsunoyama, H. Sakurai, Y. Negishi, T. Tsukuda, Size-Specific Catalytic Activity of Polymer-Stabilized Gold Nanoclusters for Aerobic Alcohol Oxidation in Water, J. Am. Chem. Soc. 127 (2005) 9374–9375. doi:10.1021/ja052161e.

[19] T.W. Hansen, P.L. Hansen, S. Dahl, C.J. Jacobsen, Support effect and active sites on promoted ruthenium catalysts for ammonia synthesis, Catal. Lett. 84 (2002) 7–12.

[20] A. Abad, C. Almela, A. Corma, H. García, Efficient chemoselective alcohol oxidation using oxygen as oxidant. Superior performance of gold over palladium catalysts, Tetrahedron. 62 (2006) 6666–6672. doi:10.1016/j.tet.2006.01.118.

[21] V.R. Choudhary, A. Dhar, P. Jana, R. Jha, B.S. Uphade, A green process for chlorine-free benzaldehyde from the solvent-free oxidation of benzyl alcohol with molecular oxygen over a supported nano-size gold catalyst, Green Chem. 7 (2005) 768. doi:10.1039/b509003b.

[22] S. Klitgaard, A. Riva, S. Helveg, R. Werchmeister, C. Christensen, Aerobic Oxidation of Alcohols over Gold Catalysts: Role of Acid and Base, Catal. Lett. 126 (2008) 213–217. doi:10.1007/s10562-008-9688-x.

[23] G.C.; Louis, C.; Thompson, D.T Bond, Catalysis by Gold, Book. - (2006) -.

[24] N. Russo, D. Fino, G. Saracco, V. Specchia, Supported gold catalysts for CO oxidation, Catal. Today. 117 (2006) 214–219. doi:10.1016/j.cattod.2006.05.027.

[25] M. Haruta, Catalysis of gold nanoparticles deposited on metal oxides, Cattech. 6 (2002) 102–115.

[26] C.T. Campbell, PHYSICS: The Active Site in Nanoparticle Gold Catalysis, Science. 306 (2004) 234–235. doi:10.1126/science.1104246.

[27] R. Grisel, K.-J. Weststrate, A. Gluhoi, B.E. Nieuwenhuys, Catalysis by gold nanoparticles, Gold Bull. 35 (2002) 39–45.

[28] G.C. Bond, D.T. Thompson, Gold-catalysed oxidation of carbon monoxide, Gold Bull. 33 (2000) 41–50.

[29] I.N. Remediakis, N. Lopez, J.K. Nørskov, CO oxidation on gold nanoparticles: Theoretical studies, Appl. Catal. Gen. 291 (2005) 13–20. doi:10.1016/j.apcata.2005.01.052.

[30] B. Zhu, R.J. Angelici, Non-Nanogold Catalysis of Carbon Monoxide Oxidative Amination, J. Am. Chem. Soc. 128 (2006) 14460–14461. doi:10.1021/ja065706t.

[31] P. Haider, B. Kimmerle, F. Krumeich, W. Kleist, J.-D. Grunwaldt, A. Baiker, Gold-Catalyzed Aerobic Oxidation of Benzyl Alcohol: Effect of Gold Particle Size on Activity and Selectivity in Different Solvents, Catal. Lett. 125 (2008) 169–176. doi:10.1007/s10562-008-9567-5.

[32] N. Zheng, and G.D. Stucky, A General Synthetic Strategy for Oxide-Supported Metal Nanoparticle Catalysts, J. Am. Chem. Soc. 128 (2006) 14278–14280. doi:10.1021/ja0659929.

[33] L. Prati, M. Rossi, Gold on Carbon as a New Catalyst for Selective Liquid Phase Oxidation of Diols, J. Catal. 176 (1998) 552 – 560. doi:http://dx.doi.org/10.1006/jcat.1998.2078.

[34] C. Bianchi, F. Porta, L. Prati, M. Rossi, Selective liquid phase oxidation using gold catalysts, Top. Catal. 13 (2000) 231–236. doi:10.1023/A:1009065812889.

[35] S. Carrettin, P. McMorn, P. Johnston, K. Griffin, C.J. Kiely, G.J. Hutchings, Oxidation of glycerol using supported Pt, Pd and Au catalysts, Phys Chem Chem Phys. 5 (2003) 1329–1336. doi:10.1039/B212047J.

[36] A. Abad, P. Concepción, A. Corma, H. García, A Collaborative Effect between Gold and a Support Induces the Selective Oxidation of Alcohols, Angew. Chem. Int. Ed. 44 (2005) 4066–4069. doi:10.1002/anie.200500382.

[37] F.-Z. Su, Y.-M. Liu, L.-C. Wang, Y. Cao, H.-Y. He, K.-N. Fan, Ga–Al Mixed-Oxide-Supported Gold Nanoparticles with Enhanced Activity for Aerobic Alcohol Oxidation, Angew. Chem. Int. Ed. 47 (2008) 334–337. doi:10.1002/anie.200704370.

[38] T. Mallat, A. Baiker, Oxidation of Alcohols with Molecular Oxygen on Solid Catalysts, Chem. Rev. 104 (2004) 3037–3058. doi:10.1021/cr0200116.

[39] B.N. Zope, D.D. Hibbitts, M. Neurock, R.J. Davis, Reactivity of the Gold/Water Interface During Selective Oxidation Catalysis, Science. 330 (2010) 74–78. doi:10.1126/science.1195055.

[40] M.C. Greca, C. Moraes, M.R. Morelli, A.M. Segadães, Evaluation of Pd/alumina catalysts, produced by combustion synthesis, in the ethanol oxidation reaction to acetic acid, Appl. Catal. Gen. 179 (1999) 87–92. doi:http://dx.doi.org/10.1016/S0926-860X(98)00297-X.

[41] G. Avgouropoulos, E. Oikonomopoulos, D. Kanistras, T. Ioannides, Complete oxidation of ethanol over alkali-promoted Pt/Al2O3 catalysts, Appl. Catal. B Environ. 65 (2006) 62–69. doi:http://dx.doi.org/10.1016/j.apcatb.2005.12.016.

[42] A.B. Gaspar, A.M.L. Esteves, F.M.T. Mendes, F.G. Barbosa, L.G. Appel, Chemicals from ethanol—The ethyl acetate one-pot synthesis, Appl. Catal. Gen. 363 (2009) 109–114. doi:10.1016/j.apcata.2009.05.001.

[43] P.-Y. Sheng, G.A. Bowmaker, H. Idriss, The Reactions of Ethanol over Au/CeO2, Appl. Catal. Gen. 261 (2004) 171–181. doi:http://dx.doi.org/10.1016/j.apcata.2003.10.046.

[44] H. Chen, Y. Dai, X. Jia, H. Yu, Y. Yang, Highly selective gas-phase oxidation of ethanol to ethyl acetate over bi-functional Pd/zeolite catalysts, Green Chem. 18 (2016) 3048–3056. doi:10.1039/C5GC02593A.

[45] F. Gonçalves, P.R.S. Medeiros, J.G. Eon, L.G. Appel, Active sites for ethanol oxidation over SnO_2-supported molybdenum oxides, Appl. Catal. Gen. 193 (2000) 195–202. doi:http://dx.doi.org/10.1016/S0926-860X(99)00430-5.

[46] P.S. Medeiros, J. Eon, L. Appel, The role of water in ethanol oxidation over SnO_2-supported molybdenum oxides, Catal. Lett. 69 (2000) 79–82. doi:10.1023/A:1019093116966.

[47] B. Jørgensen, S. Kristensen, A. Kunov-Kruse, R. Fehrmann, C. Christensen, A. Riisager, Gas-Phase Oxidation of Aqueous Ethanol by Nanoparticle Vanadia/Anatase Catalysts, Top. Catal. 52 (2009) 253–257. doi:10.1007/s11244-008-9161-5.

[48] V.I. Sobolev, E.V. Danilevich, K.Y. Koltunov, Role of vanadium species in the selective oxidation of ethanol on V_2O_5/TiO_2 catalysts, Kinet. Catal. 54 (2013) 730–734. doi:10.1134/S0023158413060128.

[49] V.V. Kaichev, Y.A. Chesalov, A.A. Saraev, A.Y. Klyushin, A. Knop-Gericke, T.V. Andrushkevich, V.I. Bukhtiyarov, Redox mechanism for selective oxidation of ethanol over monolayer V_2O_5/TiO_2 catalysts, J. Catal. 338 (2016) 82 – 93. doi:http://dx.doi.org/10.1016/j.jcat.2016.02.022.

[50] J.M. Hidalgo, Z. Tišler, D. Kubička, K. Raabova, R. Bulanek, (V)/Hydrotalcite, (V)/Al_2O_3, (V)/TiO_2 and (V)/SBA-15 catalysts for the partial oxidation of ethanol to acetaldehyde, J. Mol. Catal. Chem. 420 (2016) 178–189. doi:10.1016/j.molcata.2016.04.024.

[51] B. Beck, M. Harth, N.G. Hamilton, C. Carrero, J.J. Uhlrich, A. Trunschke, S. Shaikhutdinov, H. Schubert, H.-J. Freund, R. Schlögl, J. Sauer, R. Schomäcker, Partial oxidation of ethanol on vanadia catalysts on supporting oxides with different

redox properties compared to propane, J. Catal. 296 (2012) 120–131. doi:10.1016/j.jcat.2012.09.008.

[52] S. Fujita, N. Iwasa, H. Tani, W. Nomura, M. Arai, N. Takezawa, Dehydrogenation of Ethanol Over Cu/ZnO Catalysts Prepared from Various Coprecipitated Precursors, React. Kinet. Catal. Lett. 73 (2001) 367–372. doi:10.1023/A:1014192214324.

[53] A.G. Sato, D.P. Volanti, I.C. de Freitas, E. Longo, J.M.C. Bueno, Site-selective ethanol conversion over supported copper catalysts, Catal. Commun. 26 (2012) 122 – 126. doi:http://dx.doi.org/10.1016/j.catcom.2012.05.008.

[54] X. Yu, W. Zhu, S. Gao, L. Chen, H. Yuan, J. Luo, Z. Wang, W. Zhang, Transformation of ethanol to ethyl acetate over Cu/SiO_2 catalysts modified by ZrO_2, Chem. Res. Chin. Univ. 29 (2013) 986–990. doi:10.1007/s40242-013-3024-8.

[55] Q.-N. Wang, L. Shi, A.-H. Lu, Highly Selective Copper Catalyst Supported on Mesoporous Carbon for the Dehydrogenation of Ethanol to Acetaldehyde, ChemCatChem. 7 (2015) 2846–2852. doi:10.1002/cctc.201500501.

[56] M.V. Morales, E. Asedegbega-Nieto, B. Bachiller-Baeza, A. Guerrero-Ruiz, Bioethanol dehydrogenation over copper supported on functionalized graphene materials and a high surface area graphite, Carbon. 102 (2016) 426–436. doi:10.1016/j.carbon.2016.02.089.

[57] X. Li, E. Iglesia, Selective Catalytic Oxidation of Ethanol to Acetic Acid on Dispersed Mo-V-Nb Mixed Oxides, Chem. – Eur. J. 13 (2007) 9324–9330. doi:10.1002/chem.200700579.

[58] V.I. Sobolev, K.Y. Koltunov, MoVNbTe Mixed Oxides as Efficient Catalyst for Selective Oxidation of Ethanol to Acetic Acid, ChemCatChem. 3 (2011) 1143–1145. doi:10.1002/cctc.201000450.

[59] G.J. Hutchings, Vapor phase hydrochlorination of acetylene: Correlation of catalytic activity of supported metal chloride catalysts, J. Catal. 96 (1985) 292 – 295. doi:http://dx.doi.org/10.1016/0021-9517(85)90383-5.

[60] M. Haruta, N. Yamada, T. Kobayashi, S. Iijima, Gold catalysts prepared by coprecipitation for low-temperature oxidation of hydrogen and of carbon monoxide, J. Catal. 115 (1989) 301 – 309. doi:http://dx.doi.org/10.1016/0021-9517(89)90034-1.

[61] P.P. Edwards, J.M. Thomas, Gold in a Metallic Divided State—From Faraday to Present-Day Nanoscience, Angew. Chem. Int. Ed. 46 (2007) 5480–5486. doi:10.1002/anie.200700428.

[62] T. Takei, N. Iguchi, M. Haruta, Support effect in the gas phase oxidation of ethanol over nanoparticulate gold catalysts, New J Chem. 35 (2011) 2227–2233. doi:10.1039/C1NJ20297A.

[63] Y. Guan, E.J.M. Hensen, Ethanol dehydrogenation by gold catalysts: The effect of the gold particle size and the presence of oxygen, Appl. Catal. Gen. 361 (2009) 49–56. doi:http://dx.doi.org/10.1016/j.apcata.2009.03.033.

[64] H. Chen, X. Jia, Y. Li, C. Liu, Y. Yang, Controlled surface properties of Au/ZSM5 catalysts and their effects in the selective oxidation of ethanol, Catal. Today. 256 (2015) 153–160. doi:10.1016/j.cattod.2015.01.020.

[65] J. Mielby, J.O. Abildstrøm, F. Wang, T. Kasama, C. Weidenthaler, S. Kegnæs, Oxidation of Bioethanol using Zeolite-Encapsulated Gold Nanoparticles, Angew. Chem. Int. Ed. 53 (2014) 12513–12516. doi:10.1002/anie.201406354.

[66] J. Zhang, L. Wang, L. Zhu, Q. Wu, C. Chen, X. Wang, Y. Ji, X. Meng, F.-S. Xiao, Solvent-Free Synthesis of Zeolite Crystals Encapsulating Gold-Palladium Nanoparticles for the Selective Oxidation of Bioethanol, ChemSusChem. 8 (2015) 2867–2871. doi:10.1002/cssc.201500261.

[67] O.A. Simakova, V.I. Sobolev, K.Y. Koltunov, B. Campo, A.-R. Leino, K. Kordás, D.Y. Murzin, "Double-Peak" Catalytic Activity of Nanosized Gold Supported on Titania in Gas-Phase Selective Oxidation of Ethanol, ChemCatChem. 2 (2010) 1535–1538. doi:10.1002/cctc.201000298.

[68] V.I. Sobolev, K.Y. Koltunov, O.A. Simakova, A.-R. Leino, D.Y. Murzin, Low temperature gas-phase oxidation of ethanol over Au/TiO_2, Appl. Catal. Gen. 433–434 (2012) 88 – 95. doi:http://dx.doi.org/10.1016/j.apcata.2012.05.003.

[69] V.I. Sobolev, K.Y. Koltunov, Gas-phase oxidation of alcohols with dioxygen over an Au/TiO_2 catalyst: The role of reactive oxygen species, Kinet. Catal. 56 (2015) 343–346. doi:10.1134/S0023158415030192.

[70] M.C. Holz, K. Tolle, M. Muhler, Gas-phase oxidation of ethanol over Au/TiO_2 catalysts to probe metal-support interactions, Catal Sci Technol. 4 (2014) 3495–3504. doi:10.1039/C4CY00493K.

[71] Y. Guan, E.J.M. Hensen, Selective oxidation of ethanol to acetaldehyde by Au−Ir catalysts, J. Catal. 305 (2013) 135 – 145. doi:http://dx.doi.org/10.1016/j.jcat.2013.04.023.

[72] E.A. Redina, A.A. Greish, I.V. Mishin, G.I. Kapustin, O.P. Tkachenko, O.A. Kirichenko, L.M. Kustov, Selective oxidation of ethanol to acetaldehyde over Au–Cu catalysts prepared by a redox method, Catal. Today. 241, Part B (2015) 246 – 254. doi:http://dx.doi.org/10.1016/j.cattod.2013.11.065.

[73] K.Y. Koltunov, V.I. Sobolev, Selective gas-phase oxidation of ethanol by molecular oxygen over oxide and gold-containing catalysts, Catal. Ind. 4 (2012) 247–252. doi:10.1134/S2070050412040101.

[74] P. Liu, E.J.M. Hensen, Highly Efficient and Robust $Au/MgCuCr_2O_4$ Catalyst for Gas-Phase Oxidation of Ethanol to Acetaldehyde, J. Am. Chem. Soc. 135 (2013) 14032–14035. doi:10.1021/ja406820f.

[75] P. Liu, X. Zhu, S. Yang, T. Li, E.J.M. Hensen, On the metal–support synergy for selective gas-phase ethanol oxidation over $MgCuCr_2O_4$ supported metal nanoparticle catalysts, J. Catal. 331 (2015) 138 – 146. doi:http://dx.doi.org/10.1016/j.jcat.2015.08.025.

[76] J. Chen, X. Tang, J. Liu, E. Zhan, J. Li, X. Huang, W. Shen, Synthesis and Characterization of Ag−Hollandite Nanofibers and Its Catalytic Application in Ethanol Oxidation, Chem. Mater. 19 (2007) 4292–4299. doi:10.1021/cm070904k.

[77] Z. Li, J. Xu, X. Gu, K. Wang, W. Wang, X. Zhang, Z. Zhang, Y. Ding, Selective Gas-Phase Oxidation of Alcohols over Nanoporous Silver, ChemCatChem. 5 (2013) 1705–1708. doi:10.1002/cctc.201200862.

[78] O.V. Vodyankina, A.S. Blokhina, I.A. Kurzina, V.I. Sobolev, K.Y. Koltunov, L.N. Chukhlomina, E.S. Dvilis, Selective oxidation of alcohols over Ag-containing Si_3N_4 catalysts, Catal. Today. 203 (2013) 127 – 132. doi:http://dx.doi.org/10.1016/j.cattod.2012.02.056.

[79] V.V. Dutov, G.V. Mamontov, V.I. Sobolev, O.V. Vodyankina, Silica-supported silver-containing OMS-2 catalysts for ethanol oxidative dehydrogenation, Catal. Today. 278 (2016) 164–173. doi:10.1016/j.cattod.2016.05.058.

[80] J. Xu, X.-C. Xu, X.-J. Yang, Y.-F. Han, Silver/hydroxyapatite foam as a highly selective catalyst for acetaldehyde production via ethanol oxidation, Catal. Today. 276 (2016) 19 – 27. doi:http://dx.doi.org/10.1016/j.cattod.2016.03.001.

[81] J.M.C.B. Jean Marcel R. Gallo Isabel C. Freitas, C.M.P. Marques, The Effect of Ag in the Cu/ZrO_2 Performance for the Ethanol Conversion, Top. Catal. 59 (2016) 357–365.

[82] D.D. Hibbitts, M. Neurock, Influence of oxygen and pH on the selective oxidation of ethanol on Pd catalysts, J. Catal. 299 (2013) 261–271. doi:http://dx.doi.org/10.1016/j.jcat.2012.11.016.

[83] M. Boronat, A. Corma, F. Illas, J. Radilla, T. Ródenas, M.J. Sabater, Mechanism of selective alcohol oxidation to aldehydes on gold catalysts: Influence of surface roughness on reactivity, J. Catal. 278 (2011) 50–58. doi:10.1016/j.jcat.2010.11.013.

[84] Q. Meng, Y. Shen, J. Xu, J. Gong, Mechanistic Insights into Selective Oxidation of Ethanol on Au(111): A DFT Study, Chin. J. Catal. 33 (2012) 407–415. doi:10.1016/S1872-2067(11)60340-9.

[85] T. Maihom, M. Probst, J. Limtrakul, Density Functional Theory Study of the Dehydrogenation of Ethanol to Acetaldehyde over the Au-Exchanged ZSM-5 Zeolite: Effect of Surface Oxygen, J. Phys. Chem. C. 118 (2014) 18564–18572. doi:10.1021/jp505002u.

[86] P. Aghaei, R.J. Berger, Reaction kinetics investigation of the selective oxidation of aqueous ethanol solutions with air over a Au/TiO_2 catalyst, Appl. Catal. B Environ. 132–133 (2013) 195–203. doi:http://dx.doi.org/10.1016/j.apcatb.2012.11.039.

[87] S.E. Davis, M.S. Ide, R.J. Davis, Selective oxidation of alcohols and aldehydes over supported metal nanoparticles, Green Chem. 15 (2013) 17–45. doi:10.1039/C2GC36441G.

[88] B.-S. Jiang, R. Chang, Y.-C. Lin, Partial Oxidation of Ethanol to Acetaldehyde over $LaMnO_3$-Based Perovskites: A Kinetic Study, Ind. Eng. Chem. Res. 52 (2013) 37–42. doi:10.1021/ie300348u.

[89] A. Brückner, Looking on Heterogeneous Catalytic Systems from Different Perspectives: Multitechnique Approaches as a New Challenge for In Situ Studies, Catal. Rev. 45 (2003) 97–150. doi:10.1081/CR-120015739.

[90] W.H. Bragg, W. L. Bragg, The Crystalline State, Vol 1,McMillan,New york (1949)

[91] S.R. Stock, B.D. Cullity, Elements of X-Ray Diffraction, 3rd edition, Prentice Hall (2001)

[92] S. Biz, M.L. Occelli, Synthesis and Characterization of Mesostructured Materials, Catal. Rev. 40 (1998) 329–407. doi:10.1080/01614949808007111.

[93] D. E. Newbury, D. C. Joy, P. Echlin, C.E.Fiori and J.I. Goldstein, Advanced Scanning Electron Microscopy and X-Ray Microanalysis, Plenum Press, New York (1986)

[94] D.A.M. Monti, A. Baiker, Temperature-programmed reduction. Parametric sensitivity and estimation of kinetic parameters, J. Catal. 83 (1983) 323 – 335. doi:http://dx.doi.org/10.1016/0021-9517(83)90058-1.

[95] N.W. Hurst, S.J. Gentry, A. Jones, B.D. McNicol, Temperature Programmed Reduction, Catal. Rev. 24 (1982) 233–309. doi:10.1080/03602458208079654.

[96] W.W. Paudler, Nuclear Magnetic Resonance: General Concepts and Applications, (1987).

[97] S.G. M. Jaroniec M. Kruk, S. Inagaki, Nuclear Magnetic Resonance: General Concepts and Applications, J Phys Chem B. 105 (2000) 681–689.

Chapter – 3

Liquid Phase Oxidation of Bioethanol

CHAPTER – 3
Liquid Phase Oxidation of Bioethanol

3.1 Introduction

Selective oxidation of ethanol using molecular oxygen has received considerable attention in the recent past due to its potential application in the production of intermediates in the fine chemicals industries [1]. Many heterogeneous catalysts have been reported to be active for this transformation and recently supported gold nanoparticles have been shown to be highly effective [2]. Acetic acid production in the liquid phase of aqueous ethanol was achieved only by supported Au catalysts. Christensen et al. were first to report that in a batch reactor at 180 °C, supported Au catalysts exhibited best performance for acetic acid production with a selectivity of 86% [3]. They showed that over $MgAl_2O_4$ support oxidation of ethanol with air proceeds deeper to yield acetic acid in the order of Pd, Pt, and Au. Later Au/TiO_2 [4] , Au/SiO_2 [5], Au supported on ZnO, TiO_2 and Al_2O_3 [6] were also reported for the selective oxidation of ethanol to acetic acid. Au supported on ZnO and TiO_2 provide higher conversion and higher acetic acid selectivity [6,7]. Co-precipitated Au/NiO doped with Cu calcined at 300 °C showed good activity even at 120 °C with selectivities to acetic acid above 90% [8]. The rate determining step is oxygen assisted dehydrogenation of ethanol to acetaldehyde. At ethanol concentrations above 60 wt% the main product shifts towards ethyl acetate through the esterification of acetic acid [4].

From above cited literature, it is clear that supports are playing a vital role in the ethanol oxidation reaction and also trend towards the use of more environment friendly and energy efficient catalyst is evident. The acidic nature of the supports will enhance the conversion [9]. Zeolite being a solid acid catalyst is widely used in many reactions like alkylation, condensations reactions of carbonyl compounds, isomerization, oxidations, epoxidations of olefins etc [10].

The aim of the present study is to evaluate the effect of various zeolites as a support over Au and Ag metal particles for the liquid phase oxidation of bioethanol and the various parameters affecting the oxidation of bioethanol. The experiments are carried out using aqueous ethanol solution and the effects of reaction time, initial concentration of ethanol and ethanol/O2 mole ratio have been studied.

3.2 Thermodynamic calculation

The accomplishment of any reaction depends on the reaction condition, controlling parameters etc. It is necessary to check the segments of reactant at the reaction condition. If we carried out the reaction in liquid phase then reactant required to be remained in the liquid phase at the reaction condition. The reaction pressure should be higher than the pressure where the first bubble generated from the reaction mixtures. Hence it necessary to find out the pressure at which first bubble (P_{bubble}) forms from the reaction mixture. In this section we have calculated activity coefficient to calculate P_{bubble}.

3.2.1 Calculation for activity coefficient

Various methods like NRTL, Wilson, UNIFAC, UNIQUAC etc. are available to calculate the activity coefficient. The UNIFAC method for estimation of activity coefficient depends on the concept that liquid mixture may be considered a solution of structural unit from which the molecules are formed rather than a solution of molecules themselves. These structural units are called sub groups.

A number designated k, identified each sub groups. The relative volume R_k and relative surface Q_k are the properties of the sub groups.

The UNIFAC method based on UNIQUAC equation, for which the activity co efficient given by eq. (3.1)

$$In\, \gamma_i = \ln \gamma_i\, C\, + \, \ln \gamma_i\, R \dots \dots \dots \dots \dots \dots \dots \dots (3.1)$$

$$\ln \gamma_i\, C = 1\, - J_i + \ln J_i\, - 5q_i\,(\, 1 - \frac{J_i}{L_i} + \, \ln \frac{J_i}{L_{i\,i}} \dots \dots \dots \dots \dots \dots \dots (3.2)$$

$$\ln \gamma_i\, R = q_i [1\, -\, \sum_j (\theta_k \frac{\beta_{ik}}{S_k} - e_{ki} \ln \frac{\beta_{ik}}{S_k}) \dots \dots \dots \dots \dots \dots (3.3)$$

$$J_i = \frac{r_i}{\sum_j r_j x_j} \dots \dots \dots \dots \dots \dots (3.4)$$

$$L_i = \frac{q_i}{\sum_j q_j x_j} \dots \dots \dots \dots \dots \dots (3.5)$$

$$s_i = \sum \theta_i \tau_{li} \quad \ldots\ldots\ldots\ldots\ldots. (3.6)$$

$$r_i = \sum_k \vartheta_k(i) R_k \quad \ldots\ldots\ldots\ldots (3.7)$$

$$q_i = \sum_k \vartheta_k(i) Q_k \quad \ldots\ldots\ldots\ldots (3.8)$$

$$e_{ki} = \frac{\vartheta_k(i) Q_k}{q_i} \quad \ldots\ldots\ldots\ldots\ldots (3.9)$$

$$\beta_{ki} = \sum e_{mi} \tau_{mk} \quad \ldots\ldots\ldots\ldots (3.10)$$

$$\theta_k = \frac{\sum_i x_i q_i e_{ki}}{\sum_j x_j q_j} \quad \ldots\ldots\ldots\ldots\ldots (3.11)$$

$$S_k = \sum \theta_m \tau_{mk} \quad \ldots\ldots\ldots\ldots\ldots (3.12)$$

$$\tau_{mk} = e^{\frac{-a_{mk}}{T}} \quad \ldots\ldots\ldots\ldots\ldots\ldots (3.13)$$

Where, Subscripts i identifies species and j is a dummy index running over all species. Subscript k identifies subgroups, and m is a dummy index running over all subgroups. The quantity $v_k(i)$ is the number of subgroups of type k in a species i. Values of subgroups parameter R_k and Q_k and of the a_{mk} are taken from tabulations for UNIFAC – VLE subgroup parameters and UNIFAC – VLE interaction parameters, a_{mk} [11].

P_{bubble} is calculated at constant mole fraction ($X_1 = 0.1$ and $X_2 = 0.9$) for temperature range 110 – 240 °C. Where X_1 is mole fraction ethanol and X_2 is mole fraction of water. (Detailed calculation is in APPENDIX A)

Table3.1 P_{bubble} at constant mole fraction for temperature range 110 – 240 °C

activity coefficient for $X_1 = 0.1$ and $X_2 = 0.9$				X_1	0.1
				X_2	0.9
Temp, °C	Activity coefficient		P_{bubble}, bar	P1sat (bar)	P2sat (bar)
	Y1	Y2			
110	3.3545	1.0341702	2.9303	3.14813	1.43365
120	3.341795	1.033669	3.2772	4.29552	1.97972
130	3.328729	1.033263	4.4133	5.75174	2.68707
140	3.315384	1.03288	5.8464	7.56952	3.58965
150	3.301813	1.03252	7.6292	9.80676	4.42552
160	3.288063	1.032179	9.81863	12.5234	6.13682
170	3.274173	1.031857	12.4757	15.7821	7.86974
180	3.260176	1.031557	15.6656	19.6476	9.97443
190	3.246101	1.031261	19.4571	24.1861	12.5048
200	3.231974	1.030985	23.9323	29.4645	15.5186
210	3.217816	1.030723	29.1355	35.5503	19.0763
220	3.203645	1.030472	35.17443	42.5105	23.2424
230	3.189479	1.030233	42.1179	50.4117	28.0834
240	3.175331	1.030004	50.04692	59.3192	33.6688

Table 3.1 and Figure 3.1 depicts the calculation of P_{bubble} at constant mole fraction (X_1 = 0.1 & X_2 = 0.9) for temperature range 110 – 240 °C. Initially the reactor was pressurized to 22 bar at room temperature and then increased temperature to 200 °C. It was observed that pressure also increased with temperature and reached to 45 bar. As compared to 23 bar (P_{bubble} calculated) at 200 °C, reaction pressure was 45 bar at reaction condition which sufficiently greater than P_{bubble} calculated. Thus it is confirmed that at the reaction condition reactant will remain in the liquid phase.
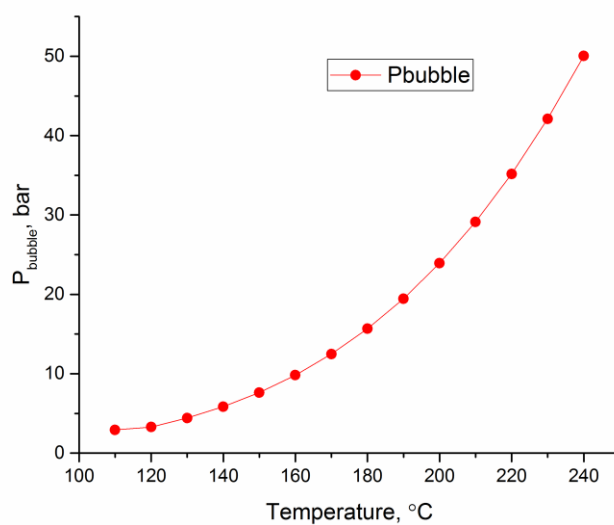
Figure 3.1 P_{bubble} at constant mole fraction for temperature range 110 – 240 °C

Further, activity coefficient was determined for different mole fraction at 200 °C and obtained values are shown in Table 3.2.

Table 3.2 Activity coefficient for different mole fraction at 200 °C

Mole fraction		Activity coefficient		P_{bubble}, bar
X_1	X_2	Y1	Y2	
0	1	6.0122	1	15.5186
0.05	0.95	4.2468	1.0087	21.12666
0.1	0.9	3.232	1.031	23.92235
0.15	0.85	2.6003	1.0633	25.51833
0.2	0.8	2.1824	1.1034	26.55895
0.25	0.75	1.8924	1.1499	27.32296
0.3	0.7	1.6836	1.2019	27.93759
0.35	0.65	1.5285	1.259	28.46251
0.4	0.6	1.4106	1.321	28.92537
0.45	0.55	1.3193	1.3879	29.33866
0.5	0.5	1.2473	1.4601	29.70445
0.55	0.45	1.19	1.5379	30.02362
0.6	0.4	1.1439	1.6222	30.29224
0.65	0.35	1.1067	1.714	30.50499
0.7	0.3	1.0767	1.8147	30.65496
0.75	0.25	1.0526	1.9263	30.73451
0.8	0.2	1.0335	2.0512	30.72836
0.85	0.15	1.019	2.1931	30.62508
0.9	0.1	1.0086	2.3567	30.40236
0.95	0.05	1.0022	2.5486	30.03028
1	0	1	2.7784	29.4645

As seen in Table 3.2 and Figure 3.2, maximum P_{bubble} was approximately 31 bar for 75 wt % ethanol and 25 wt % water. During the experiments for 2.5–10 wt % bioethanol, it was observed that reaction pressure was around 40–45 bar. Therefore, liquid reactant (bioethanol) was remained in the liquid phase is confirmed from above calculation.
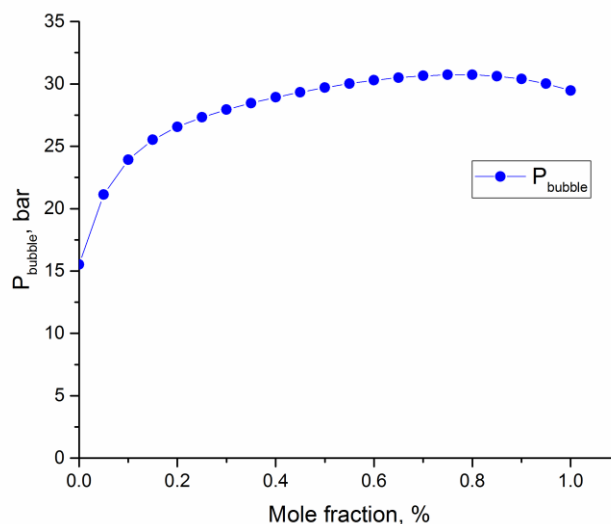
Figure 3.2 Activity coefficient for different mole fraction at 200 °C

3.3 Experimental

3.3.1 Catalyst Preparation

3.3.1.1 Method to convert as synthesized zeolite into active proton form

Zeolites obtained in as synthesized form were calcined in flowing air at 540 °C for 6 - 8 h to remove the occluded organic template. This treatment leaves zeolite in the Na-form. This Na present in the zeolite was ion exchanged with 15 ml 10% ammonium nitrate per gm of catalyst under reflux for three times, each for 4 hours followed by washing with hot distilled water. Thus zeolite in NH^{4+} form was obtained.

The NH_4^+ form zeolite was calcined at high temperature to decompose NH_4^+ ions into H^+ and NH_3. After the liberation of ammonia, protons are bonded with surface oxygen to give the bridging form SiO(H)Al- of Bronsted acid sites.

An equilibrium exists between this bridging form and the form in which silanol (-SiOH) group is adjacent to a tri-coordinate aluminum that constitutes the Lewis acid site. Higher calcination temperature (> 500 °C) of zeolite resulted in dehydroxylation process in which Bronsted acid sites were converted to Lewis acid sites. Figure 3.3 shows the diagram of a zeolite framework surface to convert as synthesized zeolite into active proton form.
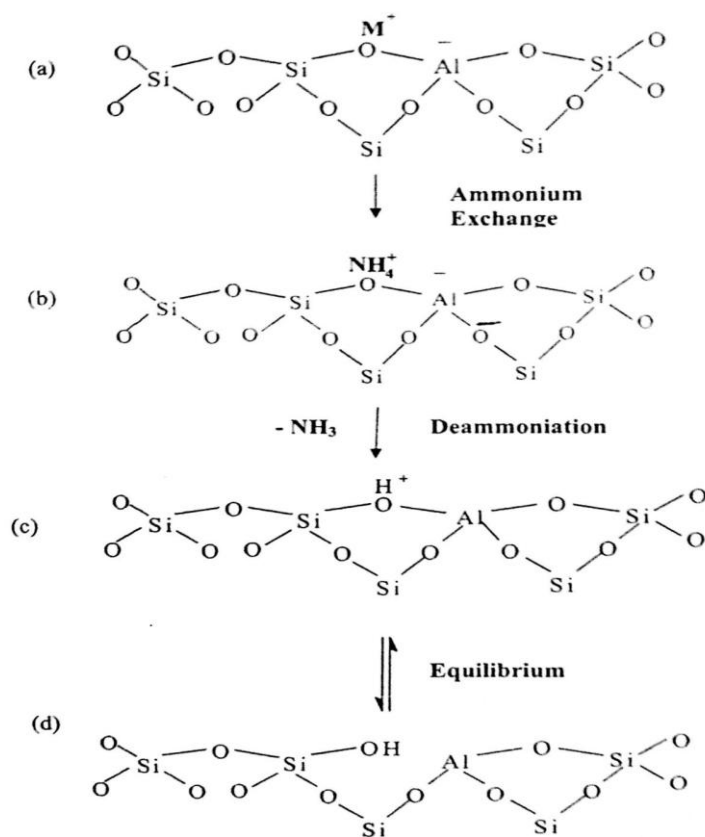
Figure 3.3 Diagram of a zeolite framework surface (a) the as- synthesized form, M^+ is either an organic cation or an alkali metal cation. (b) Ammonium ion exchange produces the NH_4^+ exchanged form. (c) Thermal treatment is used to remove ammonia, producing the H^+, acid form (d) Equilibrium form showing a silanol group adjacent to tri-coordinate aluminum.

3.3.1.2 Incipient wetness impregnation method for catalyst synthesis

Incipient wetness impregnation method also called capillary impregnation or dry impregnation is a commonly used technique for the synthesis of catalyst. Typically, the active metal precursor was dissolved in an aqueous or organic solution. Then the metal containing solution was added to a catalyst support containing the same pore volume as the volume of the solution that was added. Capillary action draws the solution into the pores. Solution added in excess of the support pore volume causes the solution transport to change from a capillary action process to a diffusion process, which is much slower. The catalyst can then be dried and calcined to drive off the volatile components within the solution, depositing the metal on the catalyst surface. The maximum loading is limited by the solubility of the precursor in the solution. The concentration profile of the impregnated compound depends on the mass transfer conditions within the pores during impregnation and drying [12].

Synthesis of Au and Ag particles supported zeolites:-

Required amount of metal precursor salt ($AgNO_3$, 1 wt %) was dissolved in 20 mL distilled water and subsequently added drop-wise to support (HZSM5) suspension in water with stirring. Resulting slurry was stirred at room temperature for 1 h. Subsequently, the mixture was dried at 100 °C for 12 h. Dry powder was then calcined at 350 °C (10 °C min^{-1}) for 4 h under air flow (50 mL/min). The catalyst was reduced under H_2 flow (50 mL/min) at 350 °C (10 °C min^{-1}) for 3 h.

Au supported on HZSM5, HY and Hβ were prepared according to above for Ag/HZSM5. However, calcinations rate for HZSM 5 and HY were 10°C/min and for Hβ was 2°C/min.

3.3.2 Catalyst evaluation for bioethanol oxidation

3.3.2.1 Catalytic activity measurement

The experiment was conducted in 100 mL stainless steel autoclave reactor (Figure 3.4). The stirrer was only used for stirring the liquid mixture inside the autoclave not for heating purposes. The autoclave was surrounded by a heating coil jacket, which was then connected to a temperature controller together with a thermocouple to control the inside temperature of the autoclave. The autoclave was charged with 20 mL of aqueous ethanol of desired concentration

ranging from 2.5 - 10 wt % ethanol diluted with water, and 150 - 250 mg of the catalyst. It was then closed and charged with technical air (80 vol% N_2, 20 vol% O_2) at the required pressure of 22 bar. The autoclave was then heated to the desired reaction temperature of 150 - 200 °C under stirring conditions for a required reaction time. Stirring was kept constant (1000 rpm) for the reactions. After each reaction, the autoclave was cooled with an ice-water mixture to a temperature below 10 °C, to ensure that volatile products did not escape. At the end of each run, the liquid reaction mixture was separated from the catalyst by centrifuge and then analyzed by gas chromatograph equipped using Agilent DB 624 column (30 m x0.25 mm id) with flame ionization detector (FID). At the end of reaction the autoclave was depressurized. We were not able to find the presence of gaseous products from the reaction such as CO_2.

Figure 3.4 Picture of autoclave used for bioethanol oxidation

To evaluate the performance of the catalytic systems, conversions of ethanol ($X_{ethanol}$, %) and selectivity to products (S) is defined as follow: ethanol conversion (X_A) was calculated from ratio of the amount of ethanol converted and initial amount of ethanol. Selectivities to the reaction products such as acetaldehyde, ethyl acetate and acetic acid (S) were calculated from the amount of the products formed divided by the amount of ethanol converted.

3.4 Results and discussion

3.4.1 Catalyst characterization

The catalysts were characterized using fourier transform infrared spectroscopy (FTIR), x-ray diffraction pattern (XRD) and scanning electron microscopy (SEM) as described in chapter 2 (section 2.7).

3.4.1.1 FTIR spectra of Ag/HZSM5 and Au over various zeolites
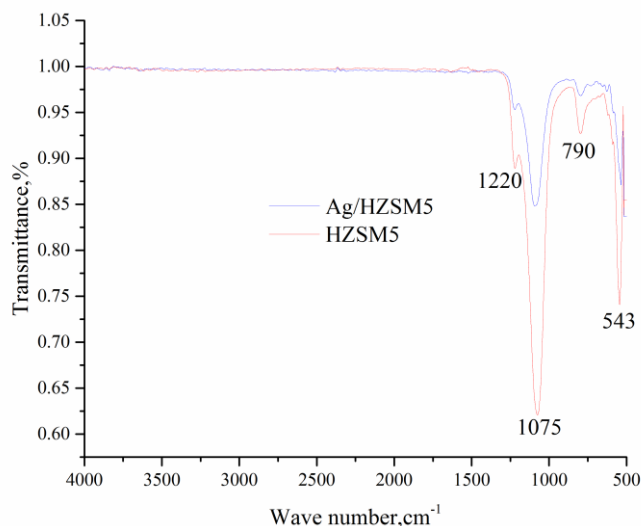
Figure 3.5 FTIR spectra of HZSM5 and Ag/HZSM5 in the region 500 – 4000 cm^{-1}

Fourier transform infra red (FTIR) spectrum of H-ZSM-5 and Ag/HZSM5 samples in the range of 400–4000 cm^{-1} are studied and shown in Figure 3.5. It can be observed that there was no significant band position shifts, hence no isomorphous substitution in zeolite framework took place[13] (Figure 3.5). This indicates that the zeolite framework had remained intact. Sharp peak at 543 cm^{-1} could be assigned to the structurally sensitive double five member ring tetrahedral vibrations and it is typical for the crystalline ZSM-5 zeolite [13,14]. IR bands around 790 and 1075 cm^{-1} can be assigned to the symmetric and asymmetric stretching vibrations of the Si–O–Si linkages of the zeolite framework, respectively. Vibration modes of 1075 and 799 cm^{-1} are assigned to the internal vibration of SiO$_4$ and AlO$_4$ tetrahedra and a small IR band near 1220 cm^{-1} is attributed to their asymmetric stretching vibration. Small H–OH bending vibrations of adsorbed water

molecules are observed at 1625 cm^{-1}. It indicates the presence of adsorbed water in samples that occurred during incipient wet impregnation process. The bands of Ag/HZSM5 demonstrated a significant change in the frequency shift or a reduction in the intensity framework. This indicates that Ag/HZSM5 catalysts experienced a significant change in the number of those forming framework bonds[14].
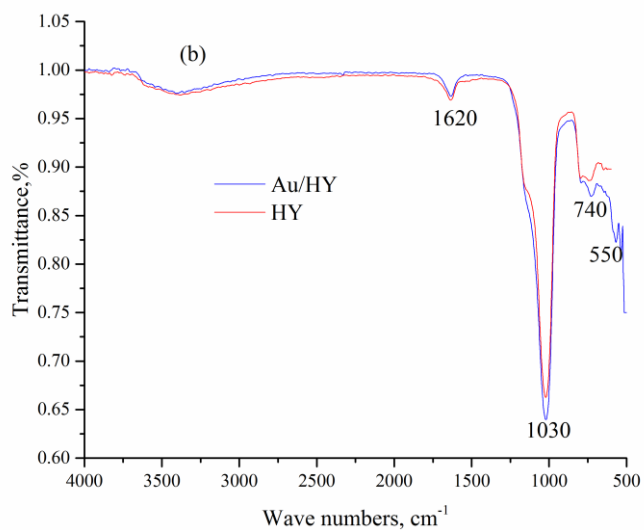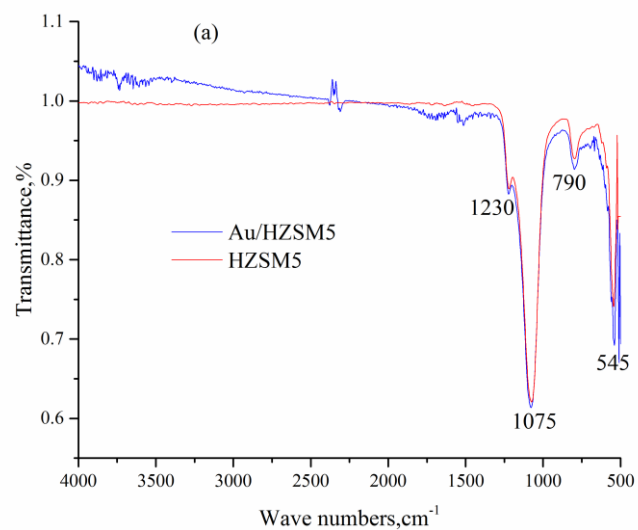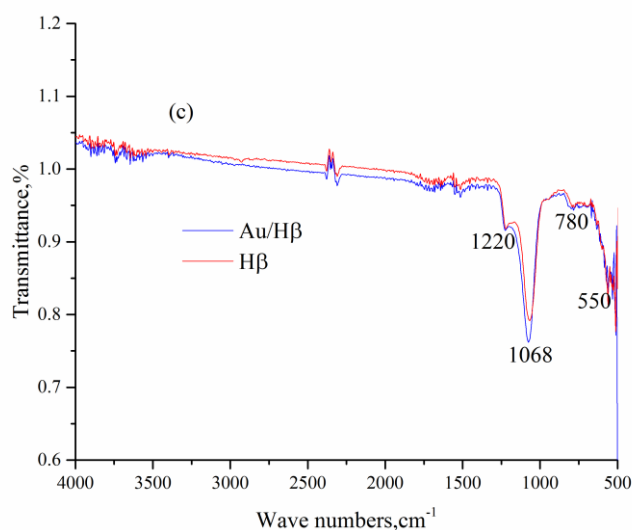
Figure 3.6 FTIR spectra of (a) HZSM5 and Au/HZSM5 (b) HY and Au/HY and (c) Hβ and Au/Hβ in the region 500 – 4000 cm^{-1}

Figure 3.6 (a) shows IR spectra of HZSM5 and Au/HZSM5 in the region 500 – 4000 cm^{-1}. In Figure 3.6 (a), bands at 1220, 1075, 790 and 545 cm^{-1} are to similar observed in Figure 3.5 and their descriptions are same as discussed for HZSM5 and Ag/HZSM5. Structure of HY (Faujasite) is characterized by the functional groups and regions found in Figure 3.6 (b). Band that appears at 1620 cm^{-1} reveals to bending vibration of water molecules in zeolite structure. Bands around 1030 cm^{-1} indicates presence of Si-O and assigned to external asymmetrical stretching while the band at about 740 cm^{-1} associated with symmetric stretching modes of external linkages [14,15]. The double ring opening vibration at 550 cm^{-1} is to the assigned to the T-O-T (T=Si/Al) bending vibration of zeolite framework [16]. Hβ and Au/Hβ spectra (Figure 3.6 (c)) also exhibit band in the region of 1630, 1220, 1068, 780 and 550 cm^{-1} are due to water bending vibration, asymmetrical stretching vibration, symmetric and asymmetric stretching vibrations of the Si–O–Si linkages of the zeolite framework and double ring opening vibration of external linkages, respectively [17]. In general FTIR spectra of various zeolites in Fig. 3.5 and 3.6 (a – c) reveal that the vibrations of zeolites are in the same range as given in Table 3.3.

Table 3.3 Assignment of zeolite lattice vibration

Internal Tetrahedra	Vibrations cm^{-1}	External Linkages	Vibrations cm^{-1}
Asymmetric Stretch	1250 - 1200	Double ring	600 -500
Symmetric Stretch	750 -800	Symmetric Stretch	800- 750
		Asymmetric stretch	1150 -1020

3.4.1.2 XRD of Au over various zeolite

XRD patterns of HZSM5 and Au/HZSM5 catalysts are shown in Figure 3.7 (a). The XRD pattern of the Au impregnated HZSM5 completely matched with that of the parent HZSM5, which indicates that the impregnation has no obvious effect on the parent zeolite structure. There was also no new phase formation during heat treatment and zeolite modification. The XRD pattern of the Au impregnated HZSM5 indicates that the structure of the zeolites remains intact after loading metal over the HZSM5 catalyst [13,15]. However a slight decrease in peak intensities of HZSM5 sample was observed. The slight decrease of crystallinity is possibly due to the removal of some silica sites from the zeolite framework, because of the impregnated Au.

A single crystalline phase of the HZSM5 structure is confirmed by observing the typical reflection peaks at 2θ of 13.96°, 23.98°, 24.57°, 26.02°, 27.05°, 29.22°, 29.46°, 30.10°, and 45.44° [14,18]. HZSM5 zeolite catalyst is hydrothermally and chemically stable and the XRD patterns are similar to that of the usual HZSM5 reported earlier in the scientific literature[18]. Compared to XRD of HZSM5 additional three new peaks around 38.2°, 44.5° and 64.58° are observed for Au/HZSM5. These peaks are characteristic diffraction peaks of Au nanoparticles and are corresponding to the (111), (200) and (220) planes, respectively [14].
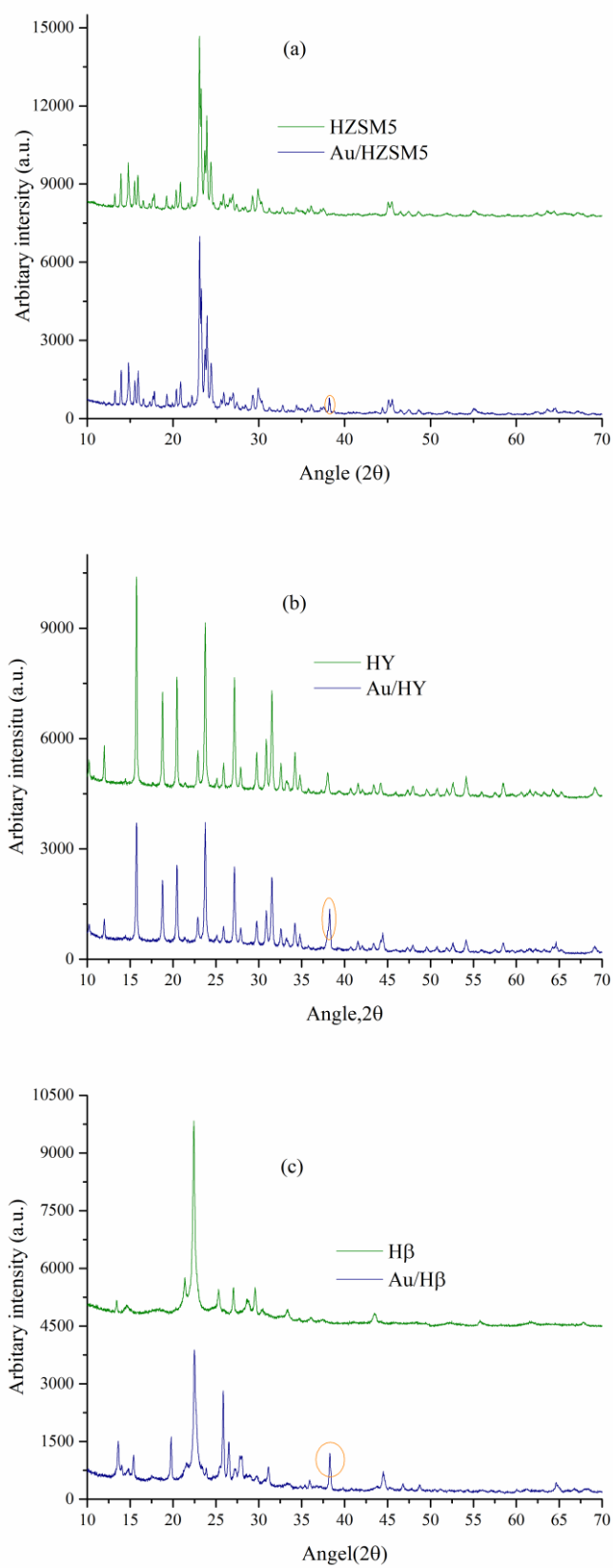
Figure 3.7 XRD of (a) HZSM5 and Au/HZSM5 (b) HY and Au/HY and (c) Hβ and Au/Hβ

The characteristic peaks at HY at 2θ of 15.8° and 23.1° confirmed the crystalline structure of HY [14,18,19] (figure 3.7 (b)). In case of Au/HY, peaks at 38.2°, 44.5° and 64.58° are observed and confirming the impregnation of Au nanoparticles to HY.

.

The XRD patterns of Hβ catalysts (Figure. 3.7 (c)) shows similar pattern to that of the parent Hβ [20] as indicated by the diffraction angle at 2θ = 16.5°, 22.5°, 25.3°, 26.9° and 29.5°. The presence of all the typical XRD peaks for Hβ in Au/Hβ indicates the framework structure has been retained after Au impregnation. Similar to Au/HZSM5 and Au/HY, peaks corresponds to Au at 38.2°, 44.5° and 64.58° are observed in Au/Hβ also.

3.4.2. Catalyst activity studies

Table 3.4 shows catalytic performance of Ag/HZSM5 and Au supported on various zeolites employed for liquid phase oxidation of bioethanol. Metal loading was approximately 1 wt % of support material. Reaction was performed at varying temperature from 150-200 °C while other parameters like pressure, time and O_2/ethanol were kept constant.

It is seen in Table 3.4 that no bioethanol conversion was found at 150 °C (entry no. 1) for 4 h of reaction time. Upon increasing temperature from 150 °C to 175 °C and from 175 °C to 200 °C, marginal increased in conversion was observed and it reached to 1.4 % (175 °C, entry 2) and 1.8 % (200 °C, entry 3) for 4 h. Further to investigate effect of reaction time, reaction was carried out for 8 h at temperatures 150, 175 and 200 °C (entry 4 to 6). However no significant change was observed in bioethanol conversion and it was around 2.5 % at 200 °C (entry 6). Acetaldehyde was found as major reaction product and its selectivity was around 80% and that of acetic acid was around 20% for Ag/HZSM5 catalyst. Little higher conversion was achieved with 200 °C (2.5 %) as compared to 150 °C (0.5%) and 175 °C (1.5 %) for 8 h; hence it was decided to carry out reaction at 200 °C for Au supported on various zeolite catalysts.

Au supported on different zeolites (HZSM5, HY and Hβ) was employed for oxidation of bioethanol with Si/Al ratio of 35, 30 and 30 respectively. As compared to Ag/HZSM5, Au/HZSM5 gave higher bioethanol conversion (8%, entry 7) for 8 h, while at the end of 24 h 10% conversion (entry 8) was obtained with same catalyst. In case of Au/HY, 10%

(entry 9) and 15% (entry 10) conversion was achieved at 8h and 24 h respectively and for Au/Hβ, it was around 10% (entry 11) and 17 % (entry 12) for 8 h and 24 h respectively.

When reaction carried out with O_2/ethanol mole ratio equal to unity (entry 13), lower bioethanol conversion (13 %) was found in compared to O_2/ethanol mole ratio = 1.3 (entry 12) where 17 % conversion obtained. This indicates that in presence of excess oxygen higher bioethanol conversion was achieved.

Significant change in product distribution was observed for Au supported on different zeolite catalysts where acetone was chief reaction product with Au/HZSM5 and Au/HY, while acetaldehyde was dominant in case of Au/ Hβ even after 24 h. This was in contrast with reported literature [3–5, 7] where acetic acid was main reaction for long reaction time.

Table 3.4 Catalytic activity of 1% Ag/HZSM-5 for aerobic oxidation of bioethanol (reaction condition: 20 ml 2.5 wt% ethanol, P = 22 atm, wt. of catalyst = 150 mg catalyst and O_2/ethanol mole ratio = 1.3) and Au supported on various zeolites (reaction condition: 20 ml 2.5 wt% ethanol, P = 22 atm, wt. of catalyst = 150 mg, T = 200 °C and O_2/ethanol mole ratio = 1.3), * reaction carried out with O_2/ethanol mole ratio = 1

No.	Catalyst	Temp., °C	Time, h	Conv., %	Selectivity, %		
					Acetaldehyde	Acetic acid	Acetone
1	Ag/HZSM-5	150	4	0	--	--	--
2		175	4	1.4	78	22	--
3		200	4	1.8	80	20	--
4		150	8	0.5	100	--	--
5		175	8	1.5	79	21	--
6		200	8	2.5	80	20	--
7	Au/HZSM5	200	8	8	20	--	80
8			24	10	12	28	60
9	Au/HY		8	10	40	--	60
10			24	15	14	33	53
11	Au/Hβ		8	10	65	--	35
12			24	17	63	10	27
13	Au/Hβ*		24	13	60	--	40

Lower bioethanol conversion with Ag and Au supported on different zeolite catalysts may be due to the hydrophilic nature of supports with water. These results are supported by

Au-Pd/zeolite silicate-1 (prepared by conventional hydrothermal route) and Au-Pd@zeolite silicate-1 (prepared by solvent free synthesis) catalysts employed for oxidation of ethanol and varying concentration of ethanol-water as feedstock. Zhang et al.have shown that Au-Pd@zeolite silicate-1 catalyst exhibited higher activity due to its hydrophobicity nature, while Au-Pd/zeolite silicate-1 catalyst had under influence of water resulted in lower ethanol conversion [21]. Generally zeolites are hydrophilic in nature at lower Si/Al ratio and this argument was confirmed by several researchers [22–24]. They have shown that water adsorption capacity depends on Si/Al ratio which decreased with increased Si/Al ratio. The present catalysts can be categorized under lower Si/Al ratio which adsorbed water on surface resulted in hindering catalytical activity. Chen et al. [25] performed oxidation of ethanol using Au/ZSM5 with high Si/Al = 360 and achieved 30% ethanol conversion with 75% selectivity towards acetaldehyde at 250 °C. It was concluded that catalytical activity of present and reported catalyst highly depends on Si/Al ratio i.e. higher Si/Al ratio favored high catalytic activity where lower ratio resulted in decline activity.

Bioethanol oxidation with Ag and Au supported on different zeolites was found low in bioethanol conversion. Literature [26–28] revealed that presence of alkali enhanced the conversion of alcohols. Therefore it was decided to check effect of alkali (NaOH) for bioethanol oxidation with Ag/HZSM5 and Au/Hβ.

Na exchanged with H of ZSM5 or Hβ was synthesized as follow: 15 ml 10% NaCl per gm of support was mixed with HZSM5 or Hβ. The mixture was kept under reflux for 1 hour at boiling condition. At the end of 1 h Na exchanged HZSM5 or Hβ was filtered and named Na-HZSM5 or Na-Hβ. Obtained powder of Na-HZSM5 or Na-Hβ was washed several times with hot water to remove impurity. Ag/Na-HZSM5 and Au/Na-Hβ were synthesized according to wet impregnation method, as described in detail in section 3.3.1.2.

Ag/Na-HZSM5 and Au/Na-Hβ catalysts were employed for bioethanol oxidation for reaction condition as follows: 20 ml 2.5 wt% ethanol, P = 22 atm, wt. of catalyst = 150 mg, T = 200 °C, t = 24 h and O_2/ethanol mole ratio = 1.3. However no significant change was observed in the bioethanol conversion and it was around 2% and 10 %, respectively.

Later on, Ag/ZrO_2 purchased from stream chemicals was used for bioethanol oxidation without any purification. Results obtained with Ag/ZrO_2 for liquid phase oxidation of

bioethanol are shown in Table 3.5 (reaction condition: P = 22 atm, wt. of catalyst = 150 mg).

Table 3.5 Catalytic activity of Ag/ZrO$_2$ for aerobic oxidation of bioethanol (P = 22 atm, wt. of catalyst = 150 mg)

Entry	Ethanol, wt %	Temp, °C	Time, h	O$_2$/ethanol, mole ratio	Conv., %	selectivity, %	
						Acetaldehyde	Acetic acid
1	10	150	24	1.3	0	-	-
2	10	175	24	1.3	5	10	90
3	30	150	6	0.3	2	100	-
4	30	150	24	0.3	30	5	95

In case of Ag/ZrO$_2$, higher bioethanol concentration was employed as compared to Ag/HZSM5 and Au supported on zeolite catalysts. At 150 °C, no bioethanol conversion was observed (entry 1) which was increased to 5 % at 175 °C (entry 2). For 30 wt % bioethanol, conversion was increased from 2 % (entry 3) and 30 % (entry 4) with reaction time from 6 h and 24 h respectively at 150 °C. As compared to Ag/HZSM5 and Au supported on zeolite catalysts, Ag/ZrO$_2$ exhibited higher bioethanol conversion at cost of higher ethanol concentration. However, direct comparison of the catalysts cannot be made because of change in the reaction condition.

3.5 Conclusion

Various catalysts Ag/HZSM5, Au over different zeolite and Ag/ZrO$_2$ (purchased from Stream chemicals) were synthesized by wet impregnation method and characterized by FTIR and XRD. The characterization result indicates that no significant change was observed in structure of HZSM5, HY and Hβ. It remains intact after the impregnation of metal over zeolites. Presence of metal has also been confirmed by their characteristic peaks observed in the characterization. Lower catalytic activity with Ag/HZSM5 and Au over different zeolite can be due to the hydrophilic nature of zeolite at lower Si/Al ratio. Water may be adsorb over the surface of the supports and block the active sites which resulted into less bioethanol conversion.

Effects of various parameters like temperature, time, ethanol concentration, effect of alkali and O$_2$/ethanol mole ratio have also been studied. Increase in bioethanol conversion was observed with increased reaction time for all employed catalyst. No bioethanol was found with low bioethanol concentration (2.5 wt %) at 150°C, while 30 % bioethanol conversion

was achieved with high bioethanol concentration (30 wt %). In case of excess oxygen (O_2/ethanol mole ratio = 1.3) higher bioethanol conversion (17 %) found as compared to 13% conversion with O_2/ethanol mole ratio = 1. Unlike reported in literature that presence of alkali enhance that rate of oxidation in present study no significant change in bioethanol conversion was observed.

In product distribution acetaldehyde was remain main reaction product with selectivity more than 78 % for Ag/HZSM5 catalyst, while 22% selectivity towards acetic acid was observed and with Au supported on zeolites acetone was major reaction product. Acetic acid was obtained with Ag/ZrO_2 at higher reaction time and bioethanol concentration

References

[1] T. Mallat, A. Baiker, Oxidation of Alcohols with Molecular Oxygen on Solid Catalysts, Chem. Rev. 104 (2004) 3037–3058. doi:10.1021/cr0200116.

[2] A. Corma, H. Garcia, Supported gold nanoparticles as catalysts for organic reactions, Chem Soc Rev. 37 (2008) 2096–2126. doi:10.1039/B707314N.

[3] C.H. Christensen, B. Jørgensen, J. Rass-Hansen, K. Egeblad, R. Madsen, S.K. Klitgaard, S.M. Hansen, M.R. Hansen, H.C. Andersen, A. Riisager, Formation of Acetic Acid by Aqueous-Phase Oxidation of Ethanol with Air in the Presence of a Heterogeneous Gold Catalyst, Angew. Chem. Int. Ed. 45 (2006) 4648–4651. doi:10.1002/anie.200601180.

[4] B. Jørgensen, S.E. Christiansen, M.L.D. Thomsen, C.H. Christensen, Aerobic oxidation of aqueous ethanol using heterogeneous gold catalysts: Efficient routes to acetic acid and ethyl acetate, J. Catal. 251 (2007) 332–337. doi:http://dx.doi.org/10.1016/j.jcat.2007.08.004.

[5] K.-Q. Sun, S.-W. Luo, N. Xu, B.-Q. Xu, Gold Nano-size Effect in Au/SiO_2 for Selective Ethanol Oxidation in Aqueous Solution, Catal. Lett. 124 (2008) 238–242. doi:10.1007/s10562-008-9507-4.

[6] S. Tembe, G. Patrick, M. Scurrell, Acetic acid production by selective oxidation of ethanol using Au catalysts supported on various metal oxide, Gold Bull. 42 (2009) 321–327. doi:10.1007/BF03214954.

[7] D. Heeskens, P. Aghaei, S. Kaluza, J. Strunk, M. Muhler, Selective oxidation of ethanol in the liquid phase over Au/TiO_2, Phys. Status Solidi B. 250 (2013) 1107–1118. doi:10.1002/pssb.201248440.

[8] T. Takei, J. Suenaga, T. Ishida, M. Haruta, Ethanol Oxidation in Water Catalyzed by Gold Nanoparticles Supported on NiO Doped with Cu, Top. Catal. 58 (2015) 295–301. doi:10.1007/s11244-015-0370-4.

[9] A.K. Patra, A. Dutta, M. Pramanik, M. Nandi, H. Uyama, A. Bhaumik, Synthesis of Hierarchical Mesoporous Mn–MFI Zeolite Nanoparticles: A Unique Architecture of Heterogeneous Catalyst for the Aerobic Oxidation of Thiols to Disulfides, ChemCatChem. 6 (2014) 220–229. doi:10.1002/cctc.201300850.

[10] M. Clerici, Zeolites for fine chemicals production, Top. Catal. 13 (2000) 373–386. doi:10.1023/A:1009063106954.

[11] J.; Vanness, H.; Abbott, M.;(Eds.) Smith, Introduction to Chemical Engineering Thermodynamics, 7th Edition, Mcgraw Hill, (2009) 756–760.

[12] D.I. Enache, J.K. Edwards, P. Landon, B. Solsona-Espriu, A.F. Carley, A.A. Herzing, M. Watanabe, C.J. Kiely, D.W. Knight, G.J. Hutchings, Solvent-Free Oxidation of Primary Alcohols to Aldehydes Using $Au-Pd/TiO_2$ Catalysts, Science. 311 (2006) 362–365. doi:10.1126/science.1120560.

[13] Z.Y. Zakaria, J. Linnekoski, N.A.S. Amin, Catalyst screening for conversion of glycerol to light olefins, Chem. Eng. J. 207-208 (2012) 803–813. doi:10.1016/j.cej.2012.07.072.

[14] N.A.S. Amin, D.D. Anggoro, Characterization and activity of Cr, Cu and Ga modified ZSM-5 for direct conversion of methane to liquid hydrocarbons, J. Nat. Gas Chem. 12 (2003) 123–134.

[15] X. Zhang, X. Ke, H. Zhu, Zeolite-Supported Gold Nanoparticles for Selective Photooxidation of Aromatic Alcohols under Visible-Light Irradiation, Chem. - Eur. J. 18 (2012) 8048–8056. doi:10.1002/chem.201200368.

[16] G. Li, FT-IR studies of zeolite materials: characterization and environmental applications, (2005). http://ir.uiowa.edu/etd/96/ (accessed February 8, 2017).

[17] K. Shanjiao, G. Yanjun, D. Tao, Z. Ying, Z. Yanying, Preparation and characterization of zeolite beta with low SiO_2/Al_2O_3 ratio, Pet. Sci. 4 (2007) 70–74.

[18] M.M.J. Treacy; J.B. Higgins;(Eds.), collection of Simulated XRD Powder Patterns for Zeolites, Book. Fifth (5th) Revised Edition (2007).

[19] K. Shameli, M. Mansor Bin Ahmad, Z. Mohsen, W.Z. Yunis, N.A. Ibrahim, Fabrication of silver nanoparticles doped in the zeolite framework and antibacterial activity, Int. J. Nanomedicine. (2011) 331. doi:10.2147/IJN.S16964.

[20] J. Perez-Pariente, J.A. Martens, P.A. Jacobs, Crystallization mechanism of zeolite beta from (TEA)$_2$O, Na$_2$O and K$_2$O containing aluminosilicate gels., Appl. Catal. 31 (1987) 35 – 64. doi:http://dx.doi.org/10.1016/S0166-9834(00)80665-X.

[21] J. Zhang, L. Wang, L. Zhu, Q. Wu, C. Chen, X. Wang, Y. Ji, X. Meng, F.-S. Xiao, Solvent-Free Synthesis of Zeolite Crystals Encapsulating Gold-Palladium Nanoparticles for the Selective Oxidation of Bioethanol, ChemSusChem. 8 (2015) 2867–2871. doi:10.1002/cssc.201500261.

[22] T. Kawai; K. Tsutsumi(Eds.), Evaluation of hydrophilic-hydrophobic character of zeolites by measurements of their immersional heats in water, Colloid Polym. Sci. 270 (1992) 711–715.

[23] K. Chen, J. Kelsey, J.L. White, L. Zhang, D. Resasco, Water Interactions in Zeolite Catalysts and Their Hydrophobically Modified Analogues, ACS Catal. 5 (2015) 7480–7487. doi:10.1021/acscatal.5b02040.

[24] P. Sharma, J.-S. Song, M.H. Han, C.-H. Cho, GIS-NaP1 zeolite microspheres as potential water adsorption material: Influence of initial silica concentration on adsorptive and physical/topological properties, Sci. Rep. 6 (2016) 22734. doi:10.1038/srep22734.

[25] H. Chen, X. Jia, Y. Li, C. Liu, Y. Yang, Controlled surface properties of Au/ZSM5 catalysts and their effects in the selective oxidation of ethanol, Catal. Today. 256 (2015) 153–160. doi:10.1016/j.cattod.2015.01.020.

[26] S.K. Klitgaard, A.T. DeLa Riva, S. Helveg, R.M. Werchmeister, C.H. Christensen, Aerobic Oxidation of Alcohols over Gold Catalysts: Role of Acid and Base, Catal. Lett. 126 (2008) 213–217. doi:10.1007/s10562-008-9688-x.

[27] S. Carrettin, P. McMorn, P. Johnston, K. Griffin, C.J. Kiely, G.J. Hutchings, Oxidation of glycerol using supported Pt, Pd and Au catalysts, Phys Chem Chem Phys. 5 (2003) 1329–1336. doi:10.1039/B212047J.

[28] T. Mitsudome, A. Noujima, T. Mizugaki, K. Jitsukawa, K. Kaneda, Efficient Aerobic Oxidation of Alcohols using a Hydrotalcite-Supported Gold Nanoparticle Catalyst, Adv. Synth. Catal. 351 (2009) 1890–1896. doi:10.1002/adsc.200900239.

Chapter – 4

Gas Phase Oxidation of Bioethanol Using Various Metal Oxides

CHAPTER – 4

Gas Phase Oxidation of Bioethanol Using Various Metal Oxides

Au and Ag supported on HZSM5, HY and Hβ catalysts are being used for the liquid phase oxidation of bioethanol in previous chapter 3. But the obtained results of bioethanol conversion are not very impressive as compared to reported in the literature. Hence it is decided to carried out gas phase oxidation of bioethanol. In this chapter, Au and Ag nanoparticles supported on CeO_2, SiO_2 and ZrO_2 are examined for gas phase bioethanol oxidation with air. Catalysts prepared are characterized by XRD, FTIR, SEM and TEM. Catalytic behavior is evaluated between 200 - 350 ℃ and 5 atm with gas hourly space velocity of 18000 mL g_{cat}^{-1} h^{-1}. Au/ZrO_2 and Au/CeO_2 are found   more active than other catalysts. Less activity of Ag/ZrO_2 and $Au-Ag/ZrO_2$ is attributed to facile oxidation of Ag under aerobic conditions. Acetaldehyde selectivity follows the order: Au/CeO_2> Ag/ZrO_2> $Au-Ag/ZrO_2$> Au/ZrO_2> Au/SiO_2 under optimal conditions.

4.1 Introduction

Continuous depletion and uncertain prices of the available fossil resources pose new challenges to the future chemical industries, as majority (>90%) of carbonaceous chemicals are produced from oil. To produce bulk and fine chemicals, chemical industry must rely on renewable resources such as biomass instead of depleting fossils. In this respect, biomass can be an alternate for the production of high value commodity chemicals and fuels. Currently, almost 90% of ethanol is produced from biomass with an annual bioethanol production reached to 114 billion liters in 2013 [1]. Bioethanol produced via, fermentation route contains typically 90% of water, which needs be removed before alcohol's further application [2]. Process of anhydrous bioethanol is energy intensive, therefore it is suggested that bioethanol to be converted to value added chemicals through reactions which are not sensitive to its water content [3]. For instance, bioethanol can be used as renewable feedstock for production of H_2 through catalytic steam reforming [4], 1-

butanol [5], isobutene [6], 1,3-butadiene [7], ethyl acetate [8], acetaldehyde [9] and acetic acid [10] through selective oxidation or dehydrogenation [11].

Use of inorganic oxidants for conversion of alcohol to aldehydes, ketones and carboxylic acids leads to toxic wastes [12]. To avoid potential contamination from inorganic oxidizers uses of molecular oxygen and air as greener oxidant have been increased in past several years.

Various heterogeneous catalysts like Ru on different oxides [13], Au/SiO$_2$ [14], Ru(OH)$_x$ supported on titania, alumina, ceria and spinel oxides [15] and Au nanoparticles supported on NiO doped with Cu [16] have been investigated for liquid phase oxidation of ethanol and found to chiefly form acetic acid.

Rossi and Biella [17] studied gas phase oxidation of primary and secondary alcohols over the 1 wt % Au/SiO$_2$ and in this case combined selectivity to aldehydes and ketones reached around 100%. This catalyst was also active in liquid phase ethanol oxidation to acetic acid [14]. Pd/Al$_2$O$_3$ [18], alkali promoted Pt/Al$_2$O$_3$ [19], Au/CeO$_2$ [20], Au on ordered mesoporous silicas and conventional silicas [21] ,V$_2$O$_5$/TiO$_2$ [22,23], zeolite encapsulated Au nanoparticles [24], Au/TiO$_2$ [25], Au supported on metal oxides [26], MoVNbTe mixed oxides [27], Mo$_{0.61}$V$_{0.31}$Nb$_{0.08}$Ox/TiO$_2$ [28], Sn–Mo–O catalysts [29] and Au/ZSM-5 [30] with high Si/Al ratio (360:1) were employed for ethanol oxidation to carbonyl compounds. Among these catalysts, supported Au nanoparticles were found to be most promising for aerobic oxidation of ethanol mainly due to good stability against metal oxidation. Catalytic performance of supported Au nanoparticles in presence of oxygen was confirmed to be superior to non-oxidative ethanol dehydrogenation [21]. Catalytic performance depends on particles size [21,24,31] and acid - base or redox properties of the support [11]. Supported bimetallic Au-Cu [32] and Au-Ir [33]catalysts have also been reported for aerobic oxidation of ethanol. However with these catalysts, higher reaction temperature resulted in lower acetaldehyde selectivity and poor catalyst stability.

Cerium oxide (CeO$_2$) is a rare earth oxide and because of its unique properties which include oxygen mobility, non-toxicity, high chemical stability and high charge transfer capacity has received attention from many researchers [34]. CeO$_2$ has two valence states- Ce^{3+} and Ce^{4+} and easy transformation between these two states is an imperative factor in its catalytic activity. This rapid change of oxidation states is related to its ability to store

and release oxygen, a property often measured as Oxygen Storage Capacity (OSC) [35]. It serves as an active oxygen donor in many reactions, such as three-way catalytic reactions, low temperature water gas shift reaction, oxygen sensors, oxygen permeation membrane systems and fuel cells [36].

Zirconia (ZrO_2), due to its acidity, basicity, superficial vacancies and oxygen mobility [37,38] is used as solid support that can improve catalytic activity of transition metals. ZrO_2 has been applied for many organic reactions such as water-gas shift reaction, cumene decomposition, alcohols oxidation and acrylic ester synthesis [39].

Most previous reported work on ethanol oxidation used high ethanol concentration (50-100%) in water. Though CeO_2 and ZrO_2 are well known solid supports but have not been considered for bioethanol oxidation using group 1B metals. In this study, we have examined catalytic behavior of (1) Au supported on CeO_2, ZrO_2 and SiO_2 and (2) Ag and Au-Ag supported on ZrO_2 for gas phase oxidation of aqueous ethanol (10 wt %).

4.2 Experimental section

4.2.1 Synthesis of catalyst

Catalysts are prepared using the wet impregnation method. 1% Au over CeO_2, ZrO_2 and SiO_2 are synthesized according to this method, as described in detail in chapter 3 (section 3.3.1.2). Other catalysts, Au, Ag (1 wt%) and Au-Ag (0.5-0.5 wt%) on ZrO_2 are prepared as described elsewhere [40], in which prepared catalysts were calcined at 450 °C (3 °C min-1) for 5 h under air flow and reduced under H_2 flow at 250 °C (10 °C min-1) for 1.5 h.

4.2.2 Catalyst characterization

Surface morphology of the catalyst is investigated with scanning electron microscopy (SEM) (JEOL make model 7600F FESEM) and transmission electron microscopy (TEM) (Philips CM 200 operated at 200kV). Catalyst structures are examined by X-ray diffraction (XRD) on a Bruker - D8 Discover equipped with a Ni-filtered Cu Kα radiation source (λ = 1.542 Å) of 40 kV and 30 mA. FTIR spectra of samples are collected in

reflection mode using ZnSe optics in Bruker Alpha Eco-ATR spectrometer. The instrument was operated in the range of 400 - 4000 cm^{-1}.

4.2.3 Catalyst activity test

Catalysts were tested for ethanol conversion using heated stainless steel continuous fixed bed down flow reactor. For reaction, 1g of catalyst was loaded in the reactor. Prior to entering the reactor, reactant (aqueous ethanol, 10 wt %) was vaporized in a pre heater and mixed with synthetic air (21 % O_2, 79% N_2). Volumetric composition of feed mixture ethanol/O_2/N_2 is 0.002:20.95:78.84. Corresponding air flow rate was 300 mL/min and the GHSV is 18000 mL g_{cat}^{-1} h^{-1} for all experiments. The mixture passed through catalyst bed for 1 h before monitoring reaction product. Temperature inside the reactor was measured by an internally positioned thermocouple placed on the catalyst bed. Reaction products were analyzed by a gas chromatography using Shimadzu Equity-5 innowax column (30 m, 0.32 mm, 0.25 μm) with both a flame ionization detector (FID) and thermal conductivity detector (TCD).

Catalytic performance of the system was evaluated on the basis of conversion of bioethanol and products selectivity as defined in section 3.3.2.1.

Figure 4.1 Picture of reactor used for Gas phase oxidation of bioethanol

4.3 Result and discussion

4.3.1 Catalyst characterization

The catalysts were characterized using Fourier transform infrared spectroscopy (FTIR), x-ray diffraction pattern (XRD), Transmission electron microscopy (TEM) and scanning electron microscopy (SEM).

4.3.1.1 Scanning electron microscope

SEM images of supported metal (Au, Ag and Au-Ag) particles, as shown in Figure 4.2, show the metal particles to be uniformly distributed on the surface. In some surface areas, clusters containing several metal nanoparticles are observed however it is difficult to identify the size of metal cluster. In addition, presence of small metal particles identified on SEM images was consistent with X-ray diffraction results.
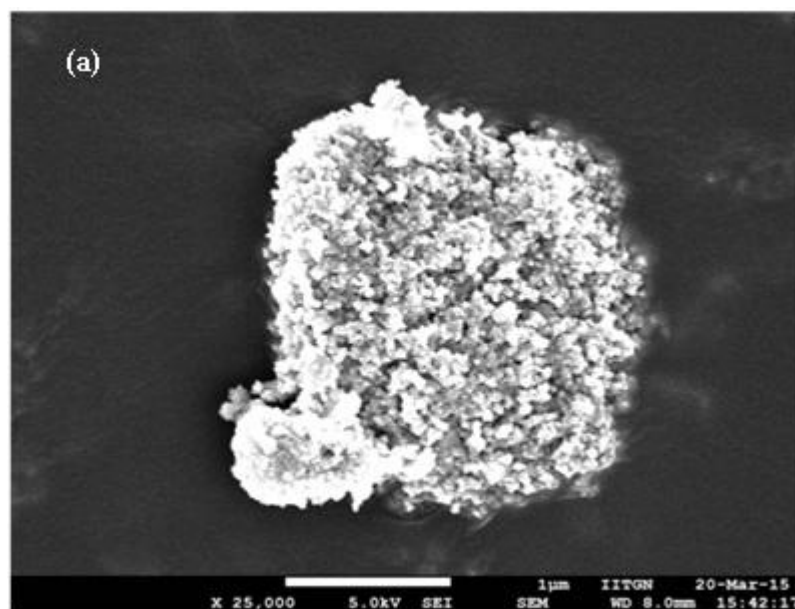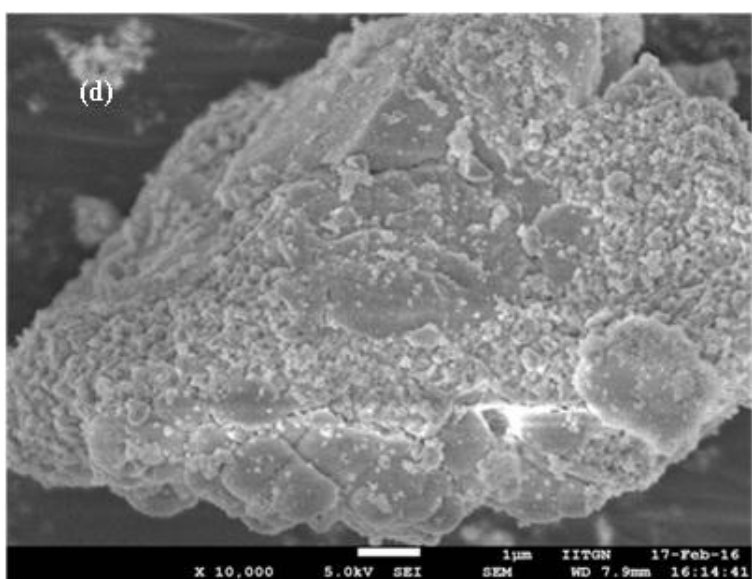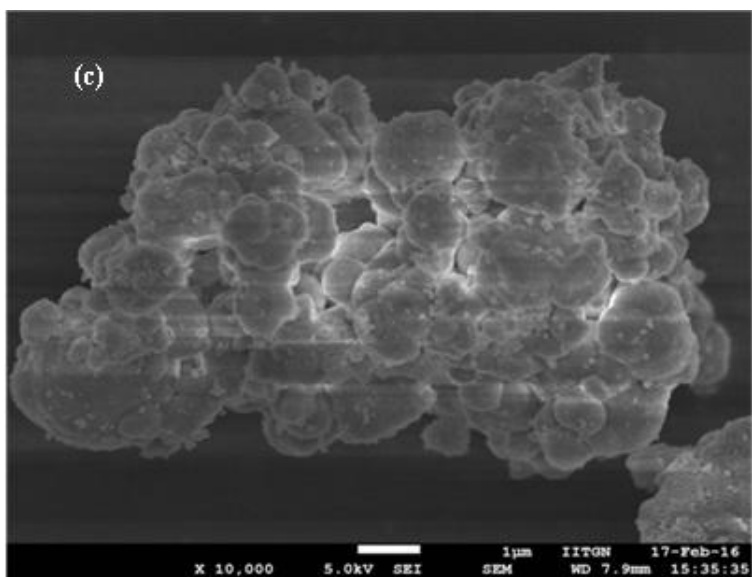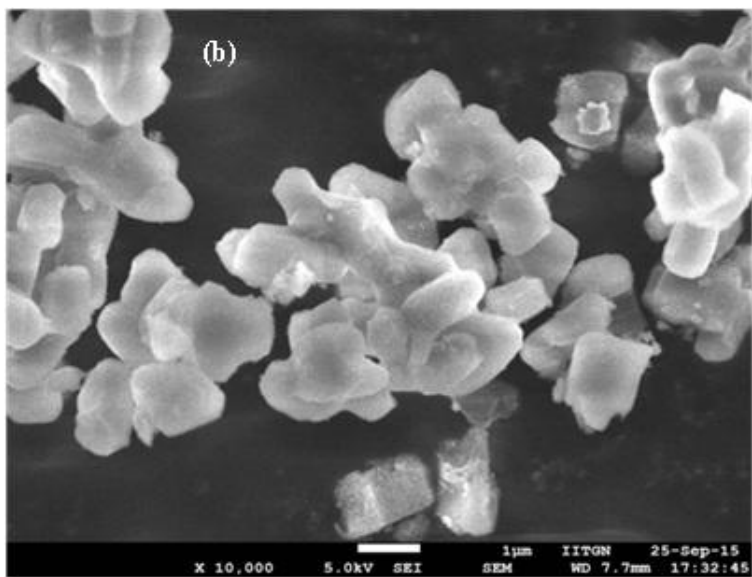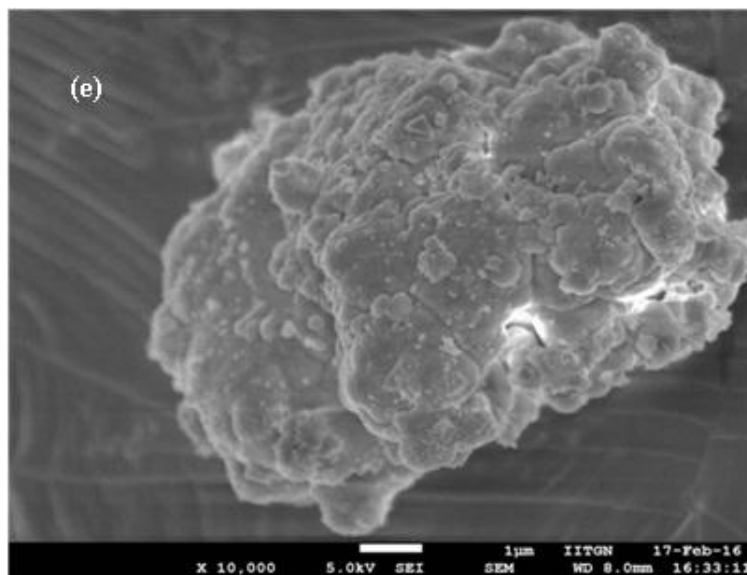
Figure 4.2 SEM images of (a) Au/CeO$_2$ (b) Au/SiO$_2$ (c) Au/ZrO$_2$ (d) Ag/ZrO$_2$ and (e) Au - Ag/ZrO$_2$

4.3.1.2 Transmission electron microscope

TEM images of metal nanoparticles supported on CeO$_2$, SiO$_2$ and ZrO$_2$ shown in Figure 4.3 (a – e) reveled that metal nanoparticles are on the surfaces of CeO$_2$, SiO$_2$ and ZrO$_2$. TEM images for Au/CeO$_2$ (Figure 4.3 (a)) and Au/SiO$_2$ (Figure 4.3 (b)) showed that average Au particles size are in the range of 15-20 nm and 25-30 nm, respectively. TEM images of Au, Ag and Au-Ag on ZrO$_2$ are Figure 2(4.3 (c), (d) and (e), respectively) which show metal particles size of 10-12 nm, 5-8 nm and 15-20 nm respectively.
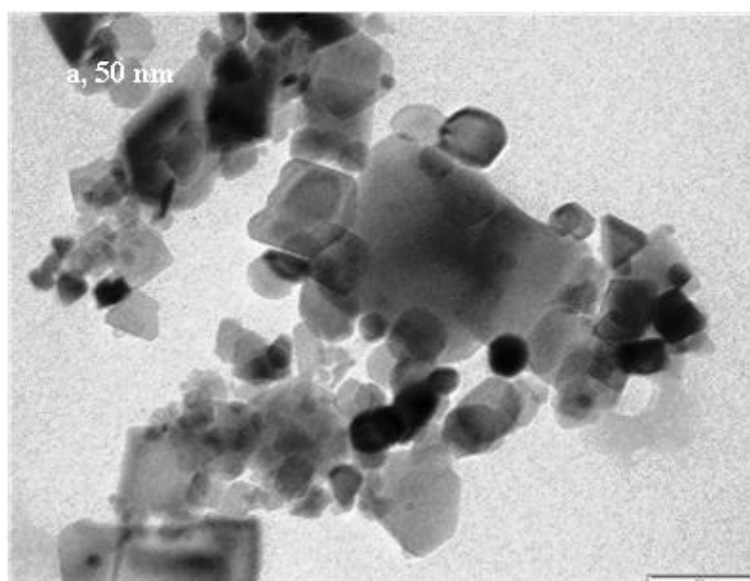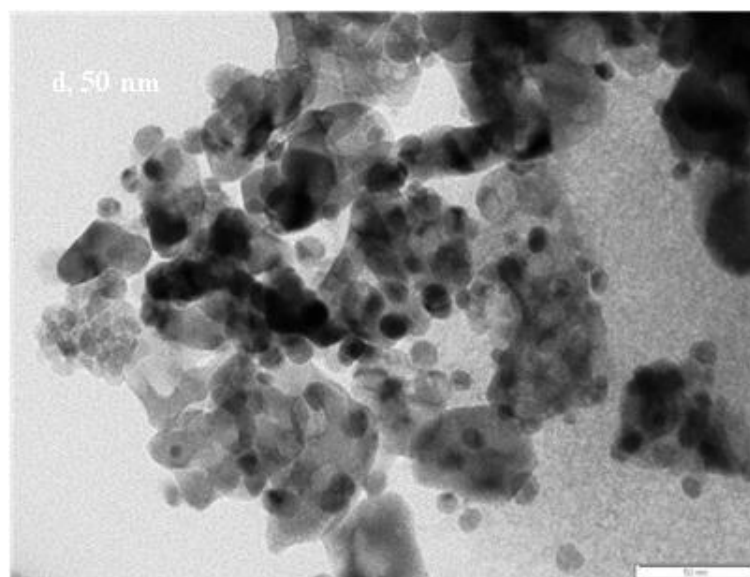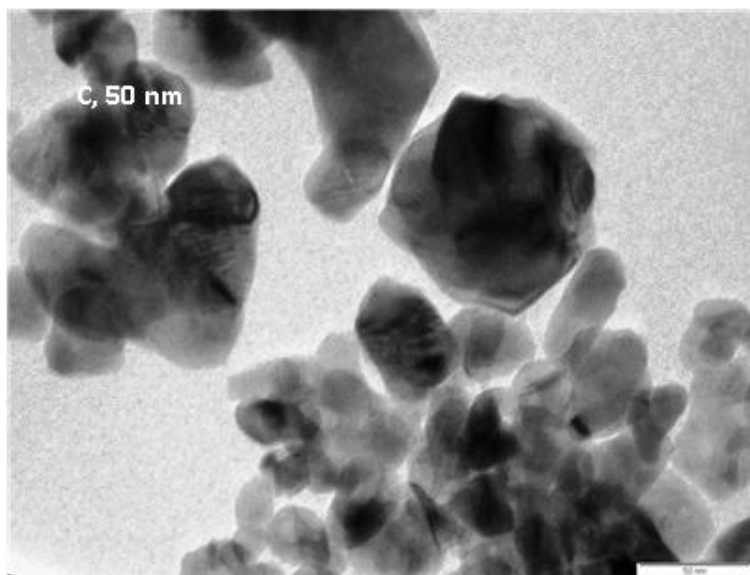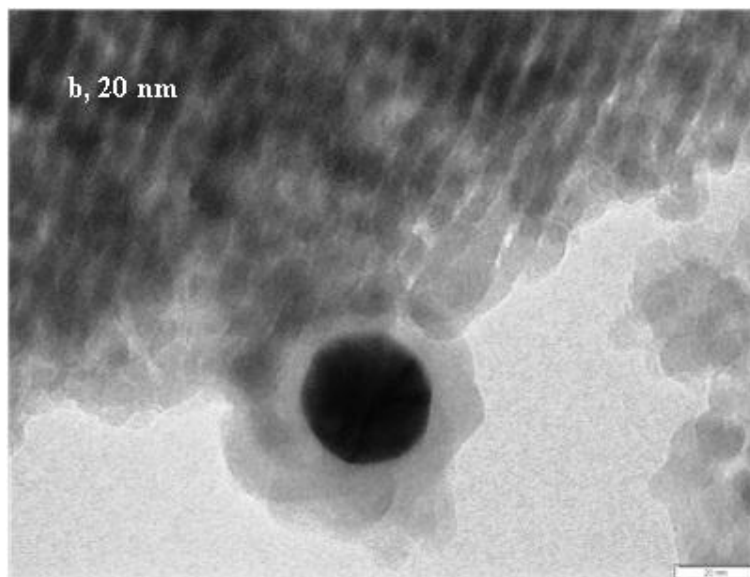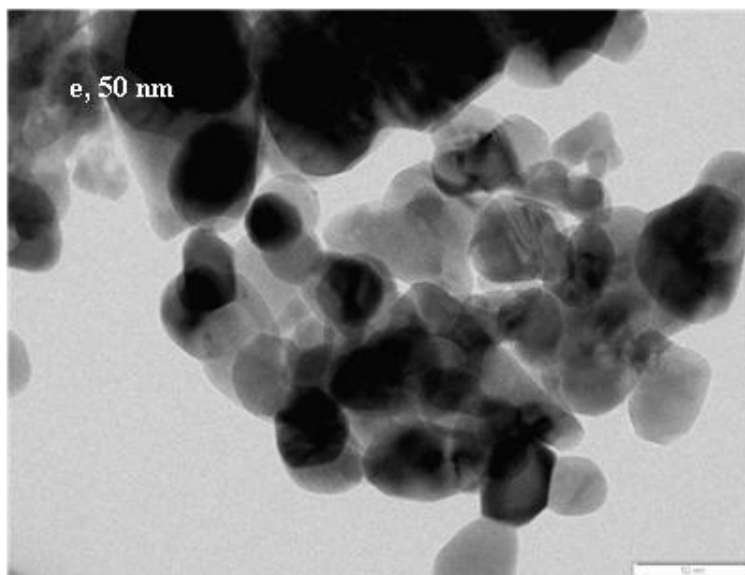
Figure 4.3 TEM images of (a) Au/CeO$_2$ (b) Au/SiO$_2$ (c) Au/ZrO$_2$ (d) Ag/ZrO$_2$ and (e) Au - Ag/ZrO$_2$. Scale bar dimensions are mentioned inset.

4.3.1.3 Powder X-ray Diffraction

Au/CeO$_2$ catalyst analyzed by XRD to confirm the crystalline phase of the support and to get an idea as to metal particle size and the result is shown in Figure 4.4 (A). Peaks observed at 2θ = 28°, 33°, 47.5°, 56°, 59° and 76° are respectively assigned to (111), (200), (220), (311), (222), and (331) planes of the cubic-fluorite structure (space group Fm3m) of CeO$_2$ (JCPDS-34-0394) [41].

Absence of peak specifically at 2θ = 38.1° (Au (111) plane), implies low loading and small cluster size. Mean crystallite size of the support CeO$_2$ calculated by the Scherrer formula is 30 nm which agrees well with that observed with TEM.

Powder XRD pattern of Au/SiO$_2$ is shown in Figure 4.4 (B). Here four sharp peaks are observed at 2θ = 38.2°, 44.3°, 64.5° and 77.6°to the(111), (200), (220) and (311) lattice planes of Au particles, respectively. Mean crystallite size of Au particles calculated by the Scherrer formula is 28 nm.
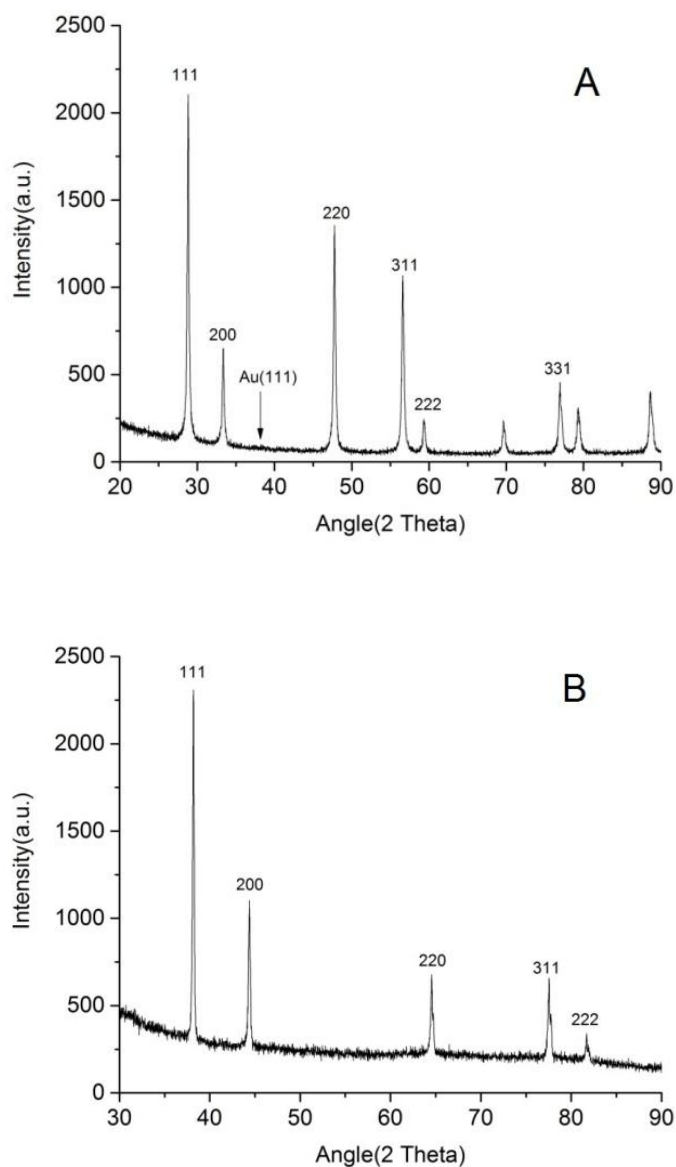
ZrO_2 supported metal catalysts have same XRD pattern as shown in Figure 4.4 (C). The diffraction peaks at 24.2°, 28.2°, 31.4° and 34.3°(JCPDS 37-1484) confirmed the mono clinic phase of ZrO_2 [40]. Au-Ag (0.5 wt % each) alloy and Au and Ag metal could not be distinguished from XRD pattern, as Au and Ag have same lattice constant [42]. Au, Ag and Au-Ag alloys have almost similar lattice plane at identical position of the 2θ such as (111) planes at 38.1°, (200) at 44.3° and (220) at 64.6 ° (Figure 4.4(C)).
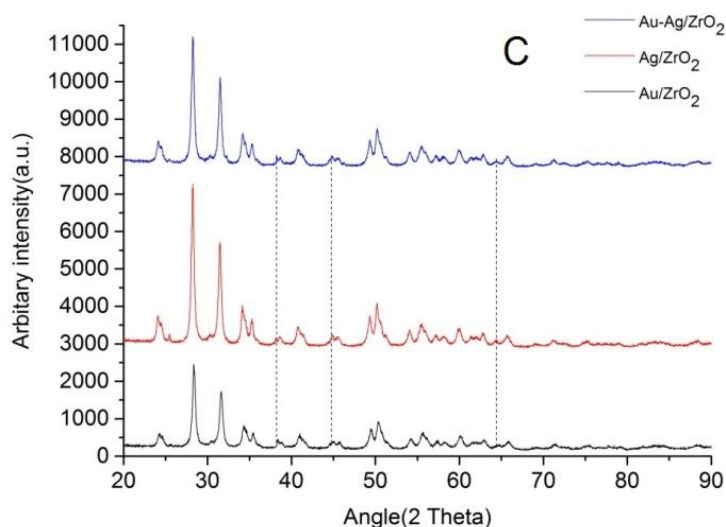
Figure 4.4 XRD pattern (A) Au/CeO$_2$ (B) Au/SiO$_2$ and (C) ZrO$_2$ supported metal particles

4.3.1.4 Fourier Transform Infrared Spectroscopy

FTIR spectra of Au/CeO$_2$ in the region of 600 -1800 cm^{-1} are shown in Figure 4.5 (A). Here band observed at around 1640 cm^{-1} is attributed to bending vibrations due to the surface hydroxyl group and strong band at 1533 cm^{-1} is due to Ce-OH stretching vibration [43]. Strong absorption band at 538 cm^{-1} is assigned to the stretching vibration of Ce -O-Ce. A slight decrease in band height at 538 cm^{-1} observed for Au/CeO$_2$,confirms impregnation of Au on CeO$_2$ [44].

FTIR spectra of Au/SiO$_2$ in the region of 500-3500 cm^{-1} are shown in Figure 4.5(B). In IR spectra, water bands observed at around 3296 and 1620 cm^{-1} corresponding to stretching and bending vibrations of the SiO$_2$. Strong bands observed at 1075 cm^{-1} was assigned to the stretching vibration of Si-O-Si. A decrease in heights at 792 cm^{-1} indicates Au on SiO$_2$ [45].

IR spectra of ZrO$_2$ supported metal particles are shown in Figure 4.5(C). Here bands at 1362cm^{-1} and 668 cm^{-1} correspond to O-H bonding and mono clinic phase of ZrO$_2$. Metals impregnation on ZrO$_2$ confirmed by decreased peak height at 574 cm^{-1} [46].
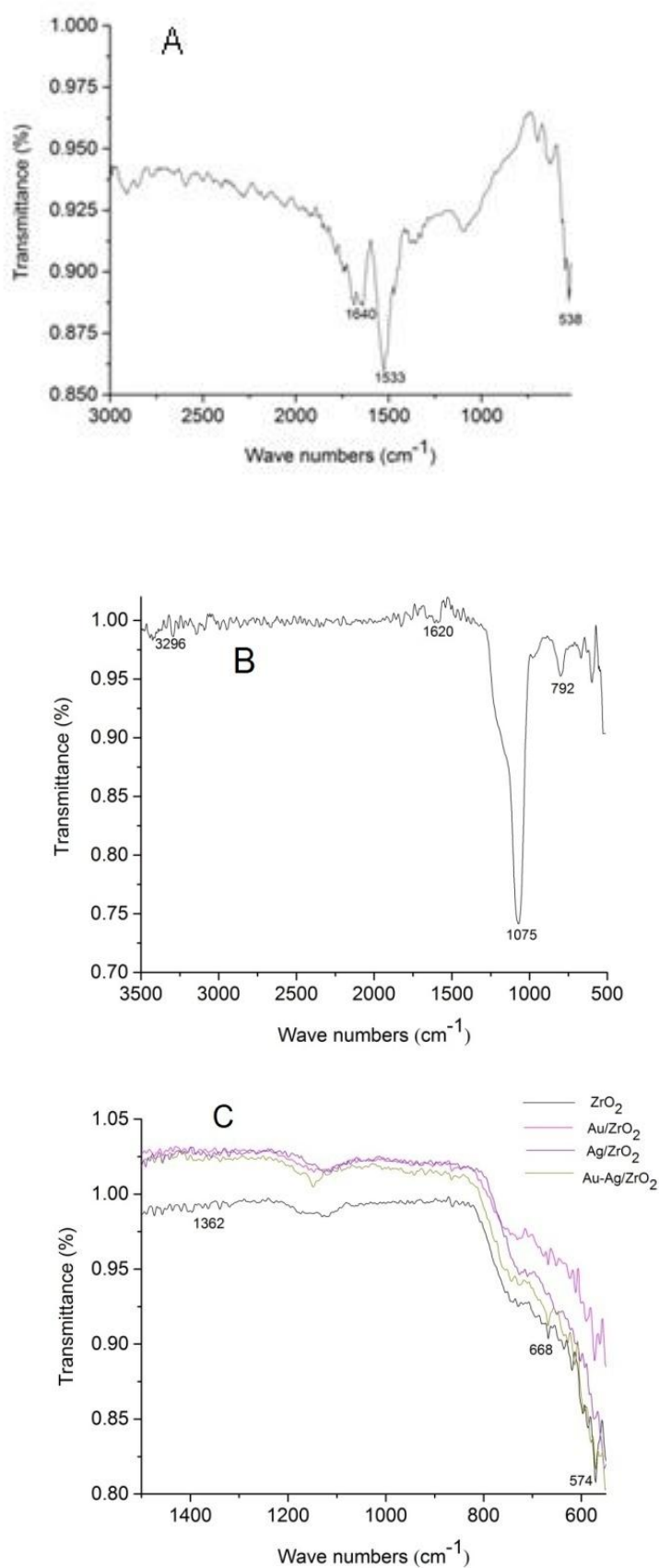
Figure 4.5 FTIR of (A) Au/CeO$_2$ (B) Au/SiO$_2$ and (C) ZrO$_2$ supported metal particles

4.3.2. Catalyst activity studies

4.3.2.1 Effect of Temperature

Figure 4.6 shows temperature dependence of gas phase oxidation of 10 wt% aqueous ethanol over various catalysts. All Au, Ag and Au-Ag nanoparticles supported on CeO_2, SiO_2 and ZrO_2 showed negligible conversions at 200°C which gradually increased with temperature. Au/ZrO_2 showed highest activity with ethanol conversion up to 38 % at 350°C followed by Au/CeO_2 (34 %, bioethanol conversion). With Au/SiO_2, ethanol conversion for entire temperature range was found to be much lower compared to that with Au supported either on ZrO_2 or CeO_2 and the least among the catalysts studied. Lower activity of Au/SiO_2 can be attributed to its reported inertness and lack of supply or activate oxygen as opposed to CeO_2 and ZrO_2 [24]. Gazsi et al. [47] reported 8% ethanol conversion with 90% selectivity towards acetaldehyde employing Au/SiO_2 at 350 °C and GHSV of 12000 $mLg_{cat}^{-1}h^{-1}$, where as in this case these values respectively are 18% and 80% with slightly higher GHSV value. We found that Ag/ZrO_2 to afford 27% ethanol conversion which was higher than that reported by Freitas et al. [40] (23%) using pure ethanol and higher loading of Ag (2 wt %) on ZrO_2. Variation in this performance may be due to less Ag dispersion in the latter case, thus high loading (2 wt%) of Ag nanoparticles may lead to larger size of metal clusters causing lower catalytic activity in the reported work by Freitas et al. [40]. Lower conversion with Ag/ZrO_2 as comparison with Au/ZrO_2 and Au/CeO_2, also reported by Liu et al. [48] and Freitas et al. [40] can be ascribed to facile oxidation of Ag^0 to Ag^+ under aerobic conditions, and oxidized Ag may not be active for oxidation reaction. Further, this also may be due to absence of electron charge transfer between Ag and ZrO_2 [49] and weaker interaction between Ag and ZrO_2 than other metals [50].

Au/CeO_2 exhibited higher catalytic activity (34 %, bioethanol conversion) compared to Ag/ZrO_2 (27 %, bioethanol conversion), $Au-Ag/ZrO_2$ (23 %, bioethanol conversion) and Au/SiO_2 (18 %, bioethanol conversion) because under reaction conditions CeO_2 was able to provide activated oxygen with concurrent creation of oxygen vacancies which could further play a role of activating reactant oxygen molecules reaching from the gas phase [51].
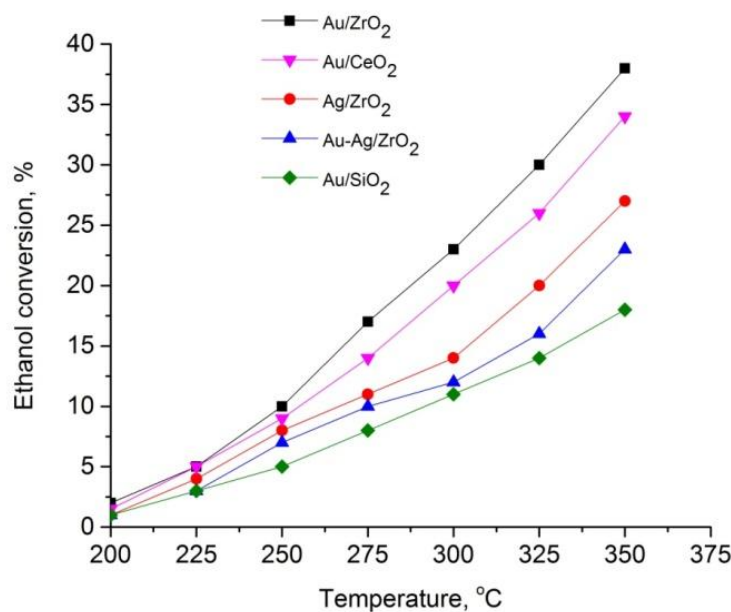
Figure 4.6 Ethanol conversions over different catalysts as function of reaction temperature. (Reaction condition: 1 g catalyst, pressure = 5 atm, time-on-stream = 4h, ethanol/O_2/N_2 (vol %) = 0.002:20.95:78.84 and GHSV =18000 mLg$_{cat}^{-1}$h^{-1}.)

In case of Au/ZrO$_2$, Au leads partial reduction of surface Zr^{4+} to Zr^{3+} which creates oxygen deficiencies on ZrO$_2$ surface. This phenomenon results into (i) enhanced concentration of anionic vacancies on ZrO$_2$ surface, and (ii) oxygen spill over from surface OH group on ZrO$_2$ to Au. This spilled over active O atom imparts catalytic activity for oxidation reaction. Li et al. [52] too advanced similar argument to explain higher activity of Au/ZrO$_2$ in water-gas shift reaction.

Stable catalytic performance of Au/ZrO$_2$, Ag/ZrO$_2$ and Au-Ag/ZrO$_2$ for ethanol oxidation was ensured by performing the reaction for prolonged duration. Catalytic activity of all of them did not change significantly even after 30 h time-on-stream (38%, 27% and 23% ethanol conversion and 72%, 80% and 80% acetaldehyde selectivity, respectively) at 350 °C, 5 atm and 18000 mLg$_{cat}^{-1}$h^{-1}GHSV.

While ethanol conversion followed the order Au/ZrO$_2$> Au/CeO$_2$> Ag/ZrO$_2$> Au-Ag/ZrO$_2$> Au/SiO$_2$, acetaldehyde selectivity showed the trend, Au/CeO$_2$> Ag/ZrO$_2$> Au-Ag/ZrO$_2$> Au/ZrO$_2$> Au/SiO$_2$.

4.3.2.2 Product selectivity for ethanol conversion over different catalysts

Figure 4.7 depicts selectivity to products, namely acetaldehyde, acetic acid, ethyl acetate, acetone and CO_2 as a function of reaction temperature. For Au/SiO$_2$, acetaldehyde selectivity changed considerably from 90% at 250 °C to 72% at 350 °C with a compensating increase in selectivity to acetic acid. This implies acetaldehyde to be a primary product which subsequently converts to acetic acid. Earlier various researchers [3,14,28] had observed similar trend in the reaction of ethanol oxidation.

Notably, with Au/CeO$_2$, selectivity to acetone and CO_2 increased with temperature at the cost of acetaldehyde selectivity implying this catalyst having higher oxidation activity. Still, it did show very high (exceeding 95%) selectivity for acetaldehyde up to 275°C. Acetone formation was explained as acetaldehyde oxidation to acetates on oxide surface and their subsequent coupling reactions yield acetone [20,53].
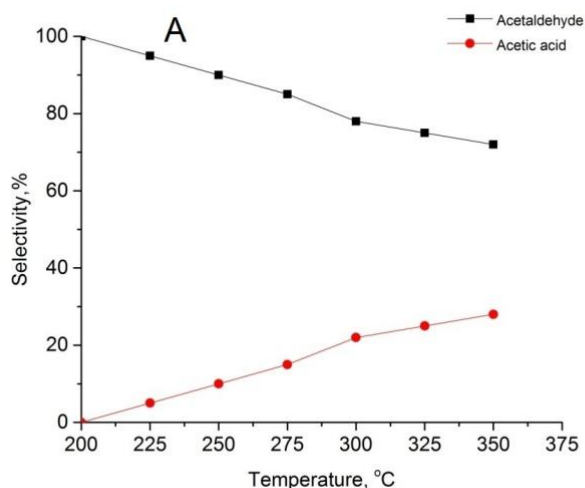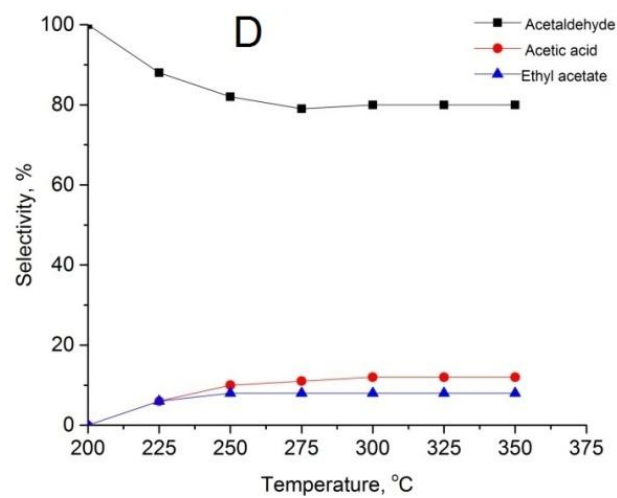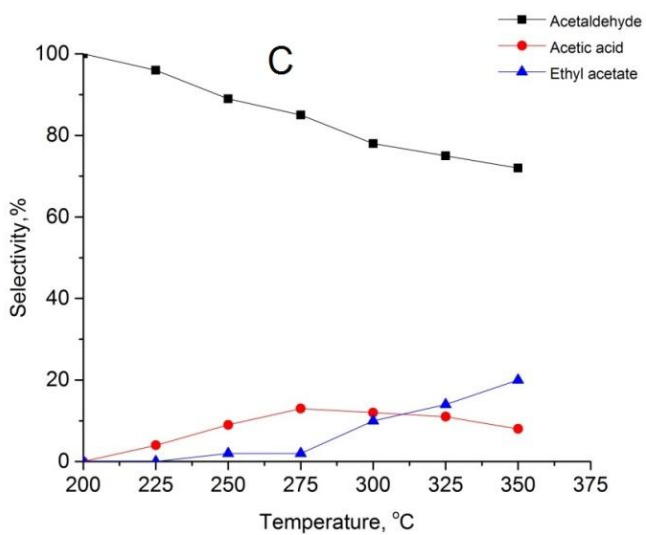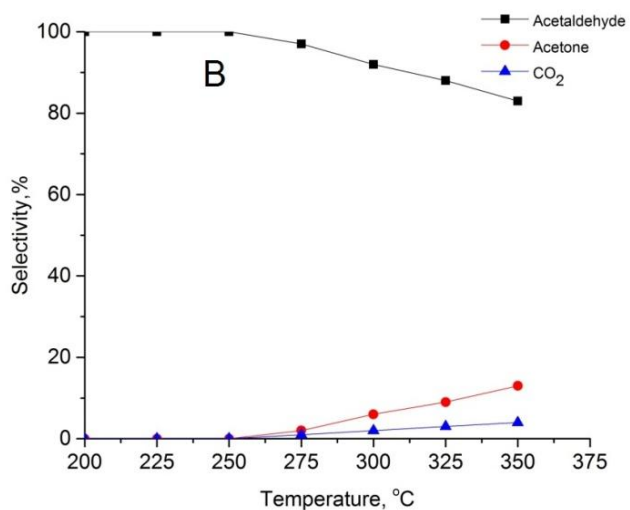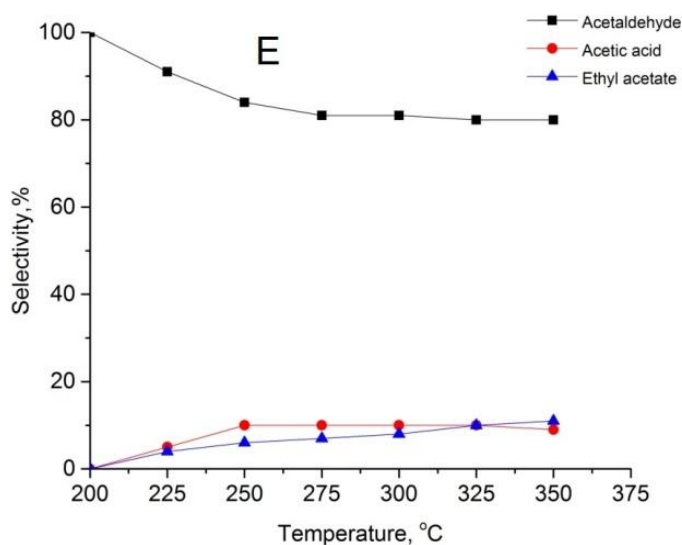
Figure 4.7 Product selectivity for ethanol conversion over different catalysts as function of reaction temperature (a) Au/SiO_2 (b) Au/CeO_2 (c) Au/ZrO_2 (d) Ag/ZrO_2 and (e) Au-Ag/ZrO_2 (reaction conditions: 1 g catalyst, pressure = 5atm, time on stream = 4h, ethanol/O_2/N_2 (vol %) = 0.02:20.99:78.99 and GHSV =18000 $mLg_{cat}^{-1}h^{-1}$.)

In case of Au, Ag and Au-Ag supported on ZrO_2, ethanol adsorbs on M^+(Au, Ag, Au-Ag), metal particles or ZrO_2 surface generating ethoxide ($CH_3CH_2O^*$) [40]. The ethoxide species adsorbed on ZrO_2 spill over to M^+ and then convert to acetaldehyde by dehydrogenation. Formed acetaldehyde was oxidized to acetic acid on metal surface or spill over toward ZrO_2 surface. Acetaldehyde activation by M^0 at metal surface and ethanol activation by the support leads to coupling reaction between acetaldehyde and ethanol at the interface between metal and support to form ethyl acetate as the mechanism proposed by Letichevsky et al. [54] and Freitas et al. [40]. Acetaldehyde spill over from metal surface to ZrO_2 has been reported by Zonetti et al. [55] and Rodrigues et al. [56].

Although acetaldehyde selectivity decreased with temperature on these catalysts, it was found to be the chief reaction product. Acetic acid and ethyl acetate are two other products formed. Selectivity to acetic acid and ethyl acetate remained almost constant with temperature in case of Ag/ZrO_2 and $Au-Ag/ZrO_2$, while for Au/ZrO_2 selectivity for acetic acid decreased and that for ethyl acetate increased after 275°C. Also, on Ag based catalysts higher selectivity towards acetaldehyde (against Au based catalysts) was observed. Metal more susceptible to oxidation (e.g., Ag) was expected to afford higher

selectivity to acetaldehyde where as metal in reduced state (e.g., Au), higher ethyl acetate selectivity has been reported for Cu [57]. Grabowsaki et al. [58] have confirmed oxidation of Ag with simultaneous reduction of its support, ZrO_2. Freitas et al. [40] too found Cu-Ag/ZrO_2 to lead to higher formation of acetaldehyde advancing the same reasoning. Freitas et al. [40] performed CO-DRIFTS and XPS analysis to investigate effect of addition of Ag in Cu nanoparticles supported on ZrO_2. They found that increased loading of Ag from 0.3 wt % to 2 wt% led to decrease Cu^0/Cu^+ ratio which facilitates higher acetaldehyde selectivity at the expense of ethyl acetate. In case of Au-Ag/ZrO_2, higher selectivity towards acetaldehyde (80%) compared to Au/ZrO_2 (72%) indicating that Ag leads to decrease Au^0/Au^+ ratio.

Formation of ethyl acetate can be explained by acetaldehyde activation on M^0 sites which couples with ethanol species activated by ZrO_2 surface. The coupling reaction occurred at the interface between metal and support [55,57,59]. Similarity in product pattern between these reports and the present work, one can safely extrapolate the reaction mechanism for Au/ZrO_2 system. Further, Cu and Au bind more strongly to ZrO_2 as compared to Ag does. Thus, this binding energy also can be envisaged to play a role in determining product selectivity.

When the reaction was carried out at higher (10 atm) pressure, all the catalysts studied showed higher activity reflected in higher conversion values, though, product distribution was relatively insensitive to pressure.

4.4 Comparison of performance of catalyst with those of the previous work

A quick glance at relevant literature would confirm that very few studies deal with ethanol concentration typical for bioethanol, i.e., about 10% aqueous solution. Table 4.1 compares the performance of catalysts studied in this work and that of the catalyst systems with common support and metals with this work. Also this summary has been limited to the reaction performed in continuous mode. To start with, our catalyst, Au/ZrO_2 (Entry 9) afforded 38% ethanol conversion and 72% acetaldehyde selectivity at 350 °C and 5 atm. Very high (80%) ethanol conversion had been reported over PdO/m-ZrO_2 (Entry 6) catalyst. However, this high conversion needed 15 h of reaction and pure ethanol. The former is impractical for continuous mode of operation and the latter necessitates energy intensive purification of bioethanol. In case of Entry 10, reaction at lower temperature

afforded complete conversion but this was accompanied by relatively poor selectivity to acetaldehyde. Entry 11 shows the system exhibiting good catalytic performance, however, it involves usage of poisonous Cr_2O_4 as support. Cu-Ag supported on ZrO_2 (Entry 13) gave higher conversion but, poor selectivity and required pure ethanol. Thus among all ZrO_2 based catalysts, the one reported in this work, outperforms in terms of catalytic performance, and "greenness" of the process. Entries 4 and 5 describe the same catalysts. However, higher selectivity observed in this work, may have to do with the presence of water. This may be substantiated by the fact that in our case higher temperature is needed to get the comparable conversion. In case of Au/SiO_2 (Entry 3), though pure ethanol was employed, conversion obtained was very poor, 17%. Though, it did give very high selectivity and that too at lower reaction temperature as compared to that in this work (Entry 2). The same catalyst, in the absence of external oxygen source did give acetaldehyde in the product, the conversion was poor (Entry 1). This comparison leads to an inference that for bioethanol oxidation, the catalyst system arrived at in this work, namely, Au/ZrO_2 is best from catalytic performance, energy consumption and toxicity of the materials points of view.

Table 4. 1 Comparison of various supported metal catalyst from literature and present work for gas phase ethanol oxidation

Entry	Catalyst	Metal loading (Wt %)	EtOH in feed (%)	T, °C	P, atm	Ethanol/O_2/carrier gas (Vol %)	x,%	S, %	Time-on-stream, h	GHSV, mLg$_{cat}^{-1}$h^{-1}	Reference
1	Au/SiO$_2$	1	10	350	-	9-10/0/90	8	90	-	12000	47
2	Au/SiO$_2$	1	10	350	5	0.02:20.99:78.99	18	72	4	18000	This work
3	Au/SiO$_2$	1	100	200	-	1:1:98	17	99	-	120000 [#]	33
4	Au/CeO$_2$	1	100	200	1	1:2 (ethanol:O$_2$)	31.8	56	-	257120	20
5	Au/CeO$_2$	1	10	350	5	0.02:20.99:78.99	34	83	-	18000	This work
6	PdO/m-ZrO$_2$	0.6	100	175	4	3.0:19.4:77.6 [#]	80	10	15	10200	54
7	Ag/ZrO$_2$	2	99.9	250	-	inert atmosphere	24	31	6	38 min [@]	40
8	Ag/ZrO$_2$	1	10	350	5	0.02:20.99:78.99	27	80	4	18000	This work

9	Au/ZrO$_2$	1	10	350	5	0.02:20.99:78.99	38	72	4	18000	This work
10	V$_2$O$_5$/TiO$_2$	15	50	215	2.7	3.3 (O$_2$/ethanol molar ratio)	100	43	-	32960	23
11	Au/MgCuCr$_2$O$_4$	0.5	100	250	-	1.5:3:95.5 [#]	92	90	10	100000	48
12	0.5Au-0.5Ag/ZrO$_2$	1	10	350	5	0.02:20.99:78.99	23	80	4	18000	This work
13	10Cu-0.3Ag/ZrO$_2$	2	99.9	250	-	inert atmosphere	75	16	6	38 min [@]	40

calculated by present author, x = ethanol conversion and S = selectivity towards acetaldehyde, EtOH = Ethanol

4.5 Conclusion

Au and/or Ag over various SiO_2, CeO_2 and ZrO_2 are successfully synthesized by wet impregnation method, characterized by different techniques and implemented for bioethanol oxidation. Synthesized metal nanoparticles were in range between 10 -30 nm. Here it has been shown that metal-support interactions strongly affect the catalytic performance of Au, Ag and Au-Ag metals for gas phase oxidation of bioethanol. Among the used catalyst Au/ZrO_2 was exhibited higher activity due to oxygen deficiencies generated by Au on ZrO_2 surface. As a result, higher concentration of anion vacancies on ZrO_2 surface prevailed and spilled over active oxygen in OH group on ZrO_2 diffused to Au. With Au/CeO_2, 34% bioethanol conversion was achieved. In this case, CeO_2 was able to provide activate oxygen with concurrent creation of oxygen vacancies which could further played a role of activating reactant oxygen molecules reaching from the gas phase. Ag/ZrO_2 and $Au-Ag/ZrO_2$ show low conversion than Au/ZrO_2 and Au/CeO_2, because Ag was more prone to oxidation than Au and also due to weaker interaction between Ag and ZrO_2. Due to inert nature of SiO_2, Au/SiO_2 exhibited lowest ethanol conversion.

Over all bioethanol conversion followed the order: **Au/ZrO_2 > Au/CeO_2 > Ag/ZrO_2 > $Au-Ag/ZrO_2$ > Au/SiO_2**, while acetaldehyde selectivity showed the trend: **Au/CeO_2 > Ag/ZrO_2 > $Au-Ag/ZrO_2$ > Au/ZrO_2 > Au/SiO_2.**

It was found that addition of Ag to Au ($Au-Ag/ZrO_2$) decreased Au^0/Au^+ ratio making the catalyst less favorable for ethanol conversion to ethyl acetate. Acetone formed as acetaldehyde oxidized to acetates on oxide surface and it undergoes coupling reaction.

References

[1] C. Angelici, B.M. Weckhuysen, P.C.A. Bruijnincx, Chemocatalytic Conversion of Ethanol into Butadiene and Other Bulk Chemicals, ChemSusChem. 6 (2013) 1595–1614. doi:10.1002/cssc.201300214.

[2] S. Kumar, N. Singh, R. Prasad, Anhydrous ethanol: A renewable source of energy, Renew. Sustain. Energy Rev. 14 (2010) 1830 – 1844. doi:http://dx.doi.org/10.1016/j.rser.2010.03.015.

[3] B. Jørgensen, S.E. Christiansen, M.L.D. Thomsen, C.H. Christensen, Aerobic oxidation of aqueous ethanol using heterogeneous gold catalysts: Efficient routes to acetic acid and ethyl acetate, J. Catal. 251 (2007) 332–337. doi:http://dx.doi.org/10.1016/j.jcat.2007.08.004.

[4] G.A. Deluga, J.R. Salge, L.D. Schmidt, X.E. Verykios, Renewable Hydrogen from Ethanol by Autothermal Reforming, Science. 303 (2004) 993–997. doi:10.1126/science.1093045.

[5] D.L. Carvalho, R.R. de Avillez, M.T. Rodrigues, L.E.P. Borges, L.G. Appel, Mg and Al mixed oxides and the synthesis of n-butanol from ethanol, Appl. Catal. Gen. 415–416 (2012) 96 – 100. doi:http://dx.doi.org/10.1016/j.apcata.2011.12.009.

[6] C. Liu, J. Sun, C. Smith, Y. Wang, A study of ZnxZryOz mixed oxides for direct conversion of ethanol to isobutene, Appl. Catal. Gen. 467 (2013) 91 – 97. doi:http://dx.doi.org/10.1016/j.apcata.2013.07.011.

[7] E.V. Makshina, W. Janssens, B.F. Sels, P.A. Jacobs, Catalytic study of the conversion of ethanol into 1,3-butadiene, Catal. Today. 198 (2012) 338 – 344. doi:http://dx.doi.org/10.1016/j.cattod.2012.05.031.

[8] M. Nielsen, H. Junge, A. Kammer, M. Beller, Towards a Green Process for Bulk-Scale Synthesis of Ethyl Acetate: Efficient Acceptorless Dehydrogenation of Ethanol, Angew. Chem. Int. Ed. 51 (2012) 5711–5713. doi:10.1002/anie.201200625.

[9] A.S. Blokhina, I.A. Kurzina, V.I. Sobolev, K.Y. Koltunov, G.V. Mamontov, O.V. Vodyankina, Selective oxidation of alcohols over Si_3N_4-supported silver catalysts, Kinet. Catal. 53 (2012) 477–481. doi:10.1134/S0023158412040015.

[10] C.H. Christensen, B. Jørgensen, J. Rass-Hansen, K. Egeblad, R. Madsen, S.K. Klitgaard, S.M. Hansen, M.R. Hansen, H.C. Andersen, A. Riisager, Formation of Acetic Acid by Aqueous-Phase Oxidation of Ethanol with Air in the Presence of a Heterogeneous Gold Catalyst, Angew. Chem. Int. Ed. 45 (2006) 4648–4651. doi:10.1002/anie.200601180.

[11] T. Takei, N. Iguchi, M. Haruta, Synthesis of Acetoaldehyde, Acetic Acid, and Others by the Dehydrogenation and Oxidation of Ethanol, Catal. Surv. Asia. 15 (2011) 80–88. doi:10.1007/s10563-011-9112-1.

[12] S. Tembe, G. Patrick, M. Scurrell, Acetic acid production by selective oxidation of ethanol using Au catalysts supported on various metal oxide, Gold Bull. 42 (2009) 321–327. doi:10.1007/BF03214954.

[13] A.B. Laursen, Y.Y. Gorbanev, F. Cavalca, P. Malacrida, A. Kleiman-Schwarsctein, S. Kegnæs, A. Riisager, I. Chorkendorff, S. Dahl, Highly dispersed supported ruthenium oxide as an aerobic catalyst for acetic acid synthesis, Appl. Catal. Gen. 433–434 (2012) 243–250. doi:http://dx.doi.org/10.1016/j.apcata.2012.05.025.

[14] K.-Q. Sun, S.-W. Luo, N. Xu, B.-Q. Xu, Gold Nano-size Effect in Au/SiO_2 for Selective Ethanol Oxidation in Aqueous Solution, Catal. Lett. 124 (2008) 238–242. doi:10.1007/s10562-008-9507-4.

[15] Y.Y. Gorbanev, S. Kegnæs, C.W. Hanning, T.W. Hansen, A. Riisager, Acetic Acid Formation by Selective Aerobic Oxidation of Aqueous Ethanol over Heterogeneous Ruthenium Catalysts, ACS Catal. 2 (2012) 604–612. doi:10.1021/cs200554h.

[16] T. Takei, J. Suenaga, T. Ishida, M. Haruta, Ethanol Oxidation in Water Catalyzed by Gold Nanoparticles Supported on NiO Doped with Cu, Top. Catal. 58 (2015) 295–301. doi:10.1007/s11244-015-0370-4.

[17] S. Biella, M. Rossi, Gas phase oxidation of alcohols to aldehydes or ketones catalysed by supported gold, Chem Commun. (2003) 378–379. doi:10.1039/B210506C.

[18] M.C. Greca, C. Moraes, M.R. Morelli, A.M. Segadães, Evaluation of Pd/alumina catalysts, produced by combustion synthesis, in the ethanol oxidation reaction to acetic acid, Appl. Catal. Gen. 179 (1999) 87–92. doi:http://dx.doi.org/10.1016/S0926-860X(98)00297-X.

[19] G. Avgouropoulos, E. Oikonomopoulos, D. Kanistras, T. Ioannides, Complete oxidation of ethanol over alkali-promoted Pt/Al_2O_3 catalysts, Appl. Catal. B Environ. 65 (2006) 62–69. doi:http://dx.doi.org/10.1016/j.apcatb.2005.12.016.

[20] P.-Y. Sheng, G.A. Bowmaker, H. Idriss, The Reactions of Ethanol over Au/CeO_2, Appl. Catal. Gen. 261 (2004) 171–181. doi:http://dx.doi.org/10.1016/j.apcata.2003.10.046.

[21] Y. Guan, E.J.M. Hensen, Ethanol dehydrogenation by gold catalysts: The effect of the gold particle size and the presence of oxygen, Appl. Catal. Gen. 361 (2009) 49–56. doi:http://dx.doi.org/10.1016/j.apcata.2009.03.033.

[22] V.I. Sobolev, E.V. Danilevich, K.Y. Koltunov, Role of vanadium species in the selective oxidation of ethanol on V_2O_5/TiO_2 catalysts, Kinet. Catal. 54 (2013) 730–734. doi:10.1134/S0023158413060128.

[23] B. Jørgensen, S. Kristensen, A. Kunov-Kruse, R. Fehrmann, C. Christensen, A. Riisager, Gas-Phase Oxidation of Aqueous Ethanol by Nanoparticle Vanadia/Anatase Catalysts, Top. Catal. 52 (2009) 253–257. doi:10.1007/s11244-008-9161-5.

[24] J. Mielby, J.O. Abildstrøm, F. Wang, T. Kasama, C. Weidenthaler, S. Kegnæs, Oxidation of Bioethanol using Zeolite-Encapsulated Gold Nanoparticles, Angew. Chem. Int. Ed. 53 (2014) 12513–12516. doi:10.1002/anie.201406354.

[25] V.I. Sobolev, K.Y. Koltunov, O.A. Simakova, A.-R. Leino, D.Y. Murzin, Low temperature gas-phase oxidation of ethanol over Au/TiO_2, Appl. Catal. Gen. 433–434 (2012) 88 – 95. doi:http://dx.doi.org/10.1016/j.apcata.2012.05.003.

[26] T. Takei, N. Iguchi, M. Haruta, Support effect in the gas phase oxidation of ethanol over nanoparticulate gold catalysts, New J Chem. 35 (2011) 2227–2233. doi:10.1039/C1NJ20297A.

[27] V.I. Sobolev, K.Y. Koltunov, MoVNbTe Mixed Oxides as Efficient Catalyst for Selective Oxidation of Ethanol to Acetic Acid, ChemCatChem. 3 (2011) 1143–1145. doi:10.1002/cctc.201000450.

[28] X. Li, E. Iglesia, Selective Catalytic Oxidation of Ethanol to Acetic Acid on Dispersed Mo-V-Nb Mixed Oxides, Chem. – Eur. J. 13 (2007) 9324–9330. doi:10.1002/chem.200700579.

[29] F. Gonçalves, P.R.S. Medeiros, J.G. Eon, L.G. Appel, Active sites for ethanol oxidation over SnO_2-supported molybdenum oxides, Appl. Catal. Gen. 193 (2000) 195–202. doi:http://dx.doi.org/10.1016/S0926-860X(99)00430-5.

[30] H. Chen, X. Jia, Y. Li, C. Liu, Y. Yang, Controlled surface properties of Au/ZSM5 catalysts and their effects in the selective oxidation of ethanol, Catal. Today. 256, Part 1 (2015) 153 – 160. doi:http://dx.doi.org/10.1016/j.cattod.2015.01.020.

[31] N. Zheng, and G.D. Stucky, A General Synthetic Strategy for Oxide-Supported Metal Nanoparticle Catalysts, J. Am. Chem. Soc. 128 (2006) 14278–14280. doi:10.1021/ja0659929.

[32] E.A. Redina, A.A. Greish, I.V. Mishin, G.I. Kapustin, O.P. Tkachenko, O.A. Kirichenko, L.M. Kustov, Selective oxidation of ethanol to acetaldehyde over Au–Cu catalysts prepared by a redox method, Catal. Today. 241, Part B (2015) 246 – 254. doi:http://dx.doi.org/10.1016/j.cattod.2013.11.065.

[33] Y. Guan, E.J.M. Hensen, Selective oxidation of ethanol to acetaldehyde by Au−Ir catalysts, J. Catal. 305 (2013) 135 – 145. doi:http://dx.doi.org/10.1016/j.jcat.2013.04.023.

[34] P. Dutta, S. Pal, and M.S. Seehra, Y. Shi, E. M. Eyring, and R.D. Ernst, Concentration of Ce^{3+} and Oxygen Vacancies in Cerium Oxide Nanoparticles, Chem. Mater. 18 (2006) 5144–5146. doi:10.1021/cm061580n.

[35] C. Sun, H. Li, L. Chen, Nanostructured ceria-based materials: synthesis, properties, and applications, Energy Env. Sci. 5 (2012) 8475–8505. doi:10.1039/C2EE22310D.

[36] S. Song, X. Wang, H. Zhang, CeO_2-encapsulated noble metal nanocatalysts: enhanced activity and stability for catalytic application, NPG Asia Mater. 7 (2015) e179.

[37] W. Hertl, Surface chemistry of zirconia polymorphs, Langmuir. 5 (1989) 96–100. doi:10.1021/la00085a018.

[38] M.V. Ganduglia-Pirovano, A. Hofmann, J. Sauer, Oxygen vacancies in transition metal and rare earth oxides: Current state of understanding and remaining challenges, Surf. Sci. Rep. 62 (2007) 219 – 270. doi:http://dx.doi.org/10.1016/j.surfrep.2007.03.002.

[39] Y.-H. Kim, S.-K. Hwang, J.W. Kim, Y.-S. Lee, Zirconia-Supported Ruthenium Catalyst for Efficient Aerobic Oxidation of Alcohols to Aldehydes, Ind. Eng. Chem. Res. 53 (2014) 12548–12552. doi:10.1021/ie5009794.

[40] J.M.C.B. Jean Marcel R. Gallo Isabel C. Freitas, C.M.P. Marques, The Effect of Ag in the Cu/ZrO_2 Performance for the Ethanol Conversion, Top. Catal. 59 (2016) 357–365.

[41] P. Periyat, F. Laffir, S.A.M. Tofail, E. Magner, A facile aqueous sol-gel method for high surface area nanocrystalline CeO_2, RSC Adv. 1 (2011) 1794–1798. doi:10.1039/C1RA00524C.

[42] X. Liu, A. Wang, L. Li, T. Zhang, C.-Y. Mou, J.-F. Lee, Synthesis of Au–Ag alloy nanoparticles supported on silica gel via galvanic replacement reaction, Prog. Nat. Sci. Mater. Int. 23 (2013) 317 – 325. doi:http://dx.doi.org/10.1016/j.pnsc.2013.04.008.

[43] S. Machmudah, M. Akmal Hadian, L. Samodro K., S. Winardi, _ W., H. Kanda, M. Goto, Preparation of Ceria-Zirconia Mixed Oxide by Hydrothermal Synthesis, Mod. Appl. Sci. 9 (2015). doi:10.5539/mas.v9n7p134.

[44] J.B.B.R. Muruganantham Chelliah, U.M. Krishnan, Synthesis and Characterization of Cerium Oxide Nanoparticles by Hydroxide Mediated Approach, J. Appl. Sci. 12 (2012) 1734–1737. doi:10.3923/jas.2012.1734.1737.

[45] V. Raji, M. Chakraborty, P.A. Parikh, Catalytic Performance of Silica-Supported Silver Nanoparticles for Liquid-Phase Oxidation of Ethylbenzene, Ind. Amp Eng. Chem. Res. 51 (2012) 5691–5698. doi:10.1021/ie2027603.

[46] A.S. Nair, T. Pradeep, I. MacLaren, An investigation of the structure of stearate monolayers on $Au@ZrO_2$ and $Ag@ZrO_2$ core-shell nanoparticles, J Mater Chem. 14 (2004) 857–862. doi:10.1039/B313850J.

[47] A. Gazsi, A. Koós, T. Bánsági, F. Solymosi, Adsorption and decomposition of ethanol on supported Au catalysts, Catal. Today. 160 (2011) 70 – 78. doi:http://dx.doi.org/10.1016/j.cattod.2010.05.007.

[48] P. Liu, X. Zhu, S. Yang, T. Li, E.J.M. Hensen, On the metal–support synergy for selective gas-phase ethanol oxidation over $MgCuCr_2O_4$ supported metal nanoparticle catalysts, J. Catal. 331 (2015) 138 – 146. doi:http://dx.doi.org/10.1016/j.jcat.2015.08.025.

[49] Y. Han, J. Zhu, Surface Science Studies on the Zirconia-Based Model Catalysts, Top. Catal. 56 (2013) 1525–1541.

[50] Ricardo Grau-Crespo ,Norge Cruz Hernández, Javier F. Sanz, and N.H. de Leeuw, Theoretical Investigation of the Deposition of Cu, Ag, and Au Atoms on the ZrO2(111) Surface, J. Phys. Chem. C. 111 (2007) 10448–10454. doi:10.1021/jp0704057.

[51] F. Vindigni, M. Manzoli, A. Damin, T. Tabakova, A. Zecchina, Surface and Inner Defects in Au/CeO_2 WGS Catalysts: Relation between Raman Properties, Reactivity and Morphology, Chem. – Eur. J. 17 (2011) 4356–4361. doi:10.1002/chem.201003214.

[52] J. Li, J. Chen, W. Song, J. Liu, W. Shen, Influence of zirconia crystal phase on the catalytic performance of Au/ZrO_2 catalysts for low-temperature water gas shift reaction, Appl. Catal. Gen. 334 (2008) 321 – 329. doi:http://dx.doi.org/10.1016/j.apcata.2007.10.020.

[53] G. Zhou, B. Gui, H. Xie, F. Yang, Y. Chen, S. Chen, X. Zheng, Influence of CeO_2 morphology on the catalytic oxidation of ethanol in air, J. Ind. Eng. Chem. 20 (2014) 160 – 165. doi:http://dx.doi.org/10.1016/j.jiec.2013.04.012.

[54] S. Letichevsky, P.C. Zonetti, P.P.P. Reis, J. Celnik, C.R.K. Rabello, A.B. Gaspar, L.G. Appel, The role of $m-ZrO_2$ in the selective oxidation of ethanol to acetic acid employing $PdO/m-ZrO_2$, J. Mol. Catal. Chem. 410 (2015) 177 – 183. doi:http://dx.doi.org/10.1016/j.molcata.2015.09.012.

[55] P.C. Zonetti, J. Celnik, S. Letichevsky, A.B. Gaspar, L.G. Appel, Chemicals from ethanol – The dehydrogenative route of the ethyl acetate one-pot synthesis, J. Mol. Catal. Chem. 334 (2011) 29–34. doi:http://dx.doi.org/10.1016/j.molcata.2010.10.019.

[56] C.P. Rodrigues, P.C. Zonetti, C.G. Silva, A.B. Gaspar, L.G. Appel, Chemicals from ethanol—The acetone one-pot synthesis, Appl. Catal. Gen. 458 (2013) 111 – 118. doi:http://dx.doi.org/10.1016/j.apcata.2013.03.028.

[57] I.C. Freitas, S. Damyanova, D.C. Oliveira, C.M.P. Marques, J.M.C. Bueno, Effect of Cu content on the surface and catalytic properties of Cu/ZrO_2 catalyst for ethanol dehydrogenation, J. Mol. Catal. Chem. 381 (2014) 26 – 37. doi:http://dx.doi.org/10.1016/j.molcata.2013.09.038.

[58] R. Grabowski, J. Słoczyński, M. Śliwa, D. Mucha, R.P. Socha, M. Lachowska, J. Skrzypek, Influence of Polymorphic ZrO_2 Phases and the Silver Electronic State on the Activity of Ag/ZrO_2 Catalysts in the Hydrogenation of CO_2 to Methanol, ACS Catal. 1 (2011) 266–278. doi:10.1021/cs100033v.

[59] A.B. Gaspar, F.G. Barbosa, S. Letichevsky, L.G. Appel, The one-pot ethyl acetate syntheses: The role of the support in the oxidative and the dehydrogenative routes, Appl. Catal. Gen. 380 (2010) 113 – 117. doi:http://dx.doi.org/10.1016/j.apcata.2010.03.034.

Chapter – 5

Bioethanol Selective Oxidation to Acetaldehyde Over Ag/CeO$_2$: Role of Metal-Support Interactions

CHAPTER – 5

Bioethanol Selective Oxidation to Acetaldehyde Over Ag-CeO$_2$: Role of Metal-Support Interactions

Outcome of work of chapter 4 indicates that synergy between metal and support plays a vital role for bioethanol conversion. Au gave higher bioethanol conversion due to its strong interaction with CeO$_2$ and ZrO$_2$. Ag is also known for strong interaction with CeO$_2$. In this part of work Ag/CeO$_2$ is tested for gas phase bioethanol oxidation with air. Ag/CeO$_2$ catalyst is prepared wet impregnation method and fully characterized by XRD, FTIR, TGA, SEM and TEM. Characterization results indicated that a part of Ag is inserted into the lattice of CeO$_2$ and expanded the support lattice. Ag/CeO$_2$ catalyst is found to outperform the reported catalyst systems (acetaldehyde selectivity of 90% and life > 36 h) at 200 °C to 350 °C, 5 atm and gas hourly space velocity of 18000 mLg$_{cat}^{-1}$h^{-1}. This study shows path for selective oxidation of other biomass-derived compounds.

5.1 Introduction

Meeting the needs of the commodity chemicals from biomass derived molecules is gaining ever increasing importance. One such compound is ethanol (bioethanol) derived from, e.g., fermentation of sugar crops and lignocellulosic residue [1]. Large fraction (~75%) of bioethanol is used as a fuel additive [2], however recent trends show diverting renewable resources to chemical products. Ethanol can be converted to a variety of chemicals such as acetaldehyde [3], acetic acid [4], ethyl acetate [5], or butanol [6] depending on the catalyst and reaction conditions. Acetaldehyde is chiefly used as an intermediate for the production of acetic acid, acetic anhydride, ethyl acetate, alkylamines and pyridines. It is produced by ethylene oxidation (Wacker process). With high availability of bioethanol (30 billion US gallons in 2016 worldwide)[7], ethanol oxidation for production of acetaldehyde can be a feasible process. Use of silver-based catalyst has been widely employed for oxidation of CO [8], methanol [9], formaldehyde [10], ethylene glycol [11],

ethyl benzene [12]. However, literature reporting bioethanol oxidation over Ag-based catalyst is rather scanty. Xu et al.[3] obtained highest ethanol conversion of about 25% with acetaldehyde selectivity of ~75% at 350˚C employing Ag/hydroxyapatite catalyst for pure ethanol. Chen et al. [13] and Li et al. [14] have reported higher (>75%) ethanol conversion at the expense of higher Ag loading of 9.8 wt% and 100 wt%, respectively again for pure ethanol.

In the present study, cerium oxide (CeO_2) is employed as solid support owing to its oxygen storage capacity (OSC) and its ability to easily create (and subsequent diffusion) of oxygen vacancies at its surface [15]. CeO_2 has been widely used as a support in various oxidation reactions such as oxidation of CO [16], styrene [17], glycerol [18], o-xylene [19], and naphthalene [20].

The OSC property of CeO_2 has not been explored for the oxidation of bioethanol to the extent that it deserves. Also the Ag/CeO_2 as a catalytic system has not been studied for bioethanol oxidation. Here, CeO_2 supported Ag nanoparticle catalyst affords high selectivity towards acetaldehyde and stable catalytic performance under reaction condition in the gas-phase aerobic oxidation of bioethanol (about 10 vol% ethanol solution in water).

5.2 Experimental section

5.2.1 Synthesis of catalyst

Catalysts are prepared using the wet impregnation method. 1% Ag over CeO_2 is synthesized according to this method, as described in detail in chapter 3 (section 3.3.1.2).

5.2.2 Catalyst characterization

Transmissions electron microscopy (TEM) images of the catalyst were recorded on a Philips CM 200 microscope operating at 200 kV. The samples were dispersed in ethanol and kept in an ultrasonic bath for 20 min, then deposited on a carbon-covered copper grid for each measurement. Surface morphology of the catalyst was investigated with scanning electron microscopy (SEM) and energy dispersive X-ray analysis (EDX) (JEOL make model 7600F FESEM) was carried out to verify the presence of Ag nanoparticles.

X-ray Diffraction (XRD) analysis was performed on a Bruker - D8 Discover equipped with Ni-filtered Cu Kα radiation source (λ = 1.542 Å) 40 kV and 30 mA. The diffractograms were recorded in the 2θ range of 20 - 90° with a 2θ step size of 0.02° and a scanning speed of 6° min^{-1}. Average crystal size was determined by the Scherer's equation. Fourier Transform Infrared Spectroscopy (FTIR) spectra of catalyst samples were collected in reflection mode using ZnSe optics in Bruker Alpha Eco-ATR spectrometer.

The Oxygen storage capacity (OSC) was measured by thermo gravimetric analysis (TGA) on a Mettler Toledo TG-SDTA apparatus. OSC measurement was carried out for specimen with heating and cooling cycles. Firstly, the sample was heated from ambient temperature to 800 °C under N_2 flow, then cooling to 150 °C in dry air and again heating to 800 °C in N_2 environment. All heating and cooling rates were 5 °C min^{-1}. Weight loss of sample during the second heating cycle was used to determine the oxygen release properties.

5.2.3 Catalyst activity test

Catalysts were tested for ethanol conversion using heated stainless steel continuous fixed bed down flow reactor. Details of the reactor set-up is presented in chapter 4 (section 4.2.3) and the sample reaction is analyzed as described in chapter 4 (section 4.2.3).

Catalytic performance of the system was evaluated on the basis of conversion of bioethanol and products selectivity as defined in section 3.3.2.1.

5.3 Result and discussion

5.3.1 Catalyst characterization

The catalyst was characterized using Fourier transform infrared spectroscopy (FTIR), x-ray diffraction pattern (XRD), Transmission electron microscopy (TEM) and scanning electron microscopy (SEM).

5.3.1.1 Transmission electron microscope

TEM measurements were carried out in order to obtain the particle size and morphology of catalysts. As seen in Fig. 1(B), CeO_2 crystallized in cubic shape with particle size of around 35 nm. The *d* spacing for CeO_2 lattice was 0.315 nm (Fig. 1(C). Selected Area Electron Diffraction (SAED) pattern corresponding to the CeO_2 (111) lattice plane of the cubic cell [21,22]. In the case of Ag/CeO_2, Fig. 1(A), average sizes of Ag particles was around 7 nm. The d spacing of Ag was 0.235 nm, which was corresponding to the Ag (111) [3,23].
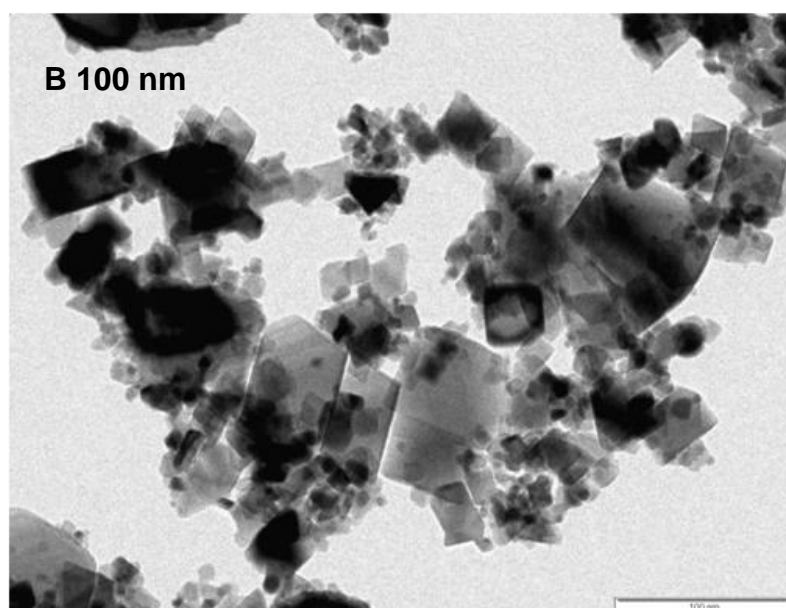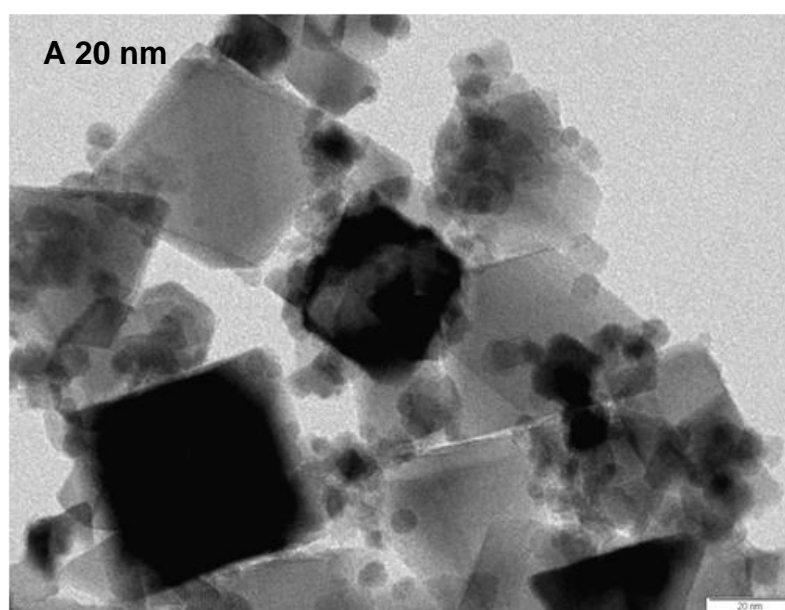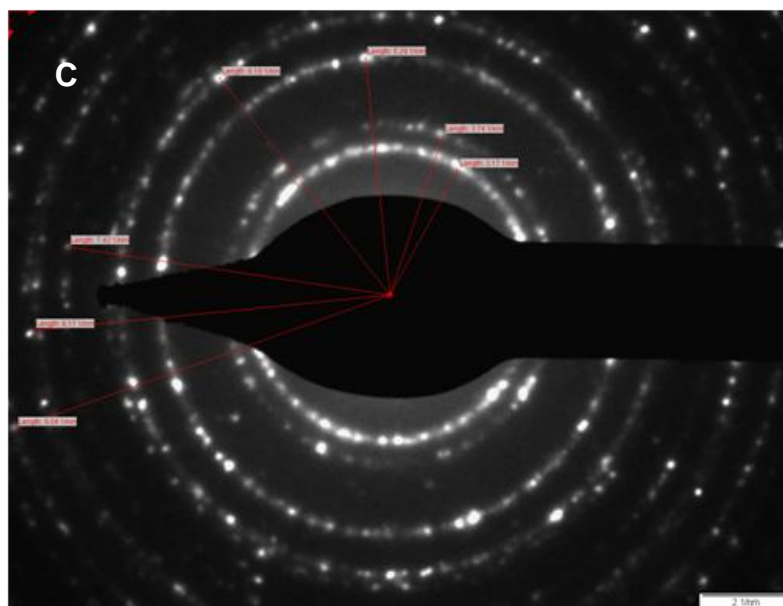
Figure 5.1 TEM images of (A) and (B) Ag/CeO$_2$ and (C) SAED pattern for Ag/CeO$_2$

5.3.1.2 Scanning electron microscope

SEM image of Ag/CeO$_2$ catalyst is shown in Figure 5.2(A). Image clearly indicates the uniform and well formed CeO$_2$ particles. Impregnation of Ag on CeO$_2$ was confirmed by EDX analysis (Figure 5.2(B)). EDX spectrum shows peaks for oxygen, silver and cerium. There is a single point at 3 keV for Ag and three peaks near about 4.3 keV, 4.7 and 5.2 keV for Ce.
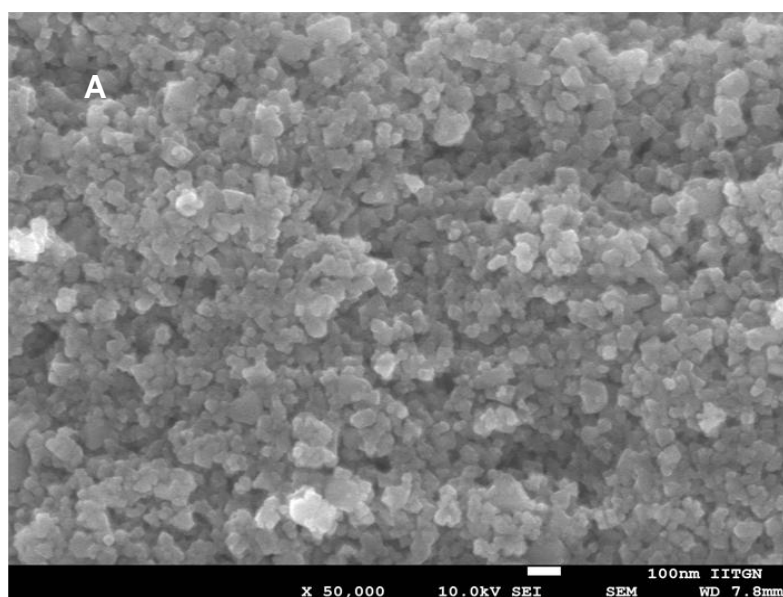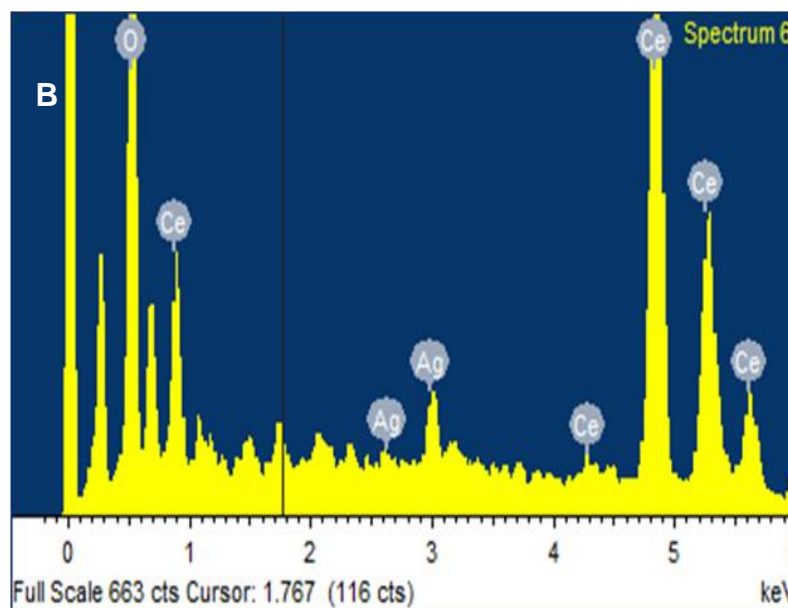
Figure 5.2 (A) SEM of Ag/CeO$_2$ catalyst and (B) EDX of Ag/CeO$_2$ catalyst

5.3.1.3 Powder X-ray Diffraction

XRD patterns of CeO$_2$ and Ag/CeO$_2$ are presented in Fig. 3. XRD of CeO$_2$ has confirmed its cubic crystal structure of fluorite type, due to the presence of diffraction peaks at 2θ of 28.2°,33°, 47.5°,56°,59° and 76° (JCPDS-34-0394) [24]. Average particle size of the CeO$_2$ was 35 nm calculated by Scherrer equation and this value was also confirmed by TEM. For the Ag/CeO$_2$, XRD analyses reveal that impregnated Ag did not lead to any significant change in the support. However, if compared to the XRD pattern of CeO$_2$, an additional weak peak at about 38.1° was observed for the Ag/CeO$_2$ catalyst, which was attributed to (111) Bragg's reflections of Ag (JCPDS 65-2871)[10,15]. It is to be noted that, the peak at 38.1° could be also the (200) Bragg's reflections of Ag$_2$O (JCPDS 65-6811) [8,10,25]. Therefore, presence of Ag$_2$O cannot be fully ignored. However, according to XRD patterns discussed in literature [25] Ag$_2$O should exhibit intense peak at 33.5°, which is not visible in the present case indicating that metallic Ag species predominated over Ag$_2$O in Ag/CeO$_2$ catalyst.

It can be seen in the insert of Fig. 3, that diffraction peak at 28.5° on Ag/CeO$_2$ catalyst shifted to lower angle compared to that for pure CeO$_2$.This may indicate that a part of Ag

has incorporated into the lattice of CeO_2 because ionic radius of Ag^+ is larger than that of Ce^{+4} [10,26]. Inserted Ag increases the crystal defects of CeO_2, which activates lattice oxygen for the reaction.
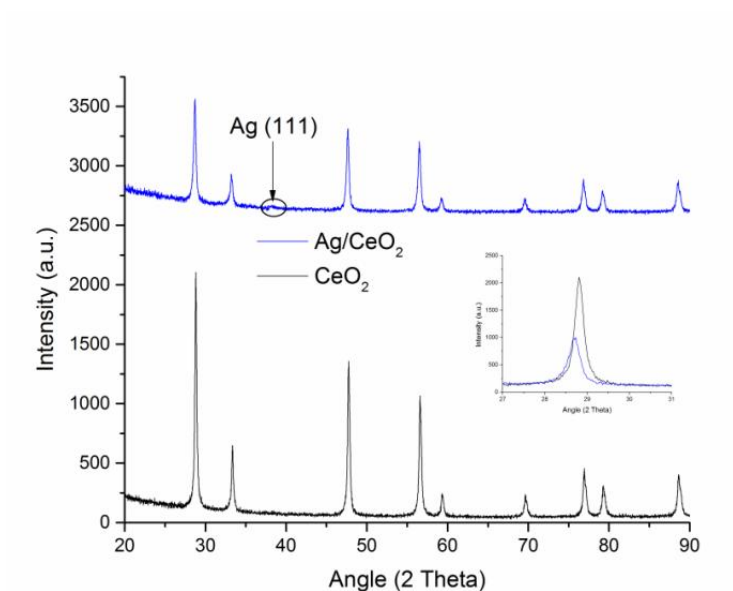
Figure 5.3 XRD pattern of CeO_2 and Ag/CeO_2 catalyst

Based on Bragg's law and Debye–Scherrer Equation, the lattice parameters and crystallite sizes of CeO_2 and Ag/CeO_2 were calculated and the results are summarized in Table 5.1. The change in lattice parameter for pure CeO_2 after impregnation of Ag (at $2\theta = 28.5$), indicates that Ag could play a significant role in activation of lattice oxygen of ceria.

Table 5. 1 Crystallite size, lattice parameter and OSC value of CeO_2 and Ag/CeO_2

Catalysts	Crystallite size (From TEM)	Crystallite size (From XRD)	Lattice parameter (nm)	OSC ($\mu mol - O\ g^{-1}$)
CeO_2	35	35	0.5418	21.38
Ag/CeO_2	7	-	0.5384	199.50

Further to confirm that impregnated Ag on CeO_2 activates the lattice oxygen of CeO_2, OSC of CeO_2 and Ag/CeO_2 was measured by thermo gravimetric analysis (TGA). As seen in Table 5.1, OSC of Ag/CeO_2 was higher by an order of magnitude than that of CeO_2 confirms that presence of Ag enhanced OSC of CeO_2.

5.3.1.4 Fourier Transform Infrared Spectroscopy

FTIR spectra of CeO_2 and Ag/CeO_2 in the region of 500 - 4000 cm^{-1} are shown in Fig. 4. It clearly shows that absorption band around 3750 cm^{-1} corresponding to the stretching vibration of the -OH function group. Here, bands observed at 1640 cm^{-1} attributed to bending vibrations due to the surface hydroxyl group and strong band at 1533 cm^{-1} due to Ce-OH stretching vibration. Absorption band at 538 cm^{-1} was assigned to the stretching vibration of Ce-O-Ce [27]. A slight decrease in band height at 538 cm^{-1} was observed for Ag/CeO_2, confirms impregnation of Ag on CeO_2 [28].
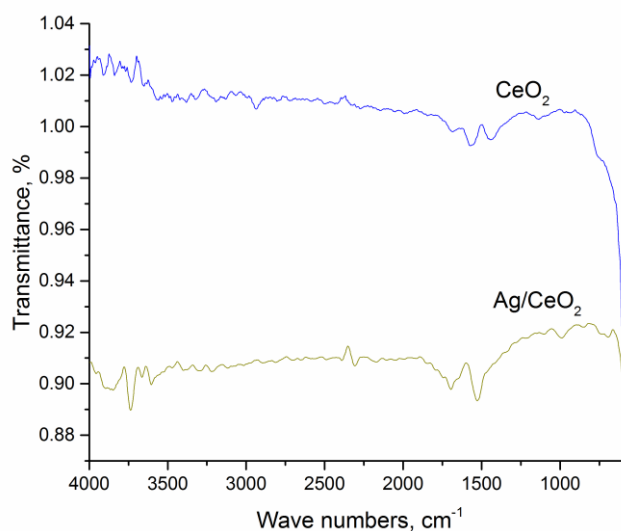
Figure 5.4 FTIR of CeO_2 and Ag/CeO_2 catalyst

5.3.2. Catalytic Performance of Ag/CeO_2 for bioethanol oxidation

5.3.2.1 Effect of temperature

Figure 5.5 shows ethanol (10 wt% aqueous solution) conversion and product selectivity as a function of reaction temperature for Ag/CeO_2 catalysts. No significant ethanol conversion was observed at reaction temperature of 225 °C ($< 10\%$), which increased with temperature (36% at 350 °C). Increased catalytic activity in this reaction may be ascribed to presence of Ag, which led to enhanced reducibility of CeO_2 surface. According to reported in literature [25,29], majority of noble metals anchored on CeO_2 and CeO_2/Al_2O_3 supports [30] were known to augment reducibility of surface ceria and were associated

with hydrogen spillover from the noble metal to the surface of the metal oxide [31]. In [29] reduction of the surface O_2^- of CeO_2 interacting with silver was observed, which agrees with our hypothesis that silver does increase reducibility of surface oxygen of CeO_2.
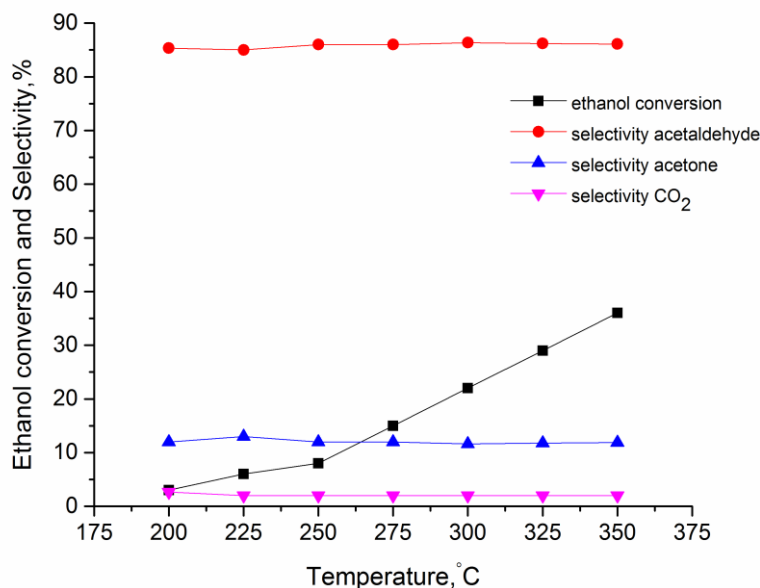
Figure 5.5 Catalytic performance of Ag/CeO_2 as a function of reaction temperature (Catalyst = 1 g, pressure = 5 atm, ethanol/H_2O/O_2/N_2 (vol %) =0.002:0.018:20.99:78.98 and GHSV =18000 mLg$_{cat}^{-1}$h^{-1})

Also, inserted Ag increases crystal defects in CeO_2 (as seen in XRD pattern, Figure 5.3), which resulted in activation of lattice oxygen for the reaction. Impregnated Ag leading to crystal defects in CeO_2 has also been reported by Kang et al.[8] and Ma et al.[10]. Atomic oxygen is transferred from the surface of ceria to the surface of silver particles through the Ag/CeO_2 interface. Effectiveness of oxygen spillover depends on nature of the supports. Mamontov et al. [32] performed temperature programmed reduction (TPR) experiments and confirmed the participation of surface oxygen of CeO_2 and ZrO_2. They also concluded that stronger interaction of Ag with CeO_2 compared to ZrO_2 and SiO_2 resulted in high catalytic activity of $Ag/CeO_2/SiO_2$ for CO oxidation. Active oxygen required for oxidation of hydrogen forms as a result of alcohol dehydrogenation. Similar mechanism was proposed for liquid phase dehydrogenation of benzyl alcohol over a mixture of Ag/SiO_2

catalyst and CeO_2 nanoparticles [33]. Hence, surface lattice oxygen is playing a key role in enhancement of catalytic activity in oxidation reactions catalyzed by CeO_2-based catalysts.

5.3.2.2 Metal Support Interactions

Intense interfacial interaction between Ag and CeO_2 may results in (i) decrease of Ce–O bond energy in CeO_2 and (ii) increase of positive charge on Ag ($Ag^{\delta+}$). Zhang et al. [29] showed the phenomena of Ag interacting with CeO_2, and decrease of Ce–O bond energy enhancing catalytic activity of Ag-CeO_2 core–shell nanospherical catalyst for CO oxidation. Presence of Ag–O bonds at the interface between Ag NPs and the surface of CeO_2 (111) was detected at the Ag K-edge by X-ray absorption fine structure spectroscopy. Small size of Ag NPs, decreases Ag–O inter atomic distance and also confirms decrease of Ce–O bond energy due to interaction of this oxygen atom of CeO_2 support with silver [34]. Ag NPs are capable of promoting surface reduction of CeO_2, which leads to increase of oxygen vacancies in CeO_2. Similar arguments was reported by Huang and Gao [35].

Here, key role of the silver on surface is: (i) to increase lattice oxygen mobility of CeO_2 by producing structural defects, as for Ag-supported CeO_2, and (ii) to weaken the Ce–O bond and thus induce the exchange between lattice oxygen and adsorbed oxygen.

Oxidation of bioethanol can proceed via breaking of C–H, or O–H bond. As stated earlier, presence of Ag decreases Ce–O bond energy and increases positive charge on $Ag^{\delta+}$. Ag-CeO_2 interface provides a pair of $Ag^{\delta+}$ acid sites and surface oxygen vacancies of CeO_2, which associatively activate alcohol molecule for dehydrogenation. Reaction begins with the interaction of a Lewis base (an alcohol molecule) with a surface Lewis acid site (Ag $^{\delta+}$). As a result, an ethoxy intermediate and OH_{ads} are formed on the catalyst surface. Further, selective oxidation of ethoxy intermediate occurs with the formation of an acetaldehyde and a water molecule. The $Ag^{\delta+}$ acid sites provide the weakening of β-C–H bond due to coordination of the H atom with subsequent detaching of the H atom from the alcohol molecule, while base sites of ceria activate the O–H bond of alcohol. This cooperative mechanism leads to easy cleavage of H atoms from the alcohol molecule. Same mechanism for partial oxidation of ethylene glycol using Ag based catalysts was proposed by Voronava et al. [11].

Close interaction between Ag NPs on a basic support CeO_2 or hydrotalcite surface over corresponding interfaces is also effective for catalytic chemo selective reduction of nitrostyrenes and epoxides to the corresponding anilines and alkenes while using alcohols as reducing reagents [36]. Interaction of Ag clusters and acid-base sites on Al_2O_3 was shown for oxidant-free dehydrogenation of alcohols over Ag/Al_2O_3 catalyst [37]. Thus, better interfacial interaction between Ag and CeO_2 provide effective way to create highly active catalysts for oxidation reaction. The higher bioethanol conversion in case of Ag/CeO_2 (36 % conversion) clearly indicated the stronger interaction of Ag with CeO_2 in comparison with Ag/ZrO_2 (27 % conversion, chapter 4, section 4.3.2).

5.3.2.3 Product Selectivity

In this work, it is found (Figure 5.5) that the increase in temperature from 200 to 350 °C does not affect selectivity for acetaldehyde. It remained practically constant (>85%) over the entire range of reaction temperature. Selectivity for acetone and CO_2 are found to be 12% and 3%, respectively for entire temperature range. Acetone formation is explained as a result of acetaldehyde oxidation to acetates on oxide surface and their subsequent coupling reactions yield acetone [38,39]. Selectivity towards acetaldehyde and CO_2 remains almost constant with temperature which is in contrast to reported literature [40–43]. Rahman et al. [44] studied effect of water in ethanol conversion using ZnO as support and concluded that presence of water inhibits dehydration of ethanol towards ethylene production via blockage of Lewis acid site and favoring dehydrogenation rate of ethanol towards acetaldehyde formation. Thus, higher and practically constant selectivity observed in this work, may have to do with the presence of water. It was reported that high ethanol conversion achieved at low temperature [13,40,45], however in our case 36% conversion was obtained at high temperature. It shows that high temperature is needed in the presence of water.

5.3.2.4 Effect of time-on-stream

Catalytic performance of Ag/CeO$_2$ catalyst is depicted in Figure 5.6, ethanol conversion and acetaldehyde selectivity are plotted against time-on-stream. Low ethanol conversion (< 10%) and high selectivity (~85%) towards acetaldehyde are observed at low temperature. Selectivity towards acetaldehyde remains virtually constant for entire duration, while conversion closely linked to the temperature. Ag/CeO$_2$ catalyst exhibited no sign of catalyst deactivation for more than 36 h on-stream.
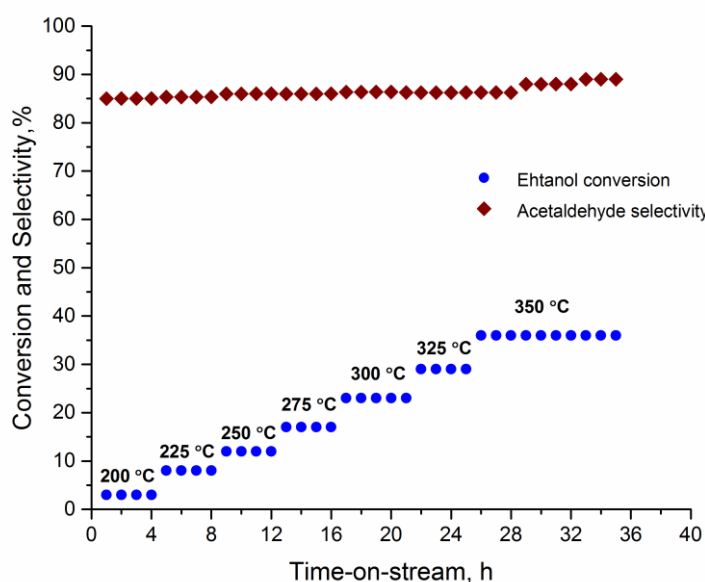
Figure 5.6 Ethanol conversion and acetaldehyde selectivity as function of time-on-stream (Catalyst = 1 g, pressure = 5 atm, ethanol/H$_2$O/O$_2$/N$_2$ (vol %) =0.002:0.018:20.99:78.98 and GHSV =18000 mLg$_{cat}^{-1}$h^{-1})

5.3.2.5 Effect of Weight hourly space velocity

Figure 5.7 elucidates the effect of weight hourly space velocity (WHSV) on acetaldehyde selectivity. As is evident, selectivity increased with WHSV at a particular temperature. Acetaldehyde selectivity was around 86 % at WHSV of 6. At 12 and 18 WHSV selectivity increased to 88% and 89%, respectively. Highest acetaldehyde selectivity (90%) was achieved at 350°C and 18 WHSV. This can be due to shorter contact time of primary

product, acetaldehyde and hence its subsequent oxidation to other products could not proceed.
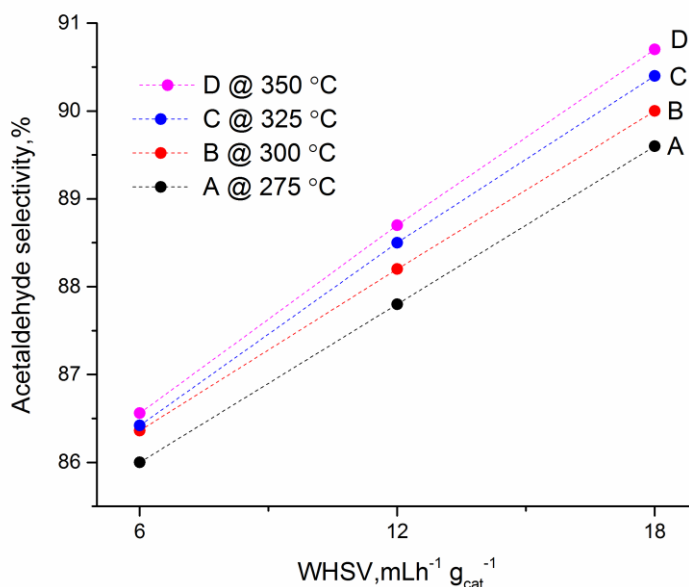
Figure 5.7 Acetaldehyde selectivity as function of weight hourly space velocity (WHSV) (Catalyst = 1 g, pressure = 5 atm, ethanol/H_2O/O_2/N_2 (vol %) =0.002:0.018:20.99:78.98)

Ethanol conversion and selectivity toward acetaldehyde for the prepared catalyst (Ag/CeO_2) and other Ag based catalysts are summarized in Table 5.2. However, straight away comparison of performance parameters cannot be made due to variation in feed composition, loading of metal and EtOH/O_2 molar ratio. As is evident here, Ag containing catalysts have been used for the gas phase mixtures with ethanol/O_2 molar ratio ranging from 0.11 to 4. Formation of byproducts such as acetic acid, ethyl acetate, and COx accompanied the formation of acetaldehyde with increased oxygen proportion in feed. The chief advantage of this catalyst is an operation in air (an industrially desirable oxidant) while maintaining high selectivity toward acetaldehyde. In general, this catalyst exhibited good activity in terms of ethanol conversion, acetaldehyde selectivity and stability. In addition, the byproducts of the reaction are acetone and CO_2. Therefore, acetaldehyde may be easily separated from the product mixture.

Table 5.2 Various Ag-containing catalysts from the literature and the present work for gas-phase ethanol oxidation

Catalyst	Ag (wt%)	EtOH in feed (vol%)	Temp., (°C)	Ethanol conversion (%)	Acetaldehyde Selectivity (%)	Ethanol/ O_2 (molar)	Reference
Ag/CeO$_2$	1	10	350	36	90	1/1	This work
Ag/HAp	0.5	100	350	25	77	4/1	[3]
Ag/OMS-2	5	100	170	53	58	1/9	[41]
Nanoporous Ag	100	100	250	85	95	2/1	[14]
Ag-Hollandite	9.8	100	250	100	71	Not mentioned	[13]
Ag/Fe-Si$_3$N$_4$	5	100	350	100	15	1/9	[46]
Ag/MgCuCr$_2$O$_4$	1	100	300	90	80	1/3	[45]

5.4 Conclusion

It is found that Ag/CeO$_2$ exhibited a higher and stable catalytic activity for bioethanol oxidation chiefly to acetaldehyde. This catalyst, outperforming the reported catalysts, afforded 36% ethanol conversion in presence of much excess water along with high (> 85 %) selectivity towards value added compound, acetaldehyde. Higher catalytic activity of Ag/CeO$_2$ upon impregnation of Ag has been ascribed to (i) increased Ag$^{\delta+}$ acid sites and/or (ii) spillover of active oxygen from ceria to Ag-CeO$_2$ interface. The cooperation of Ag$^{\delta+}$ acid sites and base sites of ceria on the Ag-CeO$_2$ interface has imparted high activity to the catalyst in bioethanol oxidation. Also presence of Ag improved the OSC of CeO$_2$, which may accelerate the activation of lattice oxygen in the reaction.

References

[1] Ó.J. Sánchez, C.A. Cardona, Trends in biotechnological production of fuel ethanol from different feedstocks, Bioresour. Technol. 99 (2008) 5270–5295. doi:10.1016/j.biortech.2007.11.013.

[2] L. Wei, L.O. Pordesimo, C. Igathinathane, W.D. Batchelor, Process engineering evaluation of ethanol production from wood through bioprocessing and chemical catalysis, Biomass Bioenergy. 33 (2009) 255–266. doi:10.1016/j.biombioe.2008.05.017.

[3] J. Xu, X.-C. Xu, X.-J. Yang, Y.-F. Han, Silver/hydroxyapatite foam as a highly selective catalyst for acetaldehyde production via ethanol oxidation, Catal. Today. 276 (2016) 19 – 27. doi:http://dx.doi.org/10.1016/j.cattod.2016.03.001.

[4] J. Zhang, L. Wang, L. Zhu, Q. Wu, C. Chen, X. Wang, Y. Ji, X. Meng, F.-S. Xiao, Solvent-Free Synthesis of Zeolite Crystals Encapsulating Gold-Palladium Nanoparticles for the Selective Oxidation of Bioethanol, ChemSusChem. 8 (2015) 2867–2871. doi:10.1002/cssc.201500261.

[5] E. Santacesaria, G. Carotenuto, R. Tesser, M. Di Serio, Ethanol dehydrogenation to ethyl acetate by using copper and copper chromite catalysts, Chem. Eng. J. 179 (2012) 209–220. doi:10.1016/j.cej.2011.10.043.

[6] D.L. Carvalho, R.R. de Avillez, M.T. Rodrigues, L.E.P. Borges, L.G. Appel, Mg and Al mixed oxides and the synthesis of n-butanol from ethanol, Appl. Catal. Gen. 415–416 (2012) 96 – 100. doi:http://dx.doi.org/10.1016/j.apcata.2011.12.009.

[7] J. Sun, Y. Wang, Recent Advances in Catalytic Conversion of Ethanol to Chemicals, ACS Catal. 4 (2014) 1078–1090. doi:10.1021/cs4011343.

[8] Y. Kang, M. Sun, A. Li, Studies of the Catalytic Oxidation of CO Over Ag/CeO$_2$ Catalyst, Catal. Lett. 142 (2012) 1498–1504. doi:10.1007/s10562-012-0893-2.

[9] X. Bao, M. Muhler, B. Pettinger, R. Schlögl, G. Ertl, On the nature of the active state of silver during catalytic oxidation of methanol, Catal. Lett. 22 (1993) 215–225. doi:doi:10.1007/BF00810368.

[10] L. Ma, D. Wang, J. Li, B. Bai, L. Fu, Y. Li, Ag/CeO$_2$ nanospheres: Efficient catalysts for formaldehyde oxidation, Appl. Catal. B Environ. 148-149 (2014) 36–43. doi:10.1016/j.apcatb.2013.10.039.

[11] G.A. Voronova, O.V. Vodyankina, V.N. Belousova, E.V. Bezrukov, L.N. Kurina, Role of the Surface Acid–Base Properties of Silver Catalysts in the Partial Oxidation of Ethylene Glycol, Kinet. Catal. 44 (2003) 652–656. doi:10.1023/A:1026194006426.

[12] V. Raji, M. Chakraborty, P.A. Parikh, Catalytic Performance of Silica-Supported Silver Nanoparticles for Liquid-Phase Oxidation of Ethylbenzene, Ind. Amp Eng. Chem. Res. 51 (2012) 5691–5698. doi:10.1021/ie2027603.

[13] J. Chen, X. Tang, J. Liu, E. Zhan, J. Li, X. Huang, W. Shen, Synthesis and Characterization of Ag−Hollandite Nanofibers and Its Catalytic Application in Ethanol Oxidation, Chem. Mater. 19 (2007) 4292–4299. doi:10.1021/cm070904k.

[14] Z. Li, J. Xu, X. Gu, K. Wang, W. Wang, X. Zhang, Z. Zhang, Y. Ding, Selective Gas-Phase Oxidation of Alcohols over Nanoporous Silver, ChemCatChem. 5 (2013) 1705–1708. doi:10.1002/cctc.201200862.

[15] S. Song, X. Wang, H. Zhang, CeO$_2$-encapsulated noble metal nanocatalysts: enhanced activity and stability for catalytic application, NPG Asia Mater. 7 (2015) e179.

[16] J. Qi, J. Chen, G. Li, S. Li, Y. Gao, Z. Tang, Facile synthesis of core-shell Au@CeO$_2$ nanocomposites with remarkably enhanced catalytic activity for CO oxidation, Energy Env. Sci. 5 (2012) 8937–8941. doi:10.1039/C2EE22600F.

[17] X. Liu, J. Ding, X. Lin, R. Gao, Z. Li, W.-L. Dai, Zr-doped CeO$_2$ nanorods as versatile catalyst in the epoxidation of styrene with tert-butyl hydroperoxide as the oxidant, Appl. Catal. Gen. 503 (2015) 117–123. doi:10.1016/j.apcata.2015.07.010.

[18] C.M. Olmos, L.E. Chinchilla, E.G. Rodrigues, J.J. Delgado, A.B. Hungría, G. Blanco, M.F.R. Pereira, J.J.M. Órfão, J.J. Calvino, X. Chen, Synergistic effect of bimetallic Au-Pd supported on ceria-zirconia mixed oxide catalysts for selective oxidation of glycerol, Appl. Catal. B Environ. 197 (2016) 222–235. doi:10.1016/j.apcatb.2016.03.050.

[19] L. He, Y. Yu, C. Zhang, H. He, Complete catalytic oxidation of o-xylene over CeO_2 nanocubes, J. Environ. Sci. 23 (2011) 160–165. doi:10.1016/S1001-0742(10)60388-9.

[20] A. Aranda, B. Puértolas, B. Solsona, S. Agouram, R. Murillo, A.M. Mastral, S.H. Taylor, T. Garcia, Total Oxidation of Naphthalene Using Mesoporous CeO_2 Catalysts Synthesized by Nanocasting from Two Dimensional SBA-15 and Three Dimensional KIT-6 and MCM-48 Silica Templates, Catal. Lett. 134 (2010) 110–117. doi:10.1007/s10562-009-0203-9.

[21] N. Barrabés, K. Föttinger, J. Llorca, A. Dafinov, F. Medina, J. Sá, C. Hardacre, G. Rupprechter, Pretreatment Effect on Pt/CeO_2 Catalyst in the Selective Hydrodechlorination of Trichloroethylene, J. Phys. Chem. C. 114 (2010) 17675–17682. doi:10.1021/jp1048748.

[22] M. Han, X. Wang, Y. Shen, C. Tang, G. Li, R.L. Smith, Preparation of Highly Active, Low Au-Loaded, Au/CeO_2 Nanoparticle Catalysts That Promote CO Oxidation at Ambient Temperatures, J. Phys. Chem. C. 114 (2010) 793–798. doi:10.1021/jp908313t.

[23] P. Wu, H. Zhang, N. Du, L. Ruan, D. Yang, A Versatile Approach for the Synthesis of ZnO Nanorod-Based Hybrid Nanomaterials via Layer-by-Layer Assembly, J. Phys. Chem. C. 113 (2009) 8147–8151. doi:10.1021/jp901896u.

[24] P. Periyat, F. Laffir, S.A.M. Tofail, E. Magner, A facile aqueous sol–gel method for high surface area nanocrystalline CeO_2, RSC Adv. 1 (2011) 1794. doi:10.1039/c1ra00524c.

[25] S. Scirè, P.M. Riccobene, C. Crisafulli, Ceria supported group IB metal catalysts for the combustion of volatile organic compounds and the preferential oxidation of CO, Appl. Catal. B Environ. 101 (2010) 109–117. doi:10.1016/j.apcatb.2010.09.013.

[26] W.Y. Hernández, M.A. Centeno, F. Romero-Sarria, J.A. Odriozola, Synthesis and Characterization of $Ce_{1-x}Eu_xO_{2-x/2}$ mixed Oxides and Their Catalytic Activities for CO Oxidation, J. Phys. Chem. C. 113 (2009) 5629–5635. doi:10.1021/jp8092989.

[27] S. Machmudah, M. Akmal Hadian, L. Samodro K., S. Winardi, _ W., H. Kanda, M. Goto, Preparation of Ceria-Zirconia Mixed Oxide by Hydrothermal Synthesis, Mod. Appl. Sci. 9 (2015) 134–139. doi:10.5539/mas.v9n7p134.

[28] J.B.B.R. Muruganantham Chelliah, U.M. Krishnan, Synthesis and Characterization of Cerium Oxide Nanoparticles by Hydroxide Mediated Approach, J. Appl. Sci. 12 (2012) 1734–1737. doi:10.3923/jas.2012.1734.1737.

[29] J. Zhang, L. Li, X. Huang, G. Li, Fabrication of $Ag-CeO_2$ core-shell nanospheres with enhanced catalytic performance due to strengthening of the interfacial interactions, J Mater Chem. 22 (2012) 10480–10487. doi:10.1039/C2JM16701H.

[30] N. Acerbi, S.C.E. Tsang, G. Jones, S. Golunski, P. Collier, Rationalization of Interactions in Precious Metal/Ceria Catalysts Using the d-Band Center Model, Angew. Chem. Int. Ed. 52 (2013) 7737–7741. doi:10.1002/anie.201300130.

[31] L.S.F. Feio, C.E. Hori, S. Damyanova, F.B. Noronha, W.H. Cassinelli, C.M.P. Marques, J.M.C. Bueno, The effect of ceria content on the properties of $Pd/CeO_2/Al_2O_3$ catalysts for steam reforming of methane, Appl. Catal. Gen. 316 (2007) 107–116. doi:10.1016/j.apcata.2006.09.032.

[32] G.V. Mamontov, V.V. Dutov, V.I. Sobolev, O.V. Vodyankina, Effect of transition metal oxide additives on the activity of an Ag/SiO_2 catalyst in carbon monoxide oxidation, Kinet. Catal. 54 (2013) 487–491. doi:10.1134/S0023158413040137.

[33] M.J. Beier, T.W. Hansen, J.-D. Grunwaldt, Selective liquid-phase oxidation of alcohols catalyzed by a silver-based catalyst promoted by the presence of ceria, J. Catal. 266 (2009) 320–330. doi:10.1016/j.jcat.2009.06.022.

[34] F. Benedetti, P. Luches, M.C. Spadaro, G. Gasperi, S. D'Addato, S. Valeri, F. Boscherini, Structure and Morphology of Silver Nanoparticles on the (111) Surface of Cerium Oxide, J. Phys. Chem. C. 119 (2015) 6024–6032. doi:10.1021/jp5120527.

[35] W. Huang, Y. Gao, Morphology-dependent surface chemistry and catalysis of CeO_2 nanocrystals, Catal Sci Technol. 4 (2014) 3772–3784. doi:10.1039/C4CY00679H.

[36] T. Mitsudome, Y. Mikami, M. Matoba, T. Mizugaki, K. Jitsukawa, K. Kaneda, Design of a Silver-Cerium Dioxide Core-Shell Nanocomposite Catalyst for Chemoselective Reduction Reactions, Angew. Chem. Int. Ed. 51 (2012) 136–139. doi:10.1002/anie.201106244.

[37] K. Shimizu, K. Sugino, K. Sawabe, A. Satsuma, Oxidant-Free Dehydrogenation of Alcohols Heterogeneously Catalyzed by Cooperation of Silver Clusters and Acid-Base Sites on Alumina, Chem. - Eur. J. 15 (2009) 2341–2351. doi:10.1002/chem.200802222.

[38] G. Zhou, B. Gui, H. Xie, F. Yang, Y. Chen, S. Chen, X. Zheng, Influence of CeO_2 morphology on the catalytic oxidation of ethanol in air, J. Ind. Eng. Chem. 20 (2014) 160 – 165. doi:http://dx.doi.org/10.1016/j.jiec.2013.04.012.

[39] P.-Y. Sheng, G.A. Bowmaker, H. Idriss, The Reactions of Ethanol over Au/CeO_2, Appl. Catal. Gen. 261 (2004) 171–181. doi:http://dx.doi.org/10.1016/j.apcata.2003.10.046.

[40] V.V. Kaichev, Y.A. Chesalov, A.A. Saraev, A.Y. Klyushin, A. Knop-Gericke, T.V. Andrushkevich, V.I. Bukhtiyarov, Redox mechanism for selective oxidation of ethanol over monolayer V_2O_5/TiO_2 catalysts, J. Catal. 338 (2016) 82 – 93. doi:http://dx.doi.org/10.1016/j.jcat.2016.02.022.

[41] V.V. Dutov, G.V. Mamontov, V.I. Sobolev, O.V. Vodyankina, Silica-supported silver-containing OMS-2 catalysts for ethanol oxidative dehydrogenation, Catal. Today. 278 (2016) 164–173. doi:10.1016/j.cattod.2016.05.058.

[42] H. Chen, X. Jia, Y. Li, C. Liu, Y. Yang, Controlled surface properties of Au/ZSM5 catalysts and their effects in the selective oxidation of ethanol, Catal. Today. 256 (2015) 153–160. doi:10.1016/j.cattod.2015.01.020.

[43] J. Mielby, J.O. Abildstrøm, F. Wang, T. Kasama, C. Weidenthaler, S. Kegnæs, Oxidation of Bioethanol using Zeolite-Encapsulated Gold Nanoparticles, Angew. Chem. Int. Ed. 53 (2014) 12513–12516. doi:10.1002/anie.201406354.

[44] M.M. Rahman, S.D. Davidson, J. Sun, Y. Wang, Effect of Water on Ethanol Conversion over ZnO, Top. Catal. 59 (2016) 37–45. doi:10.1007/s11244-015-0503-9.

[45] P. Liu, X. Zhu, S. Yang, T. Li, E.J.M. Hensen, On the metal–support synergy for selective gas-phase ethanol oxidation over $MgCuCr_2O_4$ supported metal nanoparticle catalysts, J. Catal. 331 (2015) 138 – 146. doi:http://dx.doi.org/10.1016/j.jcat.2015.08.025.

[46] A.S. Blokhina, I.A. Kurzina, V.I. Sobolev, K.Y. Koltunov, G.V. Mamontov, O.V. Vodyankina, Selective oxidation of alcohols over Si_3N_4-supported silver catalysts, Kinet. Catal. 53 (2012) 477–481. doi:10.1134/S0023158412040015.

Chapter – 6

Selective oxidation of Bioethanol: Influence of relative proportions of Ce and Zr in their mixed oxides on their catalytic performance

CHAPTER – 6

Selective oxidation of Bioethanol: Influence of relative proportions of Ce and Zr in their mixed oxides on their catalytic performance

As seen in preceding chapters 4 and 5 that reduced surface of supports plays a vital role in enhancing bioethanol conversion. This may be due to OSC of supports. Higher the OSC provides more oxygen for the reaction, resulted into higher conversion of bioethanol. In this chapter, series of $Ce_xZr_{1-x}O_2$ (x = 0.25, 0.5, 0.75) mixed oxide is prepared by precipitation method and wet impregnation method is employed for the synthesis of $Au/Ce_xZr_{1-x}O_2$ catalysts. All prepared catalysts are well characterized by powder X-ray diffraction, transmission electron microscopy, energy dispersive x-ray, thermo gravimetric analysis and fourier transform infrared spectroscopy. Catalytical activity is carried out between 200 - 350 ℃ and 5 atm with gas hourly space velocity of 18000 $mLg_{cat}^{-1}h^{-1}$ for bioethanol oxidation. The results showed that inclusion of Zr to Ce framework improved the OSC which leads to increase bioethanol conversion. $Au/Ce_xZr_{1-x}O_2$ catalysts exhibited good catalytic behavior in terms of conversion and selectivity towards acetaldehyde which is a valuable chemical for fine chemical industry.

6.1 Introduction

Over past several years, significant interest has arisen towards the green production of chemicals; and bioethanol has emerged as one of the promising feedstocks which are biomass derived. With larger availability of bioethanol (worldwide 30 billion gallons in 2016) [1] and it's still limited use in blending with fuels provide an opportunity for production of valuable chemicals such as acetaldehyde [2], acetic acid [3], ethyl acetate [4], butanol [5] etc with high selectivity. A review on the major previous works on ethanol transformation to valuable chemicals has been provided by Takei et al. [6]. The authors had summarized that supported noble metal catalysts are active in the production of acetic

acid, whereas base metal oxides favor acetaldehyde. High selectivity toward ethyl acetate has been observed for Pd/zeolite catalysts [6,7].

Acetaldehyde is commercially obtained by catalytic oxidation of ethylene following the Wacker process, which produces chlorinated wastes and is energy intensive. Therefore, special attention is paid for the development of new catalysts for production of acetaldehyde in a single step reaction of ethanol. In this efforts, Hidalgo et al. [8] investigated vanadium based catalyst for the gas phase oxidative dehydrogenation of ethanol and found that easily reducible catalysts were the most active at reaction conditions. Morales et al. [9] had shown that catalytic activity relied on nature of supports and size of metal nanoparticles. As compared to Cu/GORE-a and Cu/GOE, Cu/GORE-a exhibited high catalytic activity due to lower metal particle size, while despite of having high surface area Cu/GOE has low catalytic activity, where GORE-a was N_2 doped graphite oxide and GOE was un doped graphite oxide. Liu et al. [10] performed $M/MgCuCr_2O_4$ (M = Cu, Ag, Pd, Pt, Au) catalysts for aerobic oxidation of ethanol. Ethanol conversion for the $M/MgCuCr_2O_4$ increased in the order of Pt > Pd > Au > Ag > Cu and selectivity towards acetaldehyde follow the order Au > Pd> Ag> Pt >Cu. Among them $Au/MgCuCr_2O_4$ was the preferred catalyst due to strong synergy between Au nanoparticles and surface of Cu^+ species. Ethanol conversion of 60% with 93% acetaldehyde selectivity was observed with MWCNTs at 270°C [11]. Ag/hydroxyapatite catalyst employed for ethanol oxidation afforded 100% selectivity towards acetaldehyde at 250°C with 15% ethanol conversion. Further increase in temperature led to decline of acetaldehyde selectivity [2]. Similar trend of decreasing acetaldehyde selectivity at higher temperature was observed for silica supported Ag-containing OMS-2 (Octahedral molecular sieve) catalyst [12], V_2O_5/TiO_2 [13] and Au/ZSM5 [14]. In majority of reported work for ethanol oxidation, high concentrations of ethanol were employed for reaction. Literature available for bioethanol (typically containing 90 vol or wt% water) oxidation is rather scant. Au over silicalite-1 [15] was tested for bioethanol oxidation and it has been to yield 50% conversion of ethanol with 98% selectivity toward acetaldehyde at 200°C. Further increase in temperature resulted in decrease of both, conversion and selectivity towards acetaldehyde. Au-Pd@silicate-1 catalyst demonstrated 100% ethanol conversion in presence of 90% water but catalyst was highly selective for acetic acid [3]. Rahman et al. examined the effect of water on ethanol conversion over ZnO. In absence of water,

catalyst favored dehydration pathway whereas dehydrogenation was followed in presence of water [16].

Cerium oxide (CeO_2) is widely used in automotive three way catalytic converters to treat the emitted CO, NO_X, and unburned hydrocarbons. Mixing CeO_2 with other oxides (i.e., ZrO_2, TiO_2, Al_2O_3 and transition metal oxides) to form solid solution or mixed oxide is known to enhance the oxygen storage capacity (OSC), increase thermal stability of the materials and prevent sintering at higher temperatures [17]. Ceria doping with zirconia improves essentially its thermal stability and catalytic efficiency, which invokes application of mixed oxides in three way catalyst formulations, solid oxides fuel cells and water splitting devices [18]. Olmos et al. [19] showed the effects of OSC of $Ce_{1-x}Zr_xO_2$ on catalytic performance of Au-Pd/CZ (CZ: CeO_2, ZrO_2 mixed oxide) for oxidation of glycerol. Reduced redox properties of $Ce_{1-x}Zr_xO_2$ enhanced the catalytic properties for volatile organic compounds (VOC) combustion reaction [20]. Use of $Ce_{1-x}Zr_xO_2$ mixed oxides in some other catalytic reactions has also been studied, e.g., partial oxidation of methane, soot abatement from diesel engine exhausts, selective catalytic reduction of NO_X, fluid catalytic cracking, water gas shift reaction and selective catalytic CO oxidation [21].

As reported in chapter 4, Au/ZrO_2 and Au/CeO_2 exhibit good catalytic activity for bioethanol oxidation. This was due to reduced surface of ZrO_2 and CeO_2 provides excess oxygen for the reaction. Though $Ce_xZr_{1-x}O_2$ is known for their surface reducibility and higher OSC, they have not been reported for either pure ethanol or bioethanol oxidation reaction.

6.2 Experimental section

6.2.1 Synthesis of catalyst

The $Ce_xZr_{1-x}O_2$ (x = 0.25, 0.5 and 0.75) support was synthesized by co precipitation method as described earlier [23]. Required amounts of zirconium and cerium precursors were dissolved separately in 20 mL double distilled water. Solution of both nitrates were mixed together and stirred for 30 min at 1200 rpm. Dilute aqueous ammonia solution (30%, 20 ml) was added dropwise to the aforementioned mixture solutions with vigorous

stirring until precipitation was complete (pH = 8.5). Obtained yellowish precipitates were filtered off and washed several times with distilled water until free from anion impurities. The obtained cakes were dried overnight in an oven 120°C and finally calcined at 500°C for 5 h. The schematic diagram of $Ce_xZr_{1-x}O_2$ mixed oxide is shown in Figure 6.1.
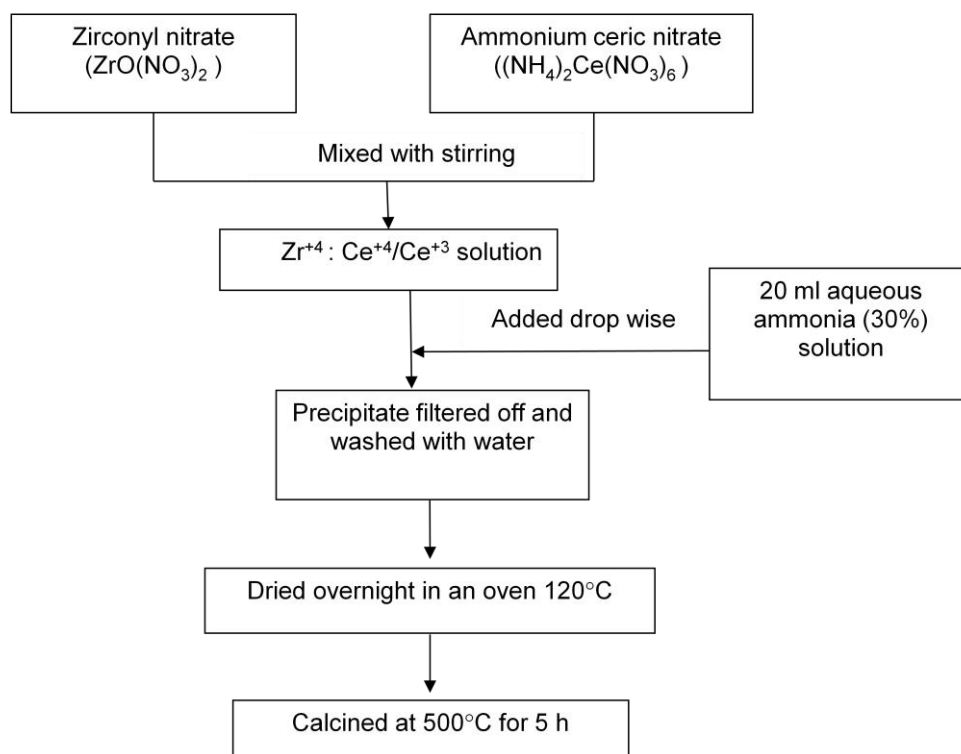
```
┌─────────────────────┐        ┌──────────────────────────┐
│  Zirconyl nitrate   │        │  Ammonium ceric nitrate  │
│   (ZrO(NO3)2 )      │        │   ((NH4)2Ce(NO3)6 )      │
└─────────────────────┘        └──────────────────────────┘
            │                              │
            └──────── Mixed with stirring ─┘
                          │
                 ┌────────────────────────┐
                 │  Zr+4 : Ce+4/Ce+3 solution │
                 └────────────────────────┘
                          │                    ┌──────────────────────┐
              Added drop wise                  │  20 ml aqueous       │
                          │ ◄───────────────── │  ammonia (30%)       │
                          │                    │  solution            │
                 ┌────────────────────────┐    └──────────────────────┘
                 │ Precipitate filtered off and │
                 │   washed with water     │
                 └────────────────────────┘
                          │
                 ┌────────────────────────┐
                 │ Dried overnight in an oven 120°C │
                 └────────────────────────┘
                          │
                 ┌────────────────────────┐
                 │ Calcined at 500°C for 5 h │
                 └────────────────────────┘
```

Figure 6.1 Schematic diagram of $Ce_xZr_{1-x}O_2$ mixed oxide

$Au/Ce_xZr_{1-x}O_2$ is synthesized using traditional wet impregnation method as described in detail in chapter 3 (section 3.3.1.2).

6.2.2 Catalyst characterization

Transmissions electron microscopy (TEM) images of the catalyst were recorded on a Philips CM 200 microscope operating at 200 kV. The samples were dispersed in ethanol and kept in an ultrasonic bath for 20 min, then deposited on a carbon-covered copper grid for each measurement. Surface morphology of the catalyst was investigated with scanning electron microscopy (SEM) and energy dispersive X-ray analysis (EDX) (JEOL make model 7600F FESEM) was carried out to verify the presence of Ag nanoparticles.

X-ray Diffraction (XRD) analysis was performed on a Bruker - D8 Discover equipped with Ni-filtered Cu Kα radiation source (λ = 1.542 Å) 40 kV and 30 mA. The diffractograms were recorded in the 2θ range of 20 - 90° with a 2θ step size of 0.02° and a scanning speed of 6° min^{-1}. Average crystal size was determined by the Scherer's equation. Fourier Transform Infrared Spectroscopy (FTIR) spectra of catalyst samples were collected in reflection mode using ZnSe optics in Bruker Alpha Eco-ATR spectrometer. Oxygen storage capacity (OSC) was measured by thermo gravimetric analysis (TGA) on a Mettler Toledo TG-SDTA apparatus.

6.2.3 Catalyst activity test

Catalysts were tested for ethanol conversion using heated stainless steel continuous fixed bed down flow reactor. Details of the reactor set-up is presented in chapter 4 (section 4.2.3) and the sample reaction is analyzed as described in chapter 4(section 4.2.3.

Catalytic performance of the system was evaluated on the basis of conversion of bioethanol and products selectivity as defined in section 3.3.2.1.

6.3 Results and discussion

6.3.1 Catalyst characterization

The catalysts were characterized using Fourier transform infrared spectroscopy (FTIR), x-ray diffraction pattern (XRD), Transmission electron microscopy (TEM) and thermo gravimetric analysis (TGA).

6.3.1.1 Powder X-ray diffraction

X-ray diffraction patterns of the prepared $Au/Ce_xZr_{1-x}O_2$ (x=0.25, 0.5 and 0.75) are shown in Figure 6.2. Diffraction peaks at 2θ values of 29.5°, 33.5°, 48.2°, 57.5°, 60.3°, 70.8°, 77.0° and 80.9° correspond to the (111), (200), (220), (311), (222), (400), (331) and (420) planes of the cubic fluorite-type structure of ceria-zirconia mixed oxide [19,24]. The characteristic peak around 2θ=28.5°(JCPDS-34-0394) of ceria is shifted to 28.62° for $Ce_{0.75}Zr_{0.25}O_2$ to 29.10° for $Ce_{0.5}Zr_{0.5}O_2$ and 29.5° for $Ce_{0.25}Zr_{0.75}O_2$. These shifts are

attributed to contraction of the lattice cells by the insertion of ZrO_2 into the CeO_2 [25,26] and has taken as formation of Ce - Zr solid solutions [27]. The shrinkage of lattice cells is an indication of the substitution of smaller ionic size Zr^{4+}(0.084 nm) for Ce^{4+}(0.097 nm) [25,28,29].

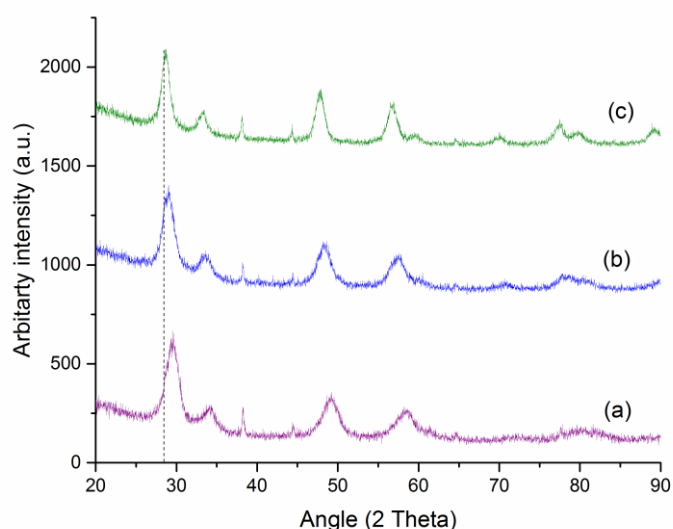An additional peak at 38.1° is observed and it can be attributed to (111) Bragg's reflections of Au.

Figure 6.2 X-ray diffraction pattern of (a) $Au/Ce_{0.25}Zr_{0.75}O_2$ (b) $Au/Ce_{0.5}Zr_{0.5}O_2$ and (c) $Au/Ce_{0.75}Zr_{0.25}O_2$

Based on Bragg's law and Debye-Scherrer equation, the lattice parameters and crystallite sizes of all samples are calculated and the results are listed in Table 1. For comparison, theoretic lattice parameters are determined from Vegard's law. According to Kim [21,30], Vegard's law for estimation of the theoretical lattice parameter of ceria-based solution as a function of the guest metal content is expressed in equation considering Zr^{4+} as dopant.

a = 0.5414 + 0.0220 (rZr – rCe) * mZr

where ''a'' (in nm) is the lattice constant of the solid solution at room temperature, rCe and rZr are the cationic radii of Ce^{4+} and Zr^{4+} (in nm), respectively and mZr is the mol% of the dopant.

Table 6.1 Particle size, lattice parameter and surface composition of prepared $Ce_xZr_{1-x}O_2$ samples

Samples	Crystalline size from XRD (nm)	Lattice parameter (nm)	Cell volume $(nm)^3$	Surface composition (at.%) determined by EDAX			
				Au	Ce	Zr	O
CeO_2 [21]	--	0.5414	0.1587				
$Ce_{0.75}Zr_{0.25}O_2$	27.50	0.5355	0.1525	--	19.05	7.60	73.35
$Ce_{0.5}Zr_{0.5}O_2$	28.65	0.5284	0.1464	--	17.16	14.41	68.43
$Ce_{0.25}Zr_{0.75}O_2$	3	0.5210	0.1405	--	8.24	19.42	72.34
Au/ $Ce_{0.75}Zr_{0.25}O_2$	7.15	--		0.18	18.98	7.51	73.33
Au/ $Ce_{0.5}Zr_{0.5}O_2$	7.25	--		0.12	17.11	14.39	68.38
Au/ $Ce_{0.25}Zr_{0.75}O_2$	8	--		0.14	8.19	19.39	72.28

Figure 6.3 depicts the corresponding lattice parameters for prepared samples in terms of Zr content. The estimated experimental lattice parameters are slightly higher than theoretic values predicted by the Vegard's rule (represented by a dotted line). This implies the existence of Ce^{3+} (1.14 Å), due to incorporation of Zr. This strongly suggests that a solid solution can be achieved with zirconium loading at least up to 75 mol %. By comparing with a most oxidative co-precipitation method, a $Ce_{0.67}Zr_{0.33}O_2$ sample yielded a value of lattice parameter of 0.5320 nm which is on the expected trend as well [31].

6.3.1.2 Energy dispersive x-ray analysis (EDX)

The energy dispersive X-ray analysis (EDX) further confirms all the cations are present in the parent mixed oxides and Au impregnated mixed oxides. EDX spectrum ratifies peaks for O_2, Au, Zr and Ce. There is a one peak at 0.5 keV for O_2, peaks at 1.7, 2.2 and 2.5 keV for Au, peaks near about 1.8, 2.1 and 2.6 keV for Zr and peaks at 4.2, 4.7, 5.3 and 5.6 keV for Ce shown in Figure 6.4 (a-c). Elemental composition analysis (Table 6.1) at several spots is uniform suggesting homogeneous material.
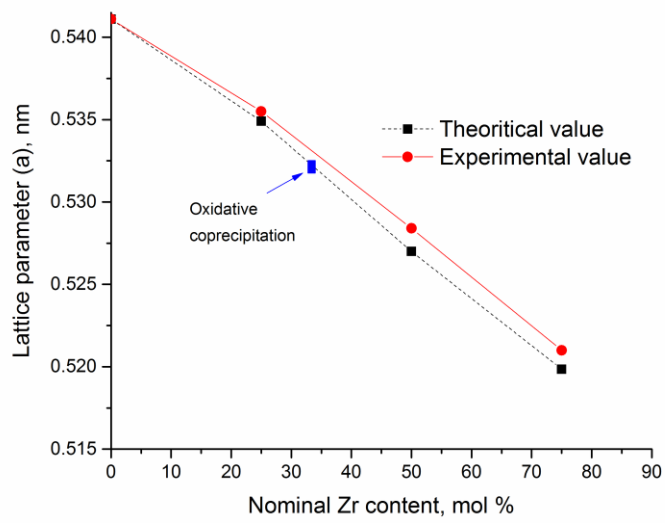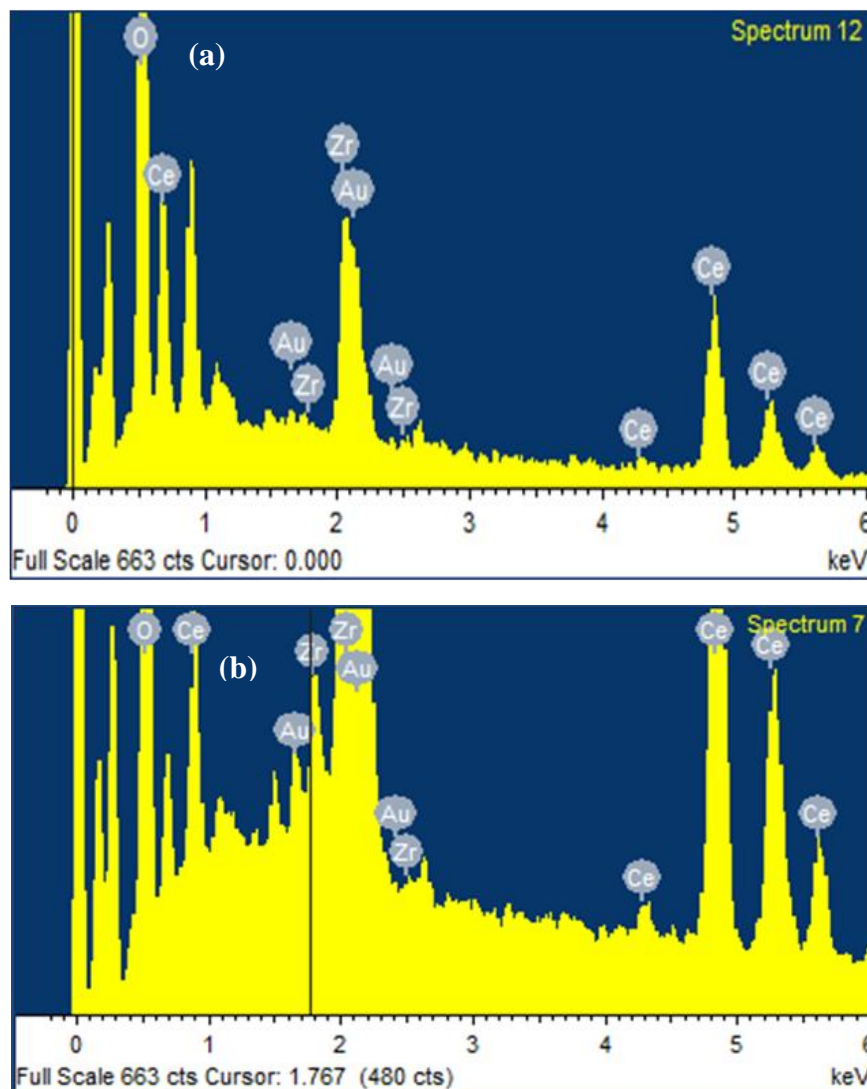
Figure 6.3 Variation of the lattice parameter (experimental) in the ceria–zirconia mixed oxides with increasing amounts of ZrO_2 inserted into the CeO_2 lattice
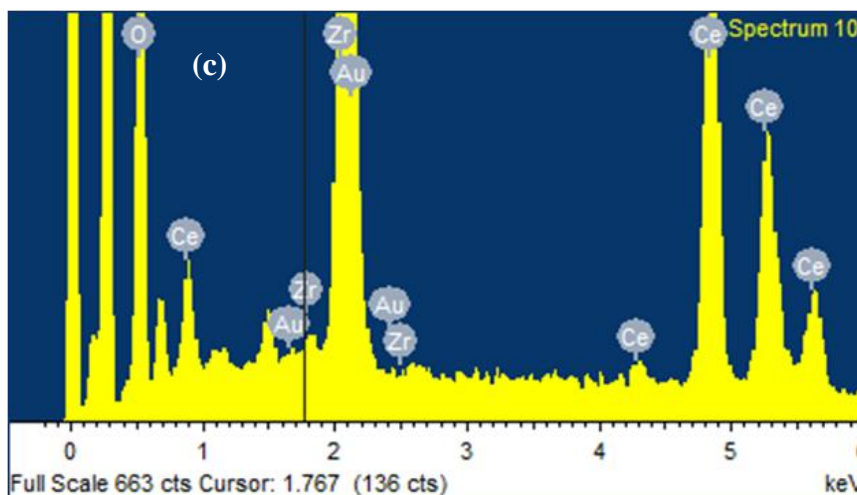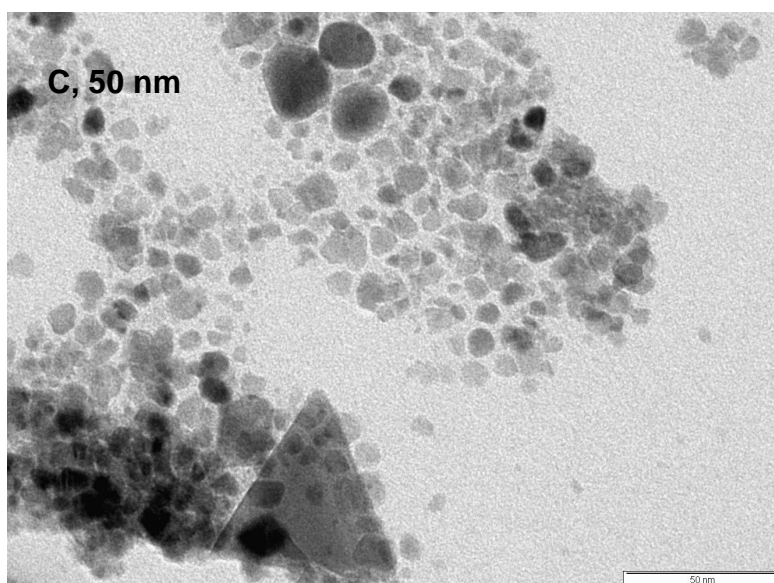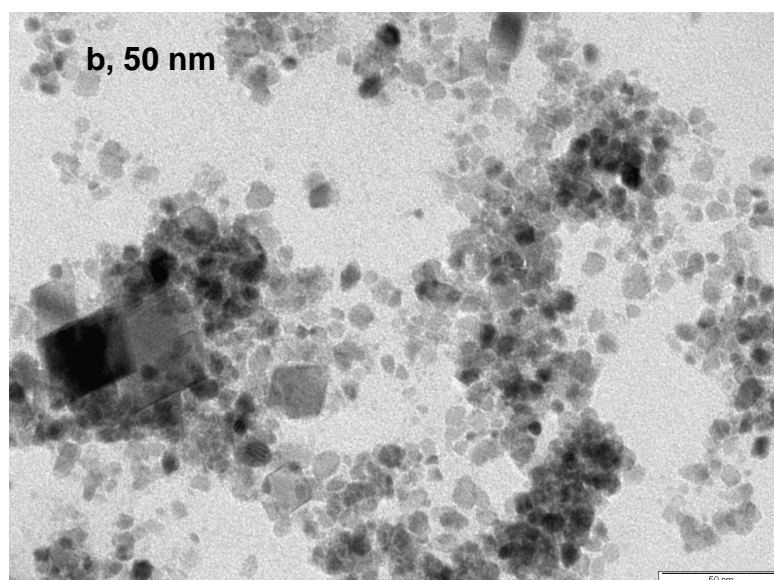
Figure 6.4 EDX analysis of (a) $Au/Ce_{0.25}Zr_{0.75}O_2$ (b) $Au/Ce_{0.5}Zr_{0.5}O_2$ and (c) $Au/Ce_{0.75}Zr_{0.25}O_2$

6.3.1.3 Transmission electron microscope (TEM)

TEM images (Figure 6.5 (a- c)) are obtained to deduce the particle size and morphology of catalysts. They revealed that Au nanoparticles were on the surfaces of $Ce_xZr_{1-x}O_2$. As indicated in Figure 6.5(a- c), the $Ce_xZr_{1-x}O_2$ crystallized in cubic shape with particle size of around 30 nm and the d spacing for the lattice was 0.312 nm. While the average sizes of Au particle was around 7 nm. The d spacing of Au was 0.235 nm, which was corresponding to the Au (111) [32]. The d spacing was calculated from SAED pattern Figure 6.5(d).
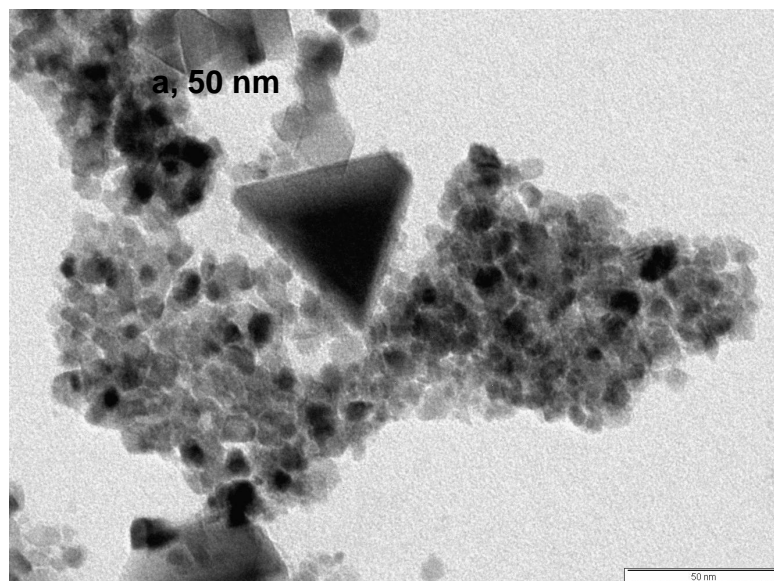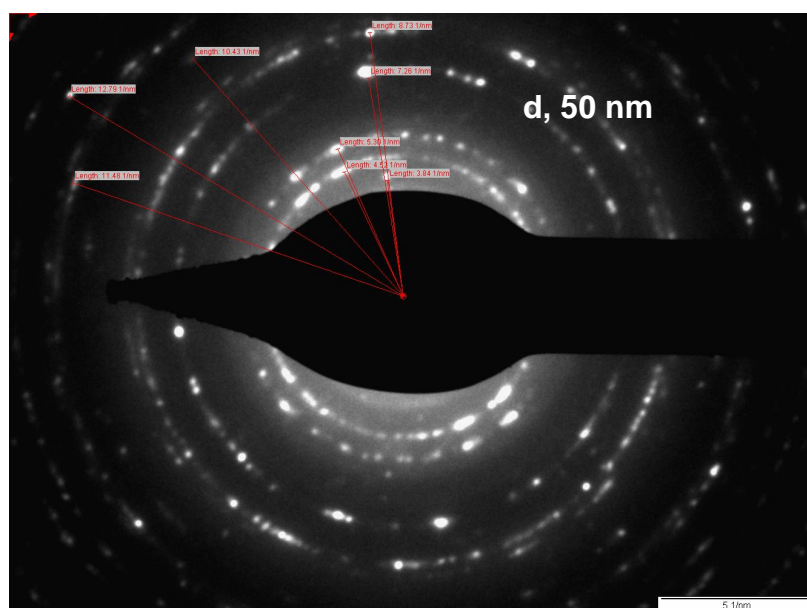
Figure 6.5 TEM images of (a) $Au/Ce_{0.25}Zr_{0.75}O_2$ (b) $Au/Ce_{0.5}Zr_{0.5}O_2$ (c) $Au/Ce_{0.75}Zr_{0.25}O_2$ and (d) SAED pattern for $Au/Ce_{0.25}Zr_{0.75}O_2$

6.3.1.4 Fourier Transform Infrared Spectroscopy

The instrument was operated in the range of 400 - 4000 cm^{-1}. The FTIR spectra of $Ce_xZr_{1-x}O_2$ samples and $Au/Ce_xZr_{1-x}O_2$ samples are shown Figures 6.6 and 6.7. They exhibited absorption band around 3750 cm^{-1} which corresponds to the stretching vibration of the –OH function group [33]. The band located at 1700 cm^{-1} represents H_2O bending vibration [18,33–35] and at around 1530 cm^{-1} is because of Ce-OH stretching vibration [34,35]. It can be seen from spectra of each sample (Figure 6.7), peak around 990 cm^{-1} assigned to M-O-M bonding (M= Au, Ce, Zr) [26,34]. Bands in the region 500 to 750 cm^{-1} are probably because of stretching vibration of metal oxide bonds [33,34].
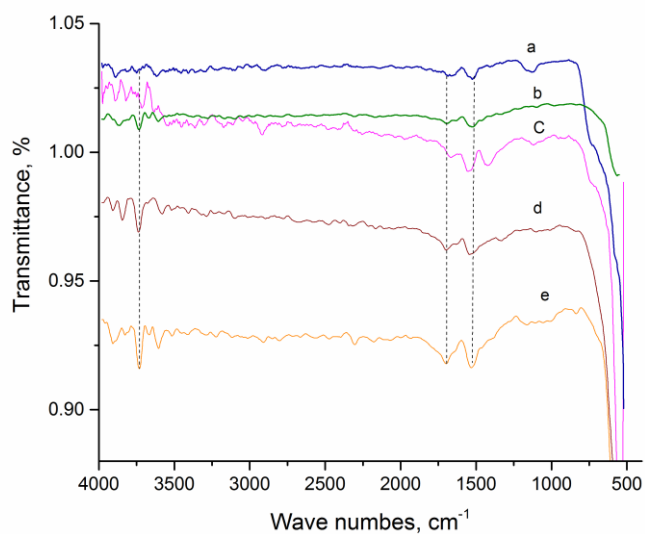
Figure 6.6 FTIR of CexZr1-xO2 samples (a) ZrO_2 (b) $Ce_{0.5}Zr_{0.5}O_2$ (c) CeO_2 (d) $Ce_{0.25}Zr_{0.75}O_2$ and (e) $Ce_{0.75}Zr_{0.25}O_2$
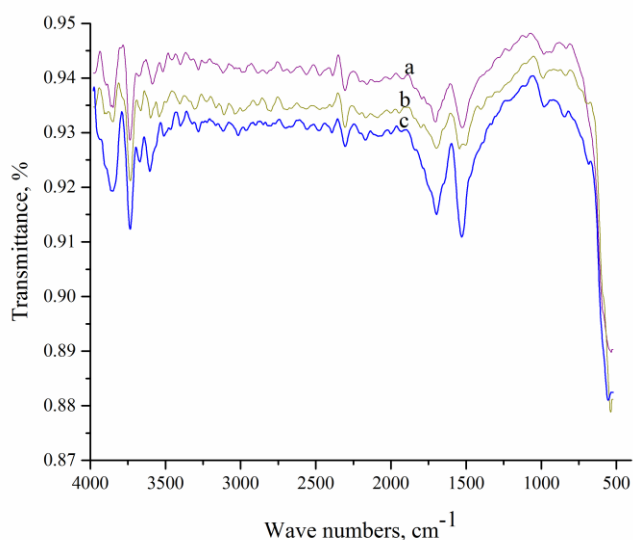
Figure 6.7 FTIR of (a) $Au/Ce_{0.75}Zr_{0.25}O_2$ (b) $Au/Ce_{0.5}Zr_{0.5}O_2$ and (c) $Au/ Ce_{0.25}Zr_{0.75}O_2$

6.3.1.5 OSC measurement

Figure 6.8 (a) and (b) are thermograms for OSC measurement of $Ce_xZr_{1-x}O_2$ and $Au/Ce_xZr_{1-x}O_2$ catalysts, respectively obtained after second heating cycle. As seen in figures (Figure 6.8 (a) and (b)) in the range of temperature $150 – 800 °C$, weight loss was observed. This change in weight loss was due to loss of adsorbed water on the surface of the sample and decomposition of unreacted nitrates. The Change in weight loss for

$Ce_{0.75}Zr_{0.25}O_2$ was lower than $Ce_{0.5}Zr_{0.5}O_2$ and $Ce_{0.25}Zr_{0.75}O_2$. Similar trend for weight loss was also observed for $Au/Ce_xZr_{1-x}O_2$ catalysts. This might be due to the more water adsorbed on the surface of the higher Zr content catalysts. In temperature range of 150 – 400 °C, weight loss was 0.3% reflecting loss of adsorbed water molecules and decomposition of unreacted nitrates. The weight loss in the latter region was <1% for all the samples, suggesting that almost all the nitrates were decomposed. While weight loss beyond 450 °C was about 0.5% for all samples, indicating that over the temperature range of 450 - 800°C, mixed oxides are quite stable in terms of chemical composition [36].

Figure 6.8 TGA results of (a) $Ce_xZr_{1-x}O_2$ and (b) $Au/Ce_xZr_{1-x}O_2$ catalysts obtained after second heating cycle.

As seen in Table 2, upon the addition of Zr to Ce, OSC of the as prepared catalysts increased in order of $Ce_{0.25}Zr_{075}O_2 > Ce_{0.5}Zr_{0.5}O_2 > Ce_{0.75}Zr_{0.25}O_2$ and for $Au/Ce_xZr_{1-x}O_2$ in the o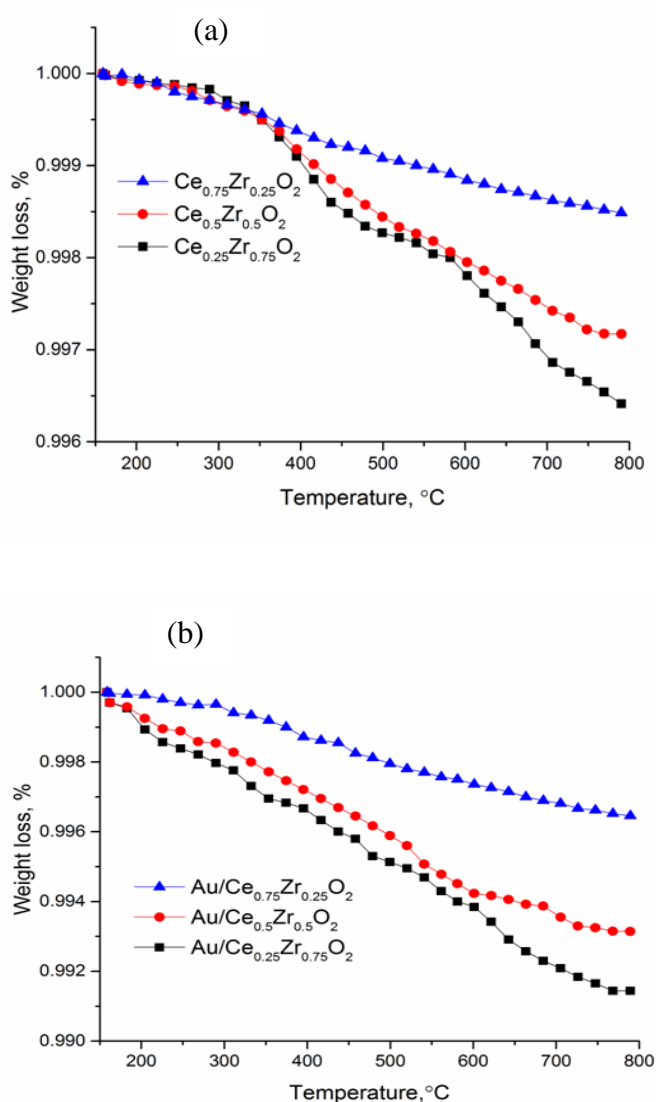rder of $Au/Ce_{0.25}Zr_{0.75}O_2 > Au/Ce_{0.5}Zr_{0.5}O_2 > Au/Ce_{0.75}Zr_{0.25}O_2$. This trend indicated that surface was more reduced at higher Zr content which implies that oxygen availability at surface increased.

Table 6.2 OSC of Prepared $Ce_xZr_{1-x}O_2$ and $Au/Ce_xZr_{1-x}O_2$ catalysts

Catalyst	OSC	$(\mu mol\ O\ g^{-1})$
	Parent mixed oxides	Au (1 wt%) containing mixed oxides
$Ce_{0.75}Zr_{0.25}O_2$	89	177
$Ce_{0.5}Zr_{0.5}O_2$	155	338
$Ce_{0.25}Zr_{0.75}O_2$	193	365

6.3.2. Catalytic activity of $Ce_xZr_{1-x}O_2$ and $Au/Ce_xZr_{1-x}O_2$ for bioethanol oxidation

6.3.2.1 Effect of Temperature

Figure 6.9 shows catalytic performance of $Ce_xZr_{1-x}O_2$ and $Au/Ce_xZr_{1-x}O_2$ catalysts for oxidation of bioethanol (10 wt%, Ethanol) at the varying temperature and pressure (5 atm) condition. All $Ce_xZr_{1-x}O_2$ and $Au/Ce_xZr_{1-x}O_2$ catalysts show negligible conversion at 200 °C which gradually increased with temperature. Increased Zr content led to enhanced bioethanol conversion. This could be ascribed to the addition of Zr to Ce causing change in lattice parameter and subsequently to modification and defects in crystalline structure. The altered lattice parameter shrinks the unit cell volume (Table 6.1), due to the smaller Zr^{+4} ionic radius compared to Ce^{+4}. Also the increased concentration of Zr^{+4} in Ce framework shortens Ce-O bond length. According to the reported literature [28,37], stress induced by decreased unit cell volume, lowers the activation energy for oxygen ion diffusion with in lattice and favors the reduction of Ce surface. Incorporation of Zr^{+4} also enhances defects in crystalline structure which are expected to play an important role in

reduction/oxidation behavior [38,39]. Structural defects could also be assigned to the oxygen vacancies since the enthalpy of formation of oxygen vacancies decreases with the reduction of crystallite size [40 - 42].
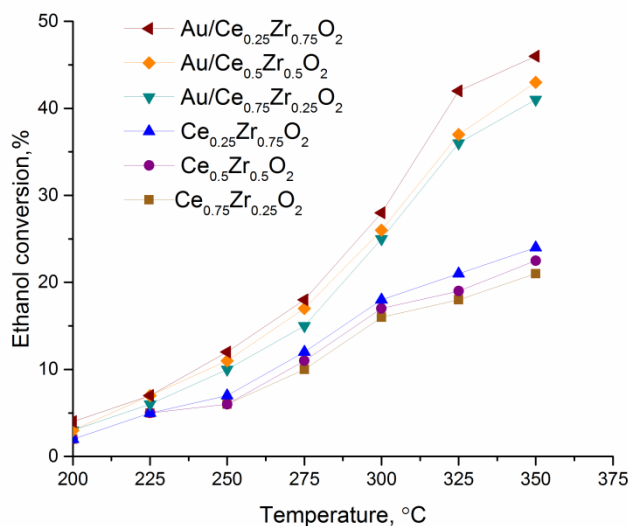
Figure 6.9 Ethanol conversion as a function of reaction temperature over different catalyst (Reaction condition: catalyst = 1 g, pressure = 5 atm, ethanol/H_2O/O_2/N_2 (vol %) = 0.002:0.018:20.99:78.98 and GHSV =18000 mLg$_{cat}^{-1}$h^{-1})

The OSC is related to the presence of defects in the structure like oxygen vacancies and crystallite planes exposed at the surface oxide. In the case of the mixed oxide ($Ce_xZr_{1-x}O_2$) higher generation of oxygen vacancies can be attributed to the incorporation of the Zr^{4+} cation in the lattice of the CeO_2 structure [29,40]. Fornasiero et al. [41] have reported that incorporation of Zr promotes Ce reduction through the generation of defects which enhances the bulk O_2^- ion mobility via vacancy diffusion. They reasoned that diffusion of O from the bulk to the surface of particles or to grain boundaries between particles is the rate limiting process for CO_2 formation. Dimitrov et al. [20] also showed that increased Zr content in Ce framework led to increase catalytic activity for ethyl acetate combustion.

As compared to parent $Ce_xZr_{1-x}O_2$ catalysts, $Au/Ce_xZr_{1-x}O_2$ exhibited better catalytic performance, which indicated that the addition of active Au metal was important for efficiently promoting bioethanol oxidation activity. Ethanol conversion for $Au/Ce_{0.75}Zr_{0.25}O_2$, $Au/Ce_{0.5}Zr_{0.5}O_2$ and $Au/Ce_{0.25}Zr_{0.75}O_2$ reached to 41%, 43% and 46 % at 350°C, respectively. Increase in conversion indicates that parent $Ce_xZr_{1-x}O_2$ samples

further reduced upon impregnation of Au nano particles. Reduction of $Ce_xZr_{1-x}O_2$ solid sample by the metals has been well reported [42 - 46]. Gomez et al. investigated CO oxidation over the Au loaded CeZr solid solutions and reported that Ce/Zr ratio, OSC and reducibility power of the solid solution to be responsible for the increased activity of the support for Au nanoparticles in CO oxidation [45].

As compared to Au/CeO_2 and Au/ZrO_2 catalysts (chapter 4) for bioethanol conversion, all $Au/Ce_xZr_{1-x}O_2$ catalyst used in this work exhibited higher catalytic activity. This indicates that Au impregnated mixed oxides catalyst play significant role in the reaction may be due to their higher OSC than their pure oxides.

6.3.2.2 Products distribution employing different catalysts as function of reaction temperature
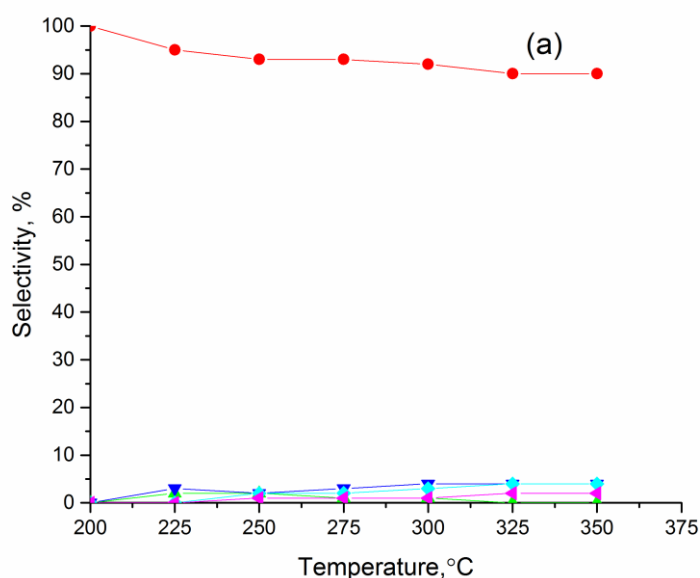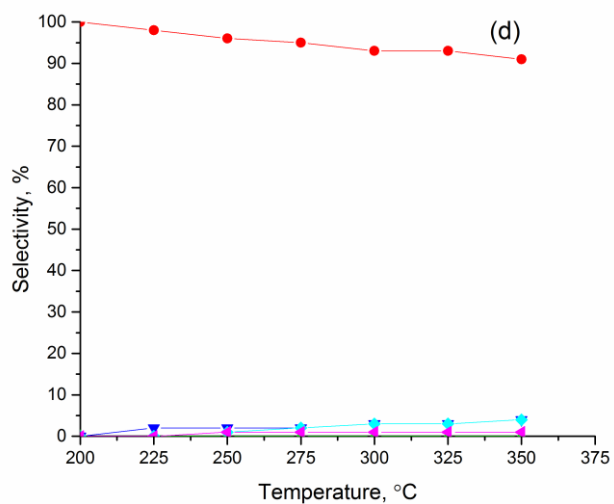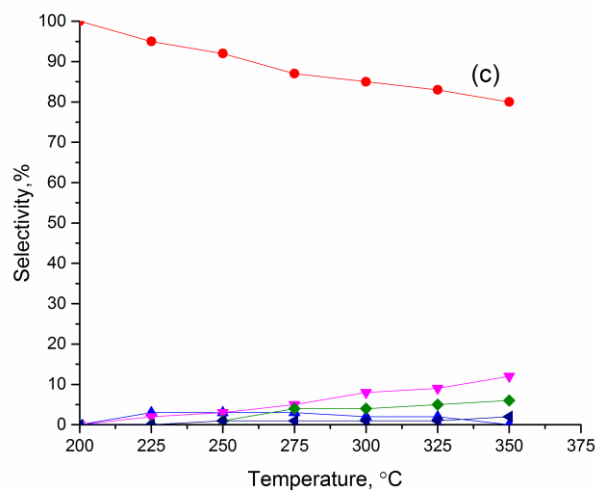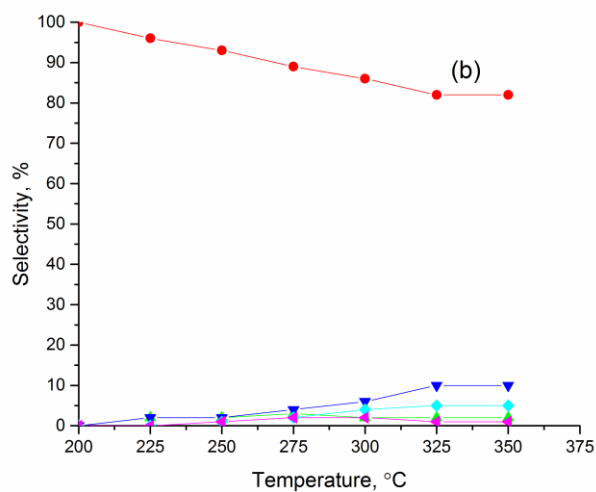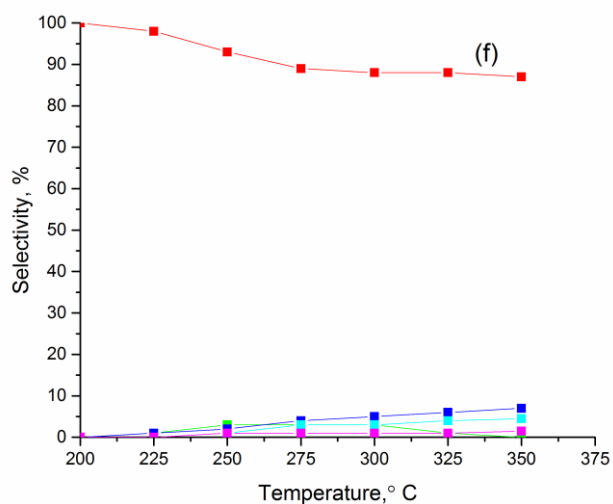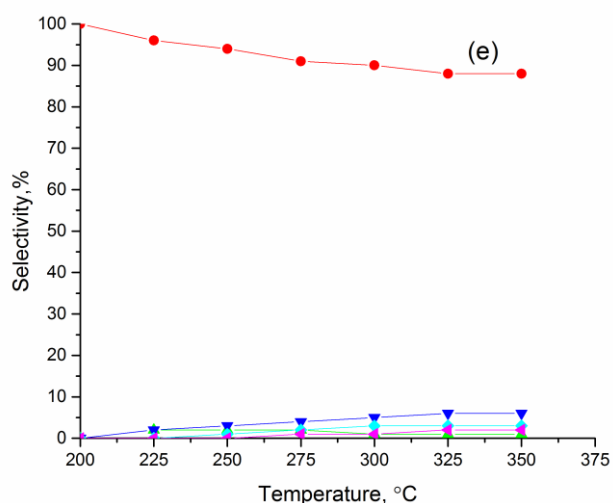
Figure 6.10 Products distribution (a) $Ce_{0.75}Zr_{0.25}O_2$ (b) $Ce_{0.5}Zr_{0.5}O_2$ (c) $Ce_{0.25}Zr_{0.75}O_2$ (d) $Au/Ce_{0.75}Zr_{0.25}O_2$ (e) $Au/Ce_{0.5}Zr_{0.5}O_2$ and (f) $Au/Ce_{0.25}Zr_{0.75}O_2$ Selectivity of acetaldehyde (●), acetic acid (▲), ethyl acetate (▼), acetone (◆) and CO_2 (*) as function of reaction temperature (Reaction condition: catalyst = 1 g, pressure = 5 atm, ethanol/H_2O/O_2/N_2 (vol %) =0.002:0.018:20.99:78.98and GHSV =18000 $mLg_{cat}^{-1}h^{-1}$)

It is worth-noting that product of the reaction over all the catalysts is acetaldehyde with selectivity in the range of 80 to 92%. Selectivity to acetaldehyde afforded by Au containing mixed oxide catalysts is higher than that by parent counterparts. Selectivity to acetaldehyde slightly declines with reaction time due to both, further surface oxidation and interface reactions. Oxidation of acetaldehyde to acetates at oxide surface and subsequent

coupling reactions yield acetone and formation of ethyl acetate can be explained by acetaldehyde activation on M^0 sites which couples with ethanol species activated by ZrO_2 surface. The coupling reaction occurs at metal surface interface. Thus, ethyl acetate and acetone are second main products, with selectivity values in the range 6 - 7% and 3 - 5 %, respectively. Selectivity to ethyl acetate over Zr rich catalyst is much higher than that of Ce rich catalyst in both parent and Au impregnated catalysts. The reverse trends shows for selectivity to acetone was observed with 3 -5 % over all the catalysts. Selectivity for acetic acid and CO_2 were in the range of 1 - 2 % for all catalysts indicating no deeper oxidation of bioethanol.

6.3.2.3 Effect of Zr proportions in ethanol conversion
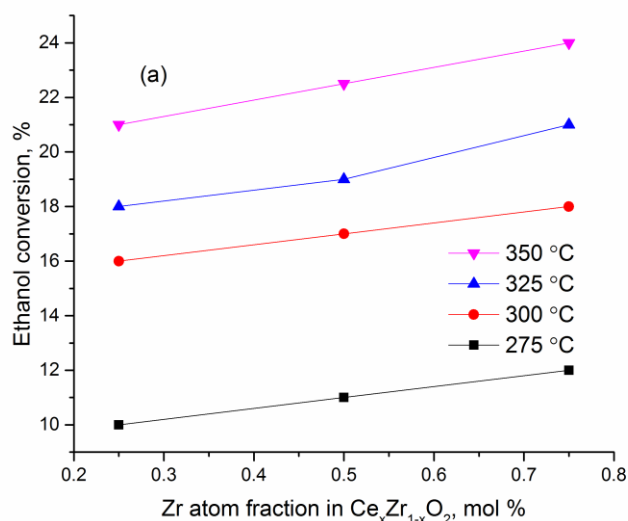
Increased Zr proportions in the mixed oxides ($Ce_xZr_{1-x}O_2$) lead to enhance OSC (Table 6.2) of catalysts, which plays significant role in the ethanol conversion. As seen in Figure 6.11(a) ethanol conversion increased from the 10 % to 12 % when Zr mol % increased from 25 % to 75% at 275 °C. Further increased in temperature from 300°C to 350 °C, ethanol conversion is increased from 16 % to 22 % for 25 mol % of Zr in parent mixed oxides and same trend is also observed for 50 mol % and 75 mol % of Zr in $Ce_xZr_{1-x}O_2$. In case of Au impregnated metal oxide catalysts, both Au and increase Zr fraction further enhanced OSC. Enhanced OSC of catalyst increased ethanol conversion for entire temperature range (Figure 6.11(b)).
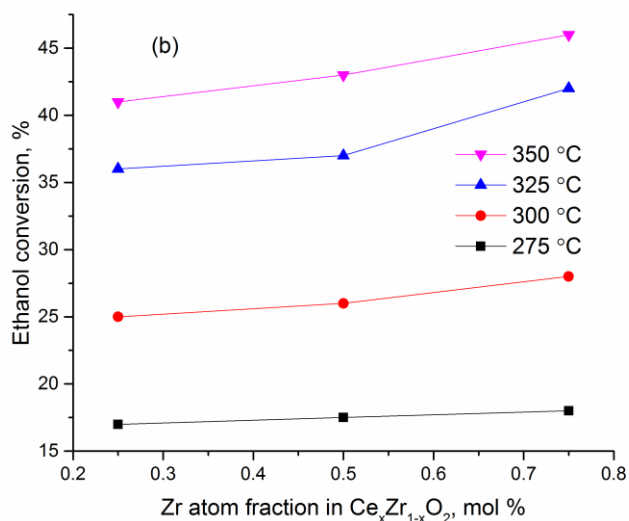
Figure 6.11 Effect of Zr proportions in ethanol conversion (a) parent mixed oxides (b) Au impregnated mixed oxides(Reaction condition: catalyst = 1 g, pressure = 5 atm, ethanol/H_2O/O_2/N_2 (vol %) = 0.002:0.018:20.99:78.98 and GHSV =18000 mLg$_{cat}^{-1}$h^{-1})

6.3.2.4 Effect of time-on-stream
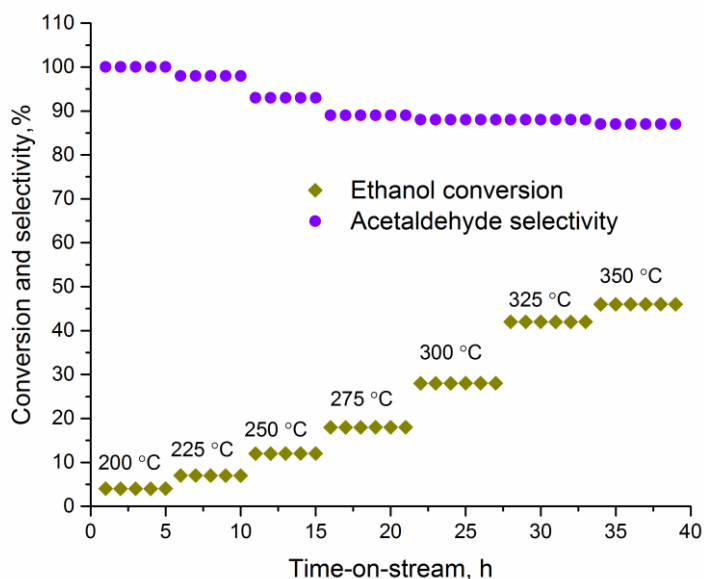
Figure 6.12 Ethanol conversion and acetaldehyde selectivity as function of time-on-stream for Au/ $Ce_{0.25}Zr_{0.75}O_2$ (Reaction condition: catalyst = 1 g, pressure = 5 atm, ethanol/H_2O/O_2/N_2 (vol %) = 0.002:0.018:20.99:78.98 and GHSV =18000 mLg$_{cat}^{-1}$h^{-1})

Catalytic performance of $Au/Ce_{0.25}Zr_{0.75}O_2$ catalyst is depicted in Figure 6.12. Ethanol conversion and acetaldehyde selectivity are plotted against time-on-stream. Low ethanol conversion (< 10%) and high selectivity (~100%) towards acetaldehyde are observed at low temperature (200 °C). Selectivity towards acetaldehyde decreased gradually with increase in temperature and reached to 90 % at 250 °C. Further increased in temperature did not change acetaldehyde selectivity, it remain almost constant for the entire duration, while conversion closely linked to the temperature. $Au/Ce_{0.25}Zr_{0.75}O_2$ catalyst exhibited no sign of catalyst deactivation for more than 40 h on-stream. It is observed that all catalysts (parent and Au impregnated mixed oxides) also displayed same stability as of $Au/Ce_{0.25}Zr_{0.75}O_2$.

The incorporation of Zr cation into the Ce unit cell modifies the surface acid-base sites, Ce^{4+} and Zr^{4+} ion acts as Lewis acid sites and O^{2-} ions as Bronsted or Lewis base sites [26]. In presence of oxygen, the intrinsic activity of ethanol dehydrogenation is considerably higher. Surface science studies have shown that co-adsorbed oxygen on late transition metals acts as a Bronsted base to facilitate O-H bond cleavage. Subsequent C-H bond cleavage leads to the corresponding aldehyde or ketone. Oxidation of ethanol can occur via activation of C-H bond or O-H bond of ethanol. As mentioned in literature [47,48] adsorbed oxygen on the transition metal act as Bronsted base to facilitate O-H bond cleavage. Later cleavage of C-H bond leads to the corresponding aldehyde. In this case, adsorbed oxygen on prepared catalysts facilitates O-H cleavage then dehydrogenation occurs via C-H cleavage to form acetaldehyde as main reaction products.

6.4 Conclusion

$Ce_xZr_{1-x}O_2$ and $Au/Ce_xZr_{1-x}O_2$ catalysts are first time reported for bioethanol oxidation reaction. Incorporation of Zr into Ce framework led to enhance the OSC which plays important role in bioethanol conversion. Bioethanol conversion increased with Zr content, while reverse trend was observed for acetaldehyde selectivity. $Au/Ce_xZr_{1-x}O_2$ catalysts exhibited good ethanol conversion compared to $Ce_xZr_{1-x}O_2$ catalysts. This is due to impregnation of Au which further reduced surface of $Ce_xZr_{1-x}O_2$ catalysts and enhanced their OSC. Among the used catalysts, $Au/Ce_{0.25}Zr_{0.75}O_2$ displayed 46% ethanol conversion and 87% selectivity towards acetaldehyde. However other two catalysts $Au/Ce_{0.75}Zr_{0.25}O_2$ and $Au/Ce_{0.5}Zr_{0.5}O_2$ showed 41% and 43 % ethanol conversion and 91% and 88 % acetaldehyde selectivity, respectively.

References

[1] J. Sun, Y. Wang, Recent Advances in Catalytic Conversion of Ethanol to Chemicals, ACS Catal. 4 (2014) 1078–1090. doi:10.1021/cs4011343.

[2] J. Xu, X.-C. Xu, X.-J. Yang, Y.-F. Han, Silver/hydroxyapatite foam as a highly selective catalyst for acetaldehyde production via ethanol oxidation, Catal. Today. 276 (2016) 19 – 27. doi:http://dx.doi.org/10.1016/j.cattod.2016.03.001.

[3] J. Zhang, L. Wang, L. Zhu, Q. Wu, C. Chen, X. Wang, Y. Ji, X. Meng, F.-S. Xiao, Solvent-Free Synthesis of Zeolite Crystals Encapsulating Gold-Palladium Nanoparticles for the Selective Oxidation of Bioethanol, ChemSusChem. 8 (2015) 2867–2871. doi:10.1002/cssc.201500261.

[4] E. Santacesaria, G. Carotenuto, R. Tesser, M. Di Serio, Ethanol dehydrogenation to ethyl acetate by using copper and copper chromite catalysts, Chem. Eng. J. 179 (2012) 209–220. doi:10.1016/j.cej.2011.10.043.

[5] D.L. Carvalho, R.R. de Avillez, M.T. Rodrigues, L.E.P. Borges, L.G. Appel, Mg and Al mixed oxides and the synthesis of n-butanol from ethanol, Appl. Catal. Gen. 415-416 (2012) 96–100. doi:10.1016/j.apcata.2011.12.009.

[6] T. Takei, N. Iguchi, M. Haruta, Synthesis of Acetoaldehyde, Acetic Acid, and Others by the Dehydrogenation and Oxidation of Ethanol, Catal. Surv. Asia. 15 (2011) 80–88. doi:10.1007/s10563-011-9112-1.

[7] H. Chen, Y. Dai, X. Jia, H. Yu, Y. Yang, Highly selective gas-phase oxidation of ethanol to ethyl acetate over bi-functional Pd/zeolite catalysts, Green Chem. 18 (2016) 3048–3056. doi:10.1039/C5GC02593A.

[8] J.M. Hidalgo, Z. Tišler, D. Kubička, K. Raabova, R. Bulanek, (V)/Hydrotalcite, (V)/Al$_2$O$_3$, (V)/TiO$_2$ and (V)/SBA-15 catalysts for the partial oxidation of ethanol to acetaldehyde, J. Mol. Catal. Chem. 420 (2016) 178–189. doi:10.1016/j.molcata.2016.04.024.

[9] M.V. Morales, E. Asedegbega-Nieto, B. Bachiller-Baeza, A. Guerrero-Ruiz, Bioethanol dehydrogenation over copper supported on functionalized graphene materials and a high surface area graphite, Carbon. 102 (2016) 426–436. doi:10.1016/j.carbon.2016.02.089.

[10] P. Liu, X. Zhu, S. Yang, T. Li, E.J.M. Hensen, On the metal–support synergy for selective gas-phase ethanol oxidation over MgCuCr$_2$O$_4$ supported metal nanoparticle catalysts, J. Catal. 331 (2015) 138 – 146. doi:http://dx.doi.org/10.1016/j.jcat.2015.08.025.

[11] J. Wang, R. Huang, Z. Feng, H. Liu, D. Su, Multi-Walled Carbon Nanotubes as a Catalyst for Gas-Phase Oxidation of Ethanol to Acetaldehyde, ChemSusChem. 9 (2016) 1820–1826. doi:10.1002/cssc.201600234.

[12] V.V. Dutov, G.V. Mamontov, V.I. Sobolev, O.V. Vodyankina, Silica-supported silver-containing OMS-2 catalysts for ethanol oxidative dehydrogenation, Catal. Today. 278 (2016) 164–173. doi:10.1016/j.cattod.2016.05.058.

[13] V.V. Kaichev, Y.A. Chesalov, A.A. Saraev, A.Y. Klyushin, A. Knop-Gericke, T.V. Andrushkevich, V.I. Bukhtiyarov, Redox mechanism for selective oxidation of ethanol over monolayer V$_2$O$_5$/TiO$_2$ catalysts, J. Catal. 338 (2016) 82 – 93. doi:http://dx.doi.org/10.1016/j.jcat.2016.02.022.

[14] H. Chen, X. Jia, Y. Li, C. Liu, Y. Yang, Controlled surface properties of Au/ZSM5 catalysts and their effects in the selective oxidation of ethanol, Catal. Today. 256 (2015) 153–160. doi:10.1016/j.cattod.2015.01.020.

[15] J. Mielby, J.O. Abildstrøm, F. Wang, T. Kasama, C. Weidenthaler, S. Kegnæs, Oxidation of Bioethanol using Zeolite-Encapsulated Gold Nanoparticles, Angew. Chem. Int. Ed. 53 (2014) 12513–12516. doi:10.1002/anie.201406354.

[16] M.M. Rahman, S.D. Davidson, J. Sun, Y. Wang, Effect of Water on Ethanol Conversion over ZnO, Top. Catal. 59 (2016) 37–45. doi:10.1007/s11244-015-0503-9.

[17] S.I. Mutinda, Hydrothermal Synthesis of Shape/Size-Controlled Cerium-Based Oxides, Youngstown State University, 2013. http://rave.ohiolink.edu/etdc/view?acc_num=ysu1378917332 (accessed October 6, 2016).

[18] T. Tsoncheva, R. Ivanova, J. Henych, M. Dimitrov, M. Kormunda, D. Kovacheva, N. Scotti, V.D. Santo, V. Štengl, Effect of preparation procedure on the formation of nanostructured ceria–zirconia mixed oxide catalysts for ethyl acetate oxidation: Homogeneous precipitation with urea vs template-assisted hydrothermal synthesis, Appl. Catal. Gen. 502 (2015) 418–432. doi:10.1016/j.apcata.2015.05.034.

[19] C.M. Olmos, L.E. Chinchilla, E.G. Rodrigues, J.J. Delgado, A.B. Hungría, G. Blanco, M.F.R. Pereira, J.J.M. Órfão, J.J. Calvino, X. Chen, Synergistic effect of bimetallic Au-Pd supported on ceria-zirconia mixed oxide catalysts for selective oxidation of glycerol, Appl. Catal. B Environ. 197 (2016) 222–235. doi:10.1016/j.apcatb.2016.03.050.

[20] M.D. Dimitrov, R.N. Ivanova, V. Štengl, J. Henych, D.G. Kovacheva, T.S. Tsoncheva, Optimization of CeO_2-ZrO_2 mixed oxide catalysts for ethyl acetate combustion, Bulg. Chem. Commun. 47 (2015) 323–329.

[21] N. Guillén-Hurtado, A. Bueno-López, A. García-García, Surface and structural characterization of co precipitated $Ce_xZr_{1-x}O_2$ ($0 \leq x \leq 1$) mixed oxides, J. Mater. Sci. 47 (2012) 3204–3213. doi:10.1007/s10853-011-6158-4.

[22] P.H. Rana, P.A. Parikh, Bioethanol valorization via its gas phase oxidation over Au &/or Ag supported on various oxides, J. Ind. Eng. Chem. 47 (2017) 228 – 235. doi:http://dx.doi.org/10.1016/j.jiec.2016.11.037.

[23] C.E. Hori, H. Permana, K.S. Ng, A. Brenner, K. More, K.M. Rahmoeller, D. Belton, Thermal stability of oxygen storage properties in a mixed CeO_2-ZrO_2 system, Appl. Catal. B Environ. 16 (1998) 105–117.

[24] C.M. Olmos, L.E. Chinchilla, J.J. Delgado, A.B. Hungría, G. Blanco, J.J. Calvino, X. Chen, CO Oxidation over Bimetallic Au–Pd Supported on Ceria–Zirconia Catalysts: Effects of Oxidation Temperature and Au:Pd Molar Ratio, Catal. Lett. 146 (2016) 144–156. doi:10.1007/s10562-015-1641-1.

[25] M.K. Devaraju, X. Liu, K. Yusuke, S. Yin, T. Sato, Solvothermal synthesis and characterization of ceria–zirconia mixed oxides for catalytic applications, Nanotechnology. 20 (2009) 405606. doi:10.1088/0957-4484/20/40/405606.

[26] S.B. Rathod, M.K. Lande, B.R. Arbad, Synthesis, Characterization and Catalytic Application of MoO_3/CeO_2-ZrO_2 Solid Heterogeneous Catalyst for the Synthesis of Benzimidazole Derivatives, Bull. Korean Chem. Soc. 31 (2010) 2835–2840. doi:10.5012/bkcs.2010.31.10.2835.

[27] S. Letichevsky, C.A. Tellez, R.R. de Avillez, M.I.P. da Silva, M.A. Fraga, L.G. Appel, obtaining CeO_2–ZrO_2 mixed oxides by coprecipitation: role of preparation conditions, Appl. Catal. B Environ. 58 (2005) 203–210.

[28] M. Rumruangwong, S. Wongkasemjit, Synthesis of ceria–zirconia mixed oxide from cerium and zirconium glycolates via sol–gel process and its reduction property, Appl. Organomet. Chem. 20 (2006) 615–625. doi:10.1002/aoc.1106.

[29] B.M. Reddy, A. Khan, Nanosized CeO$_2$–SiO$_2$, CeO$_2$–TiO$_2$, and CeO$_2$–ZrO$_2$ Mixed Oxides: Influence of Supporting Oxide on Thermal Stability and Oxygen Storage Properties of Ceria, Catal. Surv. Asia. 9 (2005) 155–171. doi:10.1007/s10563-005-7552-1.

[30] D.-J. Kim, Lattice Parameters, Ionic Conductivities, and Solubility Limits in Fluorite-Structure MO$_2$ Oxide [M= Hf^{4+}, Zr^{4+}, Ce^{4+}, Th^{4+}, U^{4+}] Solid Solutions, J. Am. Ceram. Soc. 72 (1989) 1415–1421.

[31] J. Fan, D. Weng, X. Wu, X. Wu, R. Ran, Modification of CeO$_2$–ZrO$_2$ mixed oxides by coprecipitated/impregnated Sr: Effect on the microstructure and oxygen storage capacity, J. Catal. 258 (2008) 177–186. doi:10.1016/j.jcat.2008.06.009.

[32] S. Sareen, V. Mutreja, S. Singh, B. Pal, Highly dispersed Au, Ag and Cu nanoparticles in mesoporous SBA-15 for highly selective catalytic reduction of nitroaromatics, RSC Adv. 5 (2015) 184–190. doi:10.1039/C4RA10050F.

[33] P. Saikia, A.T. Miah, B. Malakar, A. Bordoloi, Enhanced Catalytic Activity of Supported Gold Catalysts for Oxidation of Noxious Environmental Pollutant CO, Indian J. Mater. Sci. 2015 (2015) 1–10. doi:10.1155/2015/658346.

[34] S.S. Cimi A Daniel, Surfactant-assisted Hydrothermal Synthesis of Ceria-Zirconia Nanostructured Materials for Catalytic Applications, IOSR J. Appl. Chem. IOSR-JAC. 5 (2013) 23–29.

[35] S. Machmudah, M. Akmal Hadian, L. Samodro K., S. Winardi, _ W., H. Kanda, M. Goto, Preparation of Ceria-Zirconia Mixed Oxide by Hydrothermal Synthesis, Mod. Appl. Sci. 9 (2015) 134–139. doi:10.5539/mas.v9n7p134.

[36] B.M. Reddy, G.K. Reddy, I. Ganesh, J.M.F. Ferreira, Single step synthesis of nanosized CeO$_2$–M$_x$O$_y$ mixed oxides (M$_x$O$_y$ = SiO$_2$, TiO$_2$, ZrO$_2$, and Al$_2$O$_3$) by microwave induced solution combustion synthesis: characterization and CO oxidation, J. Mater. Sci. 44 (2009) 2743–2751. doi:10.1007/s10853-009-3358-2.

[37] A. Trovarelli, Structural and Oxygen Storage/Release Properties of CeO$_2$ -Based Solid Solutions, Comments Inorg. Chem. 20 (1999) 263–284. doi:10.1080/02603599908021446.

[38] A. Trovarelli, F. Zamar, J. Llorca, C. de Leitenburg, G. Dolcetti, J.T. Kiss, Nanophase Fluorite-Structured CeO$_2$–ZrO$_2$ Catalysts Prepared by High-Energy Mechanical Milling, J. Catal. 169 (1997) 490 – 502. doi:http://dx.doi.org/10.1006/jcat.1997.1705.

[39] P.P. Silva, F.A. Silva, L.S. Portela, L.V. Mattos, F.B. Noronha, C.E. Hori, Effect of Ce/Zr ratio on the performance of Pt/CeZrO$_2$/Al$_2$O$_3$ catalysts for methane partial oxidation, Catal. Today. 107 (2005) 734–740. doi:10.1016/j.cattod.2005.07.004.

[40] R.C.R. Neto, M. Schmal, Synthesis of CeO$_2$ and CeZrO$_2$ mixed oxide nanostructured catalysts for the iso-syntheses reaction, Appl. Catal. Gen. 450 (2013) 131–142. doi:10.1016/j.apcata.2012.10.002.

[41] P. Fornasiero, R. Dimonte, G.R. Rao, J. Kaspar, S. Meriani, A. Trovarelli, M. Graziani, Rh-Loaded CeO$_2$-ZrO$_2$ Solid-Solutions as Highly Efficient Oxygen Exchangers: Dependence of the Reduction Behavior and the Oxygen Storage Capacity on the Structural-Properties, J. Catal. 151 (1995) 168 – 177. doi:http://dx.doi.org/10.1006/jcat.1995.1019.

[42] C. Diagne, H. Idriss, K. Pearson, M.A. Gómez-García, A. Kiennemann, Efficient hydrogen production by ethanol reforming over Rh catalysts. Effect of addition of Zr on CeO$_2$ for the oxidation of CO to CO$_2$, Comptes Rendus Chim. 7 (2004) 617–622. doi:10.1016/j.crci.2004.03.004.

[43] P. Biswas, D. Kunzru, Steam reforming of ethanol for production of hydrogen over Ni/CeO$_2$–ZrO$_2$ catalyst: Effect of support and metal loading, Int. J. Hydrog. Energy. 32 (2007) 969–980. doi:10.1016/j.ijhydene.2006.09.031.

[44] C. Pojanavaraphan, A. Luengnaruemitchai, E. Gulari, Effect of catalyst preparation on Au/Ce$_{1-x}$Zr$_x$O$_2$ and Au–Cu/ Ce$_{1-x}$Zr$_x$O$_2$ for steam reforming of methanol, Int. J. Hydrog. Energy. 38 (2013) 1348–1362. doi:10.1016/j.ijhydene.2012.10.117.

[45] J. Rynkowski, I. Dobrosz-Gómez, Ceria-zirconia supported gold catalysts, Ann. UMCS Chem. 64 (2009). doi:10.2478/v10063-008-0015-6.

[46] J. Gaálová, P. Topka, L. Kaluža, O. Šolcová, Gold versus platinum on ceria–zirconia mixed oxides in oxidation of ethanol and toluene, Catal. Today. 175 (2011) 231–237. doi:10.1016/j.cattod.2011.05.011.

[47] Y. Guan, E.J.M. Hensen, Ethanol dehydrogenation by gold catalysts: The effect of the gold particle size and the presence of oxygen, Appl. Catal. Gen. 361 (2009) 49–56. doi:http://dx.doi.org/10.1016/j.apcata.2009.03.033.

[48] G.M. Mullen, L. Zhang, E.J. Evans, T. Yan, G. Henkelman, C.B. Mullins, Control of selectivity in allylic alcohol oxidation on gold surfaces: the role of oxygen adatoms and hydroxyl species, Phys Chem Chem Phys. 17 (2015) 4730–4738. doi:10.1039/C4CP04739G.

Chapter – 7

Conclusion and Future prospective

CHAPTER – 7
<u>Summary and Future Prospective</u>

7.1 Summary

Worldwide increase in high-scale production of biomass derived chemicals leads to sustainable feedstocks for high value added commodity chemicals. The transformation of biomass derived chemicals to fine chemicals requires less stages compared to tradition developed process. Bioethanol is one of the promising candidates for its conversion to various chemicals like acetaldehyde, acetic acid, ethyl acetate etc. For this conversion oxidation of bioethanol is carried out by oxygen or air as green oxidant instead of traditional inorganic oxidants. This thesis describes oxidation of bioethanol by both liquid phase and gas phase reaction assisted by different catalysts. The solid supports used in this work have been purchased and mixed oxides of $CeZrO_2$ (chapter 6) was synthesized using co-precipitation method. Au and Ag metals were anchored on the supports by wet impregnation method. Detail characterization of catalysts has been carried out using different techniques. This thesis involves study of role of supports, nature of metals and metal support interaction for bioethanol oxidation. This chapter provides summary and conclusions of the work described in previous chapters and scope of future work based on this thesis.

Chapter 1 summaries the importance of replacement of fossil fuel to alternative feedstock for producing of value added chemicals, availability of biomass derived chemicals, and the motivation of the study.

Chapter 2 provides mainly a review on the literature of oxidation of ethanol by both liquid and gas phase reaction using various catalysts, influence of reaction parameters like effect of temperature, pressure, and time on stream etc. has been discussed in detail. It also provides detail mechanism of ethanol oxidation. It concluded that ethanol conversion highly depends on nature of supports and metals as well influenced parameters. Various analytical techniques used for the characterization of catalysts are also described.

Chapter 3 involves synthesis of Au and Ag supported on various zeolite. These catalysts were tested for bioethanol oxidation in liquid phase where comparable bioethanol

conversion was not achieved. With Au/Hβ maximum 17 % bioethanol conversion with 63 % selectivity towards acetaldehyde was obtained at 200°C for 24 h. It was observed with increased reaction time increase bioethanol conversion for all the catalysts. The lower activity of catalysts may be due to hydrophilic nature of supports (zeolite). Hydrophilic nature of zeolite was confirmed by various researchers as mentioned in the chapter in detail. Effect of alkali for the reaction was checked with Ag/Na-HZSM5 and Au/Na-Hβ catalysts. However no significant change was observed in the bioethanol conversion and it was around 2% and 10 %, respectively. Later on Ag/ZrO$_2$ catalyst was prepared and evaluated for oxidation of bioethanol. With Ag/ZrO$_2$, 30 % bioethanol conversion with 95 % selectivity for acetic acid at 150° C and 24 h was achieved and it was highest among the used catalysts.

Chapter 4 describes gas phase oxidation of bioethanol using Au/SiO$_2$, Au/CeO$_2$, Au/ZrO$_2$, Ag/ZrO$_2$ and Au-Ag/ZrO$_2$ catalysts. All catalyst were prepared by wet impregnation method, characterized and tested for bioethanol oxidation reaction. The reaction conditions were kept constant for all catalysts. Au based catalysts exhibited higher bioethanol conversion than Ag based catalysts. Au/ZrO$_2$, Au/CeO$_2$ and Au/SiO$_2$ displayed 38%, 34% and 18% conversion of bioethanol respectively, while Ag/ZrO$_2$ and Au-Ag/ZrO$_2$ catalysts showed 27% and 23% bioethanol conversion respectively. Acetaldehyde was major reaction product for all catalyst and selectivity order as follow: Au/CeO$_2$> Ag/ZrO$_2$> Au-Ag/ZrO$_2$> Au/ZrO$_2$> Au/SiO$_2$. In case of Au/ZrO$_2$, Au leads partial reduction of surface Zr^{4+} to Zr^{3+} which creates oxygen deficiencies on ZrO$_2$ surface. With Au/CeO$_2$, CeO$_2$ was able to provide activate oxygen with concurrent creation of oxygen vacancies which could further played a role of activating reactant oxygen molecules reaching from the gas phase. It was also found that addition of Ag to Au (Au-Ag/ZrO$_2$) decreased Au^0/Au$^+$ ratio and making the catalyst less favorable for ethanol conversion to ethyl acetate.

Chapter 5 shows role of metal support interaction using Ag-CeO$_2$ as catalyst for selective oxidation of bioethanol to acetaldehyde. This catalyst showed good catalytic performance with 36% bioethanol conversion and > 85% acetaldehyde selectivity. Higher catalytic activity of Ag/CeO$_2$ was due to the cooperation of Ag$^{\delta+}$ acid sites and base sites of ceria on the Ag-CeO$_2$ interface. Here key role of Ag on surface is: (i) to increase lattice oxygen mobility of CeO$_2$ by producing structural defects, and (ii) to weaken the Ce–O bond and

thus induce the exchange between lattice oxygen and adsorbed oxygen. Ag/CeO_2 catalyst exhibited no sign of catalyst deactivation for more than 36 h on-stream.

Chapter 6 report the effect of proportions of Ce and Zr in their mixed oxide on their catalytic performance for bioethanol oxidation. It was observed that addition of Zr to Ce framework led to increase OSC which played crucial role in bioethanol conversion. Bioethanol conversion increase with increased Zr content, while reverse trend was observed for acetaldehyde selectivity. $Au/Ce_xZr_{1-x}O_2$ catalysts exhibited good ethanol conversion compared to $Ce_xZr_{1-x}O_2$ catalysts. Among the used catalysts, $Au/Ce_{0.25}Zr_{0.75}O_2$ displayed highest bioethanol conversion (46%) and 87% selectivity towards acetaldehyde.

7.2 Future Prospective

This dissertation work has demonstrated that supported Au and Ag nanoparticles are promising as heterogeneous catalysts in selective oxidation of bioethanol under reaction conditions, particularly from the viewpoint of green chemistry. The results obtained from this reaction and investigations have led to some possible questions and suggestions for further work and development. The following suggestions may be beneficial to understanding more about the mechanism of oxidation of bioethanol, Au based bimetallic catalysts' performance, to study effect of various noble metals supported on $CeZrO_2$ mixed oxides, as well as improving the conversion for bioethanol and employing mesoporous $CeZrO_2$ mixed oxides as solid support.

(1) It was shown in chapter 4 that Au/ZrO_2 catalyst exhibited higher bioethanol conversion. Although the catalytic activity was reduced with $Au-Ag/ZrO_2$ bimetallic catalyst compared to that observed with Au/ZrO_2. Formulation of different Au bimetal supported catalyst for example Au-Pd, Au-Cu for bioethanol oxidation, may improve the activity for reaction and selectivity of the products.

(2) To understand and explain the difference in the activity and selectivity that has been obtained using different supports, more high definition characterization techniques are needed such as STEM and sorption analysis of supports. Other techniques like *in situ* ATR-IR and DRIFT spectroscopic studies on catalysts prepared by different supports for alcohol oxidation are also required.

Investigations from this aspect may help in understanding the support effect and the interface effect between the metal nanoparticles and the supports, and also the products molecular composition with the supports and metals. This will help in understanding the possible molecular mechanism processes of the reactions.

(3) As shown in chapter 5 that Ag/CeO_2 outperforms the reported catalyst for bioethanol oxidation with no sign of deactivation for longer reaction time. By varying the loading of Ag on CeO_2, oxidation reaction can be carried out to further improve and optimize the catalytic performance.

(4) As chapter 6 demonstrated the OSC of the $CeZrO_2$ mixed oxide increases with incorporation of Zr which was further improved upon the impregnation of Au. Improved OSC of catalyst enhances conversion of bioethanol. Hence it would be interesting to carry out an evaluation of the oxidation of bioethanol with different noble nanoparticle supported $CeZrO_2$ mixed oxide.

(5) Finally, we propose to employ mesoporous $CeZrO_2$ mixed oxide for this reaction, additionally experiment should be carried out to evaluate role of surface area of this catalyst in OSC and its effect on activity.
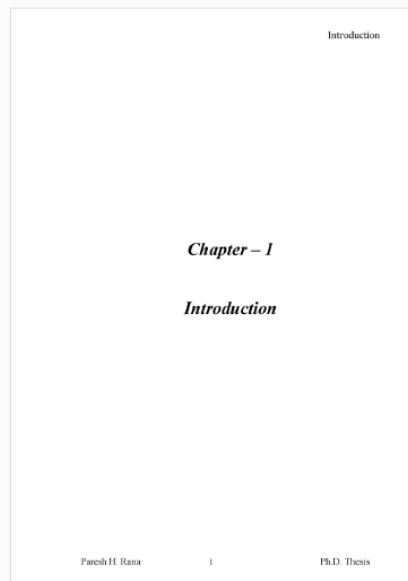
Appendix – I

Calculation of activity coefficient by UNIFAC method

		Mole fraction	Temp K		Pisat ,bar
	Ethanol	0.1	473	1CH3, 1 Ch2,1OH	29.4645
	water	0.9		1h2O	15.5186

Main group	sub group	k (sub group no)	Rk	Qk	Vk(Etha)	Vk(H2O)
1	CH3	1	0.9011	0.848	1	0
1	CH2	2	0.6744	0.54	1	0
5	OH	15	1	1.2	1	0
7	H2O	17	0.92	1.4	0	1

sub group(amk)	1	2	15	17
1	0	0	986.5	1318
2	0	0	986.5	1318
15	156.4	156.4	0	353.5
17	300	300	-229.1	0

r1	2.5755					
r2	0.92					
q1	2.588	5q1	12.94			
q2	1.4	5q2	7			
J1	2.37253	LnJ1	0.863957	J1/L1	1.392349	Ln J1/L1	0.330992
J2	0.847497	In j2	-0.16547	J2/L2	0.919413	Ln J2/L2	-0.08402
L1	1.703977					
L2	0.92178					

T1,1	1	T2,1	1	T15,1	0.718453	T17,1	0.530333
T1,2	1	T2,2	1	T15,2	0.718453	T17,2	0.530333
T1,15	0.12423	T2,15	0.12423	T15,17	1	T17,15	1.623128
T1,17	0.061638	T2,17	0.061638	T15,17	0.473617	T17,17	1

						For Compo 1		For Compo2	
e1,1	0.327666	e1,2	0			A1	0.082542	B1	0.050348
e2,1	0.208655	e2,2	0			A2	0.052562	B2	0.032061
e15,1	0.463679	e15,2	0			A15	0.029159	B15	0.089249
e17,1	0	e17,2	1			A17	0.240198	B17	0.950664
						A	0.404462	B	1.122322
B1,1	0.869453	B2,1	0.530333			P1	0.128096	Q1	0
B1,2	0.869453	B2,2	0.530333			P2	0.081571	Q2	0
B1,15	0.530306	B2,15	1.623128			P15	-0.46219	Q15	0
B1,17	0.252664	B2,17	1			P17	0	Q17	0.136214
x1q1 +x2q2	1.5188					P	-0.25253	Q	0.136214

Theta1	0.055834	Theta2	0.035554	Theta15	0.07901	Theta17	0.829602
s1	0.588118	s2	0.588118	s15	1.436914	s17	0.872656

In Y1C	0.285382			In Y1R	0.887711
In Y2C	0.011065			In Y2R	0.01945

		In Y1	1.173093165	Y1	3.231974
		In Y2	0.030514809	Y2	1.030985

Pbubble	23.92235209	bar

Appendix – II

PhD

6 Li, and Emiel J.M. Hensen. "On the metal–support synergy for selective gas-phase ethanol oxidation over MgCuCr2O4 supported metal nanoparticle catalysts", Journal of Catalysis, 2015.
Publication

%1

7 Kaichev, Vasily V., Yuriy A. Chesalov, Andrey A. Saraev, Alexander Yu. Klyushin, Axel Knop-Gericke, Tamara V. Andrushkevich, and Valerii I. Bukhtiyarov. "Redox mechanism for selective oxidation of ethanol over monolayer V2O5/TiO2 catalysts", Journal of Catalysis, 2016.
Publication

%1

| EXCLUDE QUOTES | ON | EXCLUDE MATCHES | < 1% |
| EXCLUDE BIBLIOGRAPHY | ON | | |

LIST OF PUBLICATION

1. Paresh H. Rana, Parimal A. Parikh, "Bioethanol Valorization *via* its Gas Phase Oxidation over Au and/or Ag supported on various Oxides**" Journal of Industrial and Engineering chemistry**, 2017, 47, 228 – 235, doi:10.1016/j.jiec.2016.11.037, (**IMPACT FACTOR: 4.179)**

2. Paresh H. Rana, Parimal A. Parikh, "Bioethanol Selective Oxidation to Acetaldehyde over Ag-CeO$_2$: Role of Metal -Support Interactions" **New Journal of Chemistry**, 2017, 41, 2636-2641, doi:10.1039/C6NJ03853K (**IMPACT FACTOR: 3.227)**

Papers submitted to International Peer-Reviewed Journal

1. Paresh H. Rana, Parimal A. Parikh, "Selective oxidation of bioethanol: Influence of relative proportions of Ce and Zr in their mixed oxides on their catalytic performance" under review in Industrial and Engineering Chemistry Research

Presentation at International Conference

1. Paresh H. Rana, Parimal A. Parikh, Gas phase oxidation of aqueous ethanol using Au supported cerium oxide catalyst. Sustainable Chemistry & Engineering sponsored by American chemical society & Royal society of chemistry, 8-9th, October, 2015.

2. Paresh H. Rana, Parimal A. Parikh, Review: Selective Oxidation of bioethanol to Produce Acetic acid. CHEMCOM 2013, 26-30th, December, 2013.